HIGHWAY RESEARCH RECORD

Number 404

Asphalt Mixture Characterization and Asphalt Grading

10 reports
prepared for the
51st Annual Meeting

Subject Areas

25 Pavement Design
31 Bituminous Materials and Mixes

HIGHWAY RESEARCH BOARD
DIVISION OF ENGINEERING NATIONAL RESEARCH COUNCIL
NATIONAL ACADEMY OF SCIENCES—NATIONAL ACADEMY OF ENGINEERING

Washington, D.C. 1972

NOTICE

The studies reported herein were not undertaken under the aegis of the National Academy of Sciences or the National Research Council. The papers report research work of the authors done at the institution named by the authors. The papers were offered to the Highway Research Board of the National Research Council for publication and are published herein in the interest of the dissemination of information from research, one of the major functions of the HRB.

Before publication, each paper was reviewed by members of the HRB committee named as its sponsor and was accepted as objective, useful, and suitable for publication by NRC. The members of the committee were selected for their individual scholarly competence and judgment, with due consideration for the balance and breadth of disciplines. Responsibility for the publication of these reports rests with the sponsoring committee; however, the opinions and conclusions expressed in the reports are those of the individual authors and not necessarily those of the sponsoring committee, the HRB, or the NRC.

Although these reports are not submitted for approval to the Academy membership or to the Council of the Academy, each report is reviewed and processed according to procedures established and monitored by the Academy's Report Review Committee.

ISBN 0-309-02076-X

Price: $3.60

Available from

Highway Research Board
National Academy of Sciences
2101 Constitution Avenue, N. W.
Washington, D. C. 20418

CONTENTS

FOREWORD

This RECORD contains reports that are of interest to asphalt paving and research engineers. The topics discussed are related to (a) measurement of stiffness of asphalt mixtures, (b) behavior of asphalt mixtures under repeated loads, (c) effects of aggregate characteristics on mixture design, and (d) asphalt cement viscosities.

Maupin's work is concerned with comparing the fatigue life to the indirect tensile stiffness of asphalt concrete mixtures. The fatigue life was obtained by testing beams under constant strain, and the stiffness was obtained from diametral deformations caused by "split-cylinder" loading on Marshall specimens. Although the data are not extensive, results indicated that the indirect tensile test may possibly be used to design asphalt concrete to withstand repeated applications of strain.

Stephenson and Manke report on determination of dynamic E-modulus, G-modulus, and Poisson's ratio of asphalt concrete. The procedure used is based on measurements of the propagation velocities of pulsed ultrasonic shear and compressional waves on standard-sized specimens. The data indicate that E and G decreased with increase in test temperature; the values ranged from 5×10^6 to 1×10^6 psi for E and 1.8×10^6 to 0.2×10^6 psi for G. An optimum asphalt content was found for maximum values of E and G.

A different method for obtaining a resilient modulus (M_R) of asphalt concrete is presented by Schmidt. His procedure is based on the analysis of deformations for a specimen loaded by the split-cylinder procedure. The report presents comparative values of M_R obtained by loadings of direct tension and compression with those obtained with the indirect tensile loading of the split-cylinder test and of flexural beams. The data indicate a range of M_R for asphalt concrete from 200,000 to 500,000 psi; also an optimum asphalt content was found for maximum value of M_R.

Gannon and Majidzadeh present and discuss data obtained from a laboratory and field study on the use of rubberized emulsified asphalt in hot-mix asphalt concrete. Measurements were made on samples taken from a field test pavement after construction and at 1-and 2-year intervals. Pavement samples were tested under compressive, Marshall, and flexural loading conditions, and the recovered binders were measured for penetration, softening point, and viscosity. The authors conclude that the mixture containing the binder with the greatest (3 percent) amount of rubber was the superior one.

A study to compare effects of cubical versus flaky aggregate on engineering properties of asphalt paving mixtures is reported by Livneh and Greenstein. The effects and differences are described in terms of (a) density, (b) Marshall values, (c) triaxial shear strength, (d) tensile splitting strength, (e) aggregate breakage, and (f) resistance to grooving. The conclusions presented are that flaky aggregate of the hard and crushed type may be used for producing asphalt concrete and that abrasion and crushing values of aggregates are not always reliable criteria for evaluating aggregates for asphalt concrete.

Howeedy and Herrin present and discuss data obtained in determining the behavior of cold-mix asphalt concrete subjected to repeated compressive loads. The mixtures were made of dense and open gradations with RC or MC asphalt. Fatigue failure was identified at the load repetition causing 1 percent residual strain, and the resilient modulus was calculated by using the corresponding resilient (repeated) strain. The results of the work indicated that the effects of temperature, binder content, and binder viscosity are comparable to those for hot-mix asphalt concrete.

Distribution of temperature within asphalt pavements in Kuwait is summarized by Bissada. In addition, comparisons of temperature among Kuwait and Arizona, New York, Melbourne, and London are presented. The author suggests means by which to overcome the weakening effects of temperature on mixture and pavement design.

Schweyer describes a new method for determining the apparent viscosity and shear susceptibility of asphalt cements. The results of the new method are compared and discussed with reference to results obtained by other procedures. The new (Florida) method is considered to be rapid and acceptable for general routine testing.

The importance of asphalt absorption by aggregates is discussed by Kandhal and Lee. Various methods for relating asphalt absorption to pore characteristics of aggregates were used, and their results are analyzed. A particularly interesting finding was that asphalt absorption by the limestone aggregate was controlled by the 0.7- to 0.05-μm pore size, whereas the pore sizes in the range of 0.1 to 0.05 μm seem to determine the amount of water absorption.

Also presented is an abridgment of McLeod's report on grading of asphalt cements, which recommends that asphalts be graded on the basis of penetration (or viscosity) at 77 F plus a viscosity requirement at 275 F.

—R. A. Jimenez

RESULTS OF INDIRECT TENSILE TESTS RELATED TO ASPHALT FATIGUE

G. W. Maupin, Jr., Virginia Highway Research Council

The purpose of this investigation was to develop a correlation among fatigue life, magnitude of strain, and indirect tensile stiffness for 4 asphaltic concrete mixes prepared and tested in the laboratory. Constant strain fatigue tests were performed on 2.5- by 3- by 14-in. beams at several strain levels to develop a strain-fatigue life correlation for each mix. Indirect tensile tests were conducted on Marshall specimens and the stiffness measured in the region of tensile failure. Stiffness values ranged from 5,431 psi for a flexible mix to 29,070 psi for an aged stiff mix. There was a trend for the stiff mixes to yield shorter fatigue lives than did the flexible mixes if aggregates and gradation were similar. The correlation developed between stiffness and fatigue life indicates possibilities for using the indirect tensile test to design asphaltic concrete with the flexibility required to withstand repeated strain applications.

•FATIGUE was recognized as a contributor to asphalt pavement distress problems in the 1950s (1) and possibly earlier. Fatigue is complicated in asphaltic mixes by viscoelasticity, heterogeneity, anisotropy, and temperature susceptibility.

Viscoelastic analysis requires model analysis, and it is difficult to obtain a mathematical model that defines the behavior of an asphaltic mix. Temperature affects the viscosity of the asphalt, which in turn influences the behavior of the mix; therefore, field fatigue behavior may be governed by the environment.

Although the fatigue mechanism for asphaltic pavements is complex, much valuable knowledge has been gained through laboratory fatigue testing. Initial investigations were concerned with the effect of load type, mixture variables, and environmental factors. Information was gathered on the effect of asphalt content, aggregate type, void content, temperature, and type of loading. The latest efforts have been directed toward incorporating fatigue analysis into the design systems for asphalt pavements (2).

The fatigue life of a bituminous mixture may be defined by

$$N = K\,(1/\epsilon)^n$$

where

N = number of cycles to failure,
K = constant dependent on material properties,
n = constant, and
ϵ = strain magnitude.

Most design methods have been concerned with limiting the strain that may be developed in a particular bituminous layer to provide a satisfactory fatigue life.

Constant stress fatigue tests and constant strain fatigue tests have been used to define the fatigue behavior of asphaltic concrete. It is the general consensus that the constant strain tests define the behavior of thin pavement layers that contribute little to the flexural stiffness of the pavement structure and that the constant stress tests apply to

Sponsored by Committee on Mechanical Properties of Bituminous Paving Mixtures.

thick bituminous layers that do contribute significantly to the stiffness of the pavement. Thin and thick layers have not been clearly defined, but a thin layer is generally considered to be less than 3 in. deep and a thick layer more than 5 in. As a result, a combination of constant stress and constant strain may be present in many pavements. For instance, a layer between 3 and 5 in. thick may behave according to both constant stress and constant strain modes. It may have ample stiffness to contribute to the load carrying ability of the pavement (constant stress mode); however, the strain is governed by the underlying layers (constant strain mode). In general, the two types of fatigue tests give opposite results. For example, under a constant stress test an increase in stiffness will result in an increased fatigue life, whereas under a constant strain test a decrease in stiffness results in an increased fatigue life (3).

The remainder of this paper will concentrate on thin asphaltic concrete layers and surface layers that behave in a constant strain mode. This mode was selected because thin surface mixes in Virginia have been observed to exhibit distress problems that hopefully may be solved through fatigue studies. The mode is used to define the fatigue behavior of thin layers and thin surface mixes, assuming that tensile strains sufficient to cause fatigue failure are developed on the top surface.

Also, as mentioned earlier, asphaltic concrete stiffness, which is measured under dynamic loading, appears to be related to fatigue behavior; therefore, the stiffness of an asphaltic mix might provide some indication of its ability to sustain repetitions of strain or stress. This investigation attempted to determine whether a relation also exists between the fatigue life of a mix and its indirect tensile stiffness, i.e., a relation that may be measured by a simple laboratory test. It was thought that, if a relation could be developed among indirect tensile stiffness, strain, and fatigue life for a constant strain testing mode and if the estimated strain and desired fatigue life were known, a mix could be designed with a stiffness indicated by the relation mentioned. Although this design method would not be as thorough and exact as the fatigue design subsystem using fatigue tests, n-layered analysis, and fatigue damage summation, it would be a method of designing mixes against fatigue failure. It would be especially useful in laboratories that lack the test equipment necessary for the fatigue design subsystem.

PURPOSE AND SCOPE

The purpose of this investigation was to determine if a correlation could be developed among fatigue life, strain, and indirect tensile stiffness. It was anticipated that the correlation might be used to predict the fatigue susceptibility of asphaltic mixes.

The correlation was developed by using controlled strain fatigue tests and indirect tensile tests. The tests were performed on 4 laboratory prepared mixes selected from those allowed under Virginia specifications, with slight modifications.

PROCEDURE

Mixes

Four mixes (Table 1) were selected to provide a wide range of stiffness values, and fatigue and indirect tension tests were performed on each mix. The aggregates for each mix were recombined by sieve sizes to obtain the desired gradation. The asphalt contents were obtained by the Marshall design method. The S-5 mixes contained 25 percent sand and 75 percent crushed granite, and the S-3 mix contained 93 percent rounded gravel and sand and 7 percent granite (-No. 200 sieve size).

The S-5 mix, with an 85- to 100-penetration asphalt cement, was aged in the oven to increase its stiffness and thus provide an indication of the effect of increased asphalt stiffness on fatigue life. The artificial aging was accomplished by placing the fresh mixture approximately 1½ in. deep in a pan and heating it in a 300 F oven for 2 hours, stirring the mixture occasionally. The aging process dropped the penetration value of the recovered asphalt cement from 47 to 23 at 77 F.

A mixture with a lower stiffness was made by substituting 120- to 150-penetration asphalt. Therefore, three of the mixes had different stiffness values because of the asphalt cement characteristics. The fourth mixture, an S-3, had a low stiffness caused by aggregate characteristics and gradation.

Fatigue Tests

The constant strain fatigue tests were conducted on 2.5- by 3- by 14-in. asphaltic concrete beams made on a modified kneading compactor. Experience had been gained with the test and compaction equipment in previous studies (4, 5). The strain magnitude was monitored with a 1-in. foil strain gauge located in the center of the lower surface of the beam, which is the point of maximum tensile strain. A large strain gauge was desirable in order to negate the effect of the large aggregate particles. However, strain at a point (maximum strain) was desired, and a small strain gauge best gives this indication. It was felt that a compromise gauge length of 1 in. would serve satisfactorily. The gauge was attached with an 85- to 100-penetration asphalt cement, thereby eliminating the influence of the adhesive stiffness. The fatigue tests were performed at room temperature (75 F) because it was convenient and because 75 F was considered to be an approximate median annual field temperature for Virginia.

Fatigue failure was defined as the cracking of the tensile bending surface. The cracks were detected by gluing parallel aluminum foil strips ½ in. from each edge of the tensile surface (Fig. 1) and connecting them in series with the cutoff mechanism. When a fatigue crack formed in the asphalt, thus cracking the foil strip, the machine stopped, and the number of cycles was recorded.

Indirect Tensile Tests

Fatigue failures occur in regions where large tensile stresses and strains are present; therefore, a simple test procedure yielding tensile stiffness seemed desirable for correlation purposes. Direct tensile tests, bending tests, and indirect tensile tests may be used to obtain the tensile characteristics of a material, and Hudson and Kennedy (6) have summarized the advantages and disadvantages of each method when used on asphaltic concrete.

The gripping procedure and the application of a pure tensile force are difficult in a direct tensile test. The bending test has the disadvantage of an undefined stress distribution across the specimen and is influenced by surface irregularities. Some of the advantages of the indirect tensile test are as follows:

1. It is simple;
2. Marshall specimens may be used;
3. Surface irregularities do not seriously affect the results; and
4. The coefficient of variation of the test results is low.

The major disadvantages of this test are concerned with the theory. The theory assumes that the test specimen is elastic, but asphaltic concrete is viscoelastic at most environmental temperatures. Also, the theory assumes a line loading on the specimen, whereas in practice the load is distributed with a loading strip. These disadvantages are not considered serious, and the advantages seem to outweigh the disadvantages. The results of the work by Hudson and Kennedy (6) and Hadley et al. (7) indicate that the indirect tensile test can be used to predict the tensile strength of asphaltic concrete reasonably accurately.

It was decided to use the indirect tensile test on Marshall specimens (2.5 by 4 in. diameter) because no special equipment was necessary and specimen fabrication was simple. A compressive strain rate of 1 in./min was used, and compressive deformation, compressive force, and tensile strain were recorded throughout each test. The tensile strain was measured over a 1-in. gauge length in the region of maximum tensile strain with a transducer as shown in Figure 2. The tensile stress was computed, and the tensile stiffness was obtained from the stress-strain relation.

RESULTS

The indirect tension test was performed on eight Marshall specimens for each mix. A summary of the results is given in Table 2. The tensile stress σ_{TF} was computed by using the formula

$$\sigma_{TF} = 2P/\pi\ td$$

Table 1. Asphaltic concrete mixtures.

Mix	Binder	Asphalt Content (percent)	Recovered Asphalt Penetration	Gradation, Percent Passing (sieve size)						
				½	⅜	4	8	30	50	200
Virginia S-5	AP-3 85 to 100 penetration	5.6	47	100	90	60	45	23	15	6
Virginia S-5 (aged in oven)	AP-3 85 to 100 penetration	5.6	23	100	90	60	45	23	15	6
Virginia S-5	120 to 150 penetration	6.0	87	100	90	60	45	23	15	6
Virginia S-3	85 to 100 penetration	7.5	48	—	100	97.5	94	49	24	7

Figure 1. Fatigue specimen with strain gauge and aluminum foil strips.

Figure 2. Tensile strain transducer.

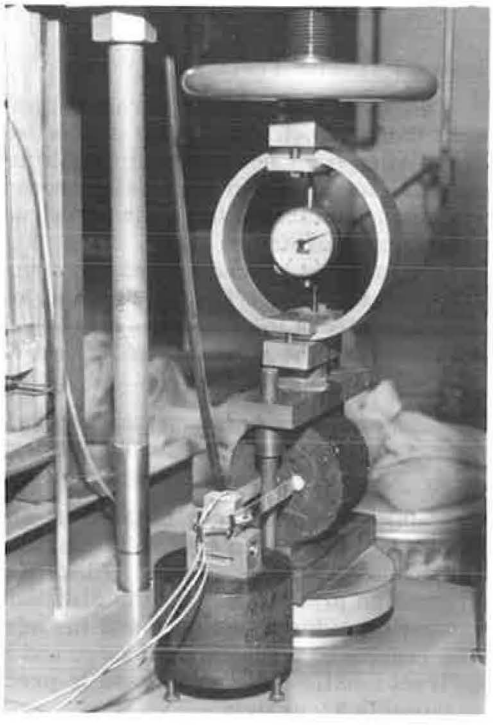

Table 2. Tensile test results.

Mix	Tensile Failure Stress (psi)	Tensile Failure Strain (in./in.)	Tensile Failure Stiffness (psi)	Tensile Stiffness at Three-Quarters of Failure Strength (psi)	Compressive Deformation at Failure (in.)
Virginia S-5	157	0.025	6,525	21,050	0.16
Aged Virgina S-5	181	0.027	7,026	29,070	0.16
Virginia S-5 (120 to 150 penetration binder)	92	0.030	3,130	10,700	0.13
S-3 (85 to 100 penetration binder)	78	0.041	1,940	5,431	0.16

where

P = the compressive force,
t = the thickness of the specimen, and
d = the diameter of the specimen.

As expected, the tensile strength and stiffness were higher for the mixtures with stiffer asphalt cements. A typical stress-strain curve is shown in Figure 3 for a point in the region of the maximum tensile stress and tensile strain. The stress-strain curve is approximately linear until three-quarters of the failure stress is reached; then, as it approaches total failure, the strain increases at a faster rate than does the stress. It was felt that a stiffness value obtained from the linear portion of the stress-strain relation would be more meaningful than the failure stiffness; therefore, a stiffness value was computed using three-quarters of the failure stress and the corresponding strain value. The stiffness computed from the stress and strain values at failure has little meaning because the failure strain is not well defined and is difficult to measure.

Strain-fatigue life data were collected for each of the four mixtures. A linear log-log relation was obtained for each mixture (Fig. 4) in the form

$$N = K\,(1/\epsilon)^n$$

which was defined previously. The K values ranged from 1.8×10^{14} to 3.1×10^{20} and the n values from 4.4 to 6.0. The n values are consistent with those found by Santucci and Schmidt (8) for constant strain fatigue tests.

It can be observed that the fatigue life of the aged S-5 mix was approximately one-tenth that of the regular S-5 mix. These results agree with past observations wherein pavements containing highly aged asphalt cements displayed excessive amounts of premature cracking.

The aged S-5 mix endured 1 million strain repetitions when the strain level was maintained below 70×10^{-6} in./in. The remaining mixes survived 1 million strain repetitions when the strain level was maintained below 140×10^{-6} in./in. Other investigators (9) have found that an asphaltic concrete tested in the laboratory will endure 1 million repetitions at 150×10^{-6} in./in., which agrees reasonably well with the results of this investigation.

The stiffness values were computed by the following formulas:

$$S_{TF} = \sigma_{TF}/\epsilon_{TF} \text{ and } S_{3/4} = {}^3/_4\sigma_{TF}/\epsilon_{3/4}$$

where

S_{TF} = secant tensile failure stiffness,
$S_{3/4}$ = secant stiffness at three-quarters of the tensile failure stress,
σ_{TF} = tensile stress at failure,
$\epsilon_{3/4}$ = tensile strain at three-quarters failure stress, and
ϵ_{TF} = tensile strain at failure.

The aged mixture containing the asphalt cement with a 23-penetration value had a three-quarter stiffness of 29,070 psi compared to 21,050 psi for the regular mixture containing an asphalt cement with a 47-penetration value. A similar mixture containing an 87-penetration value cement had a three-quarter stiffness of 10,700 psi. These values indicate that asphalt stiffness has a profound influence on mixture stiffness, and that mixture stiffness can be controlled by using certain asphalt cements. The S-3 mixture that contained an asphalt cement with a 48-penetration value and rounded gravel and sand had a three-quarter stiffness of 5,430 psi. This low stiffness value can be attributed to the aggregate type and gradation.

Fatigue investigations have indicated some correlation between asphaltic concrete stiffness and fatigue life (3). In constant strain fatigue tests, stiff mixes have shorter fatigue lives than do flexible mixes; in constant stress fatigue tests, the stiff mixes have the longer fatigue lives.

Figure 3. Typical indirect tensile test.

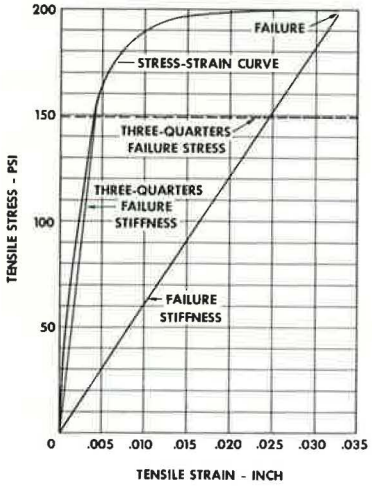

Figure 4. Constant strain fatigue tests.

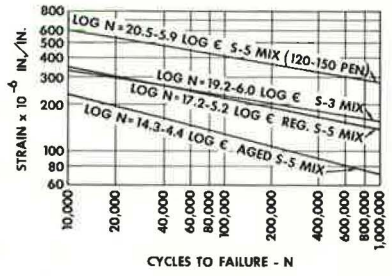

Figure 5. Fatigue versus stiffness.

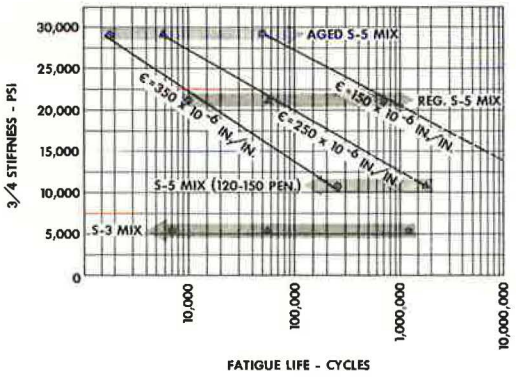

Figure 6. Fatigue versus penetration of recovered asphalt.

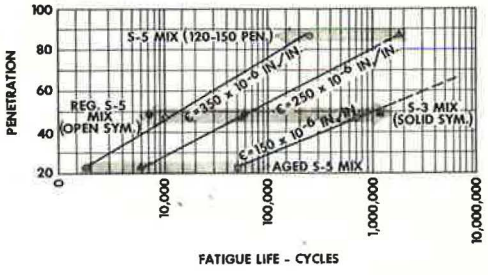

The fatigue lives of mixes having different stiffnesses can be compared at any strain level by using the information shown in Figure 4. Figure 5 shows a correlation developed between three-quarter indirect tensile stiffness and fatigue life at several strain levels for the 4 mixes tested. In general, fatigue life decreased as indirect tensile stiffness increased, except for the S-3 mix. Figure 6 shows the relation between fatigue life and the penetration of the recovered asphalt cement at 77 F. There is a linear semilog relation between the two for the four mixes. The available data indicate that stiffness correlates with fatigue life for mixes with different binders but similar aggregates. It is possible to design a mixture with a stiffness to endure a set number of repetitions with the aid of a correlation as shown in Figure 5. If it is desired to design a mix for 1 million cycles at 150×10^{-6} in./in., the stiffness of the mix should be kept less than about 20,000 psi.

The two methods of designing against fatigue failure in asphaltic concrete are as follows.

1. Method I—Design underlying layers so that the strain in the asphaltic concrete will be below a known damage level.
2. Method II—Design asphaltic concrete with fatigue characteristics that will withstand a known strain level.

Kasianchuk et al. (9) used a fatigue design subsystem (method I) to design a pavement against fatigue failure. The entire pavement structure was designed to limit the strain in the asphaltic concrete to 150×10^{-6} in./in., a value that presumably would ensure 1 million load repetitions.

Possibly a simpler and cheaper approach in some instances would be method II, in which the asphaltic concrete mixture would be designed such that it could withstand the required number of repetitions at the predicted strain level. The required stiffness, i.e., fatigue characteristics, can be obtained from a fatigue-stiffness correlation at the predicted strain value, and the mixture is then designed for that stiffness.

The amount of data obtained in this investigation is insufficient to permit broad conclusions; however, the results indicate that, for constant strain fatigue tests, fatigue life increases with decreased stiffness. It is felt that reliable correlations that will indicate fatigue susceptibility can be developed for asphaltic mixtures.

REFERENCES

1. Hveem, F. N. Pavement Deflections and Fatigue Failures. HRB Bull. 114, 1955, pp. 43-87.
2. Symposium on Fatigue of Compacted Bituminous Aggregate Mixtures, Session II, ASTM 74th Annual Meeting. Atlantic City, New Jersey.
3. Finn, F. N. Factors Involved in the Design of Asphaltic Pavement Surfaces. NCHRP Rept. 39, 1967, p. 66.
4. Maupin, G. W., Jr. Effects of Aggregate Shape on the Fatigue Behavior of an Asphaltic Surface Mixture. Virginia Highway Research Council, Charlottesville, June 1968.
5. Maupin, G. W., Jr. Effect of Some Aggregate Characteristics on the Fatigue Behavior of an Asphaltic Concrete Mixture. Virginia Highway Research Council, Charlottesville, July 1970.
6. Hudson, W. R., and Kennedy, T. W. An Indirect Tensile Test for Stabilized Materials. Center for Highway Research, University of Texas at Austin, Res. Rept. 98-1, Jan. 1968.
7. Hadley, W. O., Hudson, W. R., Kennedy, T. W., and Anderson, V. L. A Statistical Experiment to Evaluate Tensile Properties of Asphalt-Treated Materials. Proc., AAPT, Vol. 38, 1969.
8. Santucci, L. E., and Schmidt, R. J. The Effect of Asphalt Properties on the Fatigue Resistance of Asphalt Paving Mixtures. Proc., AAPT, Vol. 38, 1969.
9. Kasianchuk, D. A., Monismith, C. L., and Garrison, W. A. Asphalt Concrete Pavement Design—A Subsystem to Consider the Fatigue Mode of Distress. Highway Research Record 291, 1969, pp. 159-172.

ULTRASONIC MODULI OF ASPHALT CONCRETE

Richard W. Stephenson and Phillip G. Manke, Oklahoma State University

There has been a need for a nondestructive, dynamic technique for evaluating certain "elastic" constants of asphalt paving materials. In this study, a method is developed by which the dynamic E-modulus, G-modulus, and Poisson's ratio of compacted asphalt-aggregate specimens are determined from measurement of the propagation velocities of pulsed ultrasonic shear and compressional waves through the test material. This test procedure proved to be easily and rapidly performed on standard Hveem-gyratory specimens. The results obtained compared favorably with those reported by other investigators using different procedures. A brief study of a single asphalt-aggregate mixture, using a variety of asphalt and void contents, resulted in the following observations: (a) An increase in the temperature of the test material resulted in a decrease of the values of both the dynamic E- and G-moduli; (b) maximum moduli occurred at an "optimum" asphalt content for wave transmission of 6 percent; (c) the dynamic Poisson's ratio increased directly with increased asphalt content of the specimens; (d) at temperatures greater than approximately 100 F, Poisson's ratios increased rapidly toward the theoretical maximum of 0.50; and (e) the amount of voids contained in a compacted specimen had only a minor influence on the rate of wave transmission through the specimens at low temperatures, but above 80 F this influence was more pronounced.

•IN an effort to standardize flexible pavement design techniques, researchers have focused on procedures that treat the pavement system as a structural assembly. Because asphalt pavements are treated in this way, the major obstacle to overcome is that of determining the parameters defining the respective material's behavior under load. Although it is recognized that the system is not elastic, elastic theory has been utilized. Strength parameters predicted from various tests that have evolved over the years, in conjunction with modifications of elastic theory, have been used in pavement design.

One problem with using standard methods to determine material constants lies in the fact that most of these tests involve static loading conditions, whereas an in situ pavement is subjected primarily to dynamic loading. Another problem arises from the destructive nature of these tests. A laboratory specimen can be tested only once. This, coupled with the gross nonhomogeneity of the material under study, introduces a large degree of variation from test sample to test sample.

A testing method for road construction materials is needed, which permits the determination of material constants from evaluative procedures that more closely approximate the type of loading and the loading conditions that exist under actual use. This test should be such that a single material sample could be tested many times under varying conditions by using a repetitive or dynamic type of loading technique; i.e., a nondestructive, dynamic test procedure is desired.

In this study, a test technique used by acoustic engineers in their study of more homogeneous materials such as metals, plastics, ceramics, and glass has been applied to asphaltic paving materials. By measuring the propagation velocity of high-frequency sound waves through the material, various material constants can be determined. The advantages of this technique are threefold. First, the test procedure is nondestructive, which enables many measurements to be made on the same specimen. Second, the test

Sponsored by Committee on Mechanical Properties of Bituminous Pavement Mixtures.

procedure is dynamic and more closely corresponds to the type of loading that occurs on the in situ structure. Third, the test is easily and rapidly performed.

The primary objective of this work was to develop a test procedure by which the propagation velocity of both the ultrasonic shear and compressional waves could be directly determined. In support of this development, the ability of the testing technique to reveal the relations of certain dynamic elastic constants (E-modulus, G-modulus, and Poisson's ratio) of a compacted asphalt-aggregate mixture to changes in temperature and asphalt content was examined. The effect of void content on the shear and compressional wave velocity was also studied.

RELATION BETWEEN WAVE VELOCITIES AND MATERIAL PROPERTIES

Measurements of ultrasonic longitudinal wave velocity in asphalt concrete have been made by several investigators (1, 2, 3). However, up to this time, no pulse technique for measuring transverse wave velocities in asphalt concrete has been devised, or at least no reference to such a technique was found in a rather extensive literature review. The need for such procedures has been pointed out in various studies. Measurement of the velocity of the transverse wave through asphalt concrete, in conjunction with similar measurements of the longitudinal wave velocities, would allow the calculation of several important elastic constants that are descriptive of the dynamic nature of the test material. The technique presented in this study should provide the highway engineer with a new means to analyze nondestructively the dynamic behavioral tendencies of asphalt-aggregate mixtures.

The following relations between wave velocities and material constants can be derived from elastic theory for an extended elastic solid (4):

$$G = \rho V_s^2 \tag{1}$$

$$E = 3 - [1/(V_c/V_s)^2 - 1]\,\rho V_s^2 \tag{2}$$

$$\nu = [1 - \tfrac{1}{2}(V_c/V_s)^2]/[1 - (V_c/V_s)^2] \tag{3}$$

where

E = E-modulus,
G = G-modulus,
ν = Poisson's ratio,
V_c = longitudinal wave velocity,
V_s = transverse wave velocity, and
ρ = mass density of the medium.

In this investigation, the technique known as direct transmission was utilized to measure the time of travel of an ultrasonic wave through the test material. This method employs a cathode ray oscilloscope to measure the time lapse between the actuation of the wave source and the detection of the generated wave at a receiver.

EQUIPMENT

Electronic Equipment

The electronic equipment utilized to generate and detect ultrasonic waves consisted of a pulse generator, source and receiver piezoelectric ceramic transducers, and an oscilloscope. The pulse generator delivered a 1,100-Vdc spike pulse at a frequency of 60 Hz to the source transducer by the discharge of a condenser through an RCA 6130 hydrogen thyratron tube. Concurrently with the main voltage spike, the generator actuated a trigger pulse to the horizontal time base of the oscilloscope.

Two sets of transducers were utilized. One set generated primarily shear waves, and the other set generated primarily compressional waves. Both sets were constructed from a composition of lead zirconate titanate (PZT) manufactured by Gulton Industries.

The compressional ceramic discs had a diameter of 1.0 in. and a thickness of 0.25 in. and were poled to be thickness expanders. The resonant frequency for these discs was 308 kc/sec.

The shear mode crystals were constructed as 1.0-in. square plates with a 0.25-in. thickness. The shear plate thickness deformed into a rhombus on excitation such that a shearing action was input into the test material. The resonant frequency of the shear plates was 172 kc/sec.

The cathode ray oscilloscope was a Tectronix Type 545B with a type B wide-band, high gain preamplifier plug-in unit. The instrument had two time-base generators (A and B) with delayed sweep operation ability. Time measurements were made using the delayed sweep operation. This technique allowed time measurements to be made to an error of ±2 division of the delay-time multiplier dial on the oscilloscope. The preamplifier had a vertical deflection sensitivity of 0.005 to 20 V/cm and a horizontal time-base sweep rate of 2 μsec/cm to 1 sec/cm with an accuracy of ±3 percent. The rise time of the preamplifier unit was 18 nsec (18×10^{-12} sec).

Temperature Monitoring Equipment

Internal specimen temperatures were monitored by implanting a thermistor in the material. The thermistor's small size and adaptability to remote readout devices made it ideally suited to the needs of this study. Preliminary work revealed that the temperature gradients between the center and the outer edges of the test specimens were insignificant. This was determined by implanting thermistors at varying depths and locations within the specimen and observing the temperatures as the specimen temperature was varied over the entire testing range. Consequently, it was decided that one thermistor located at middepth and just off center of the specimen would yield sufficiently accurate temperatures. It was also determined that a thermistor placed in this location would not interfere significantly with the transmission of the sound pulse.

The thermistors and display equipment chosen for this work were manufactured by Yellow Springs Instrument Company. They had a working range of -12 to 270 F.

MATERIALS AND SAMPLE PREPARATION

Three different aggregates were utilized in the asphalt concrete. All three (fine sand, coarse sand, and crushed limestone) were obtained from a local hot-mix asphalt plant. The asphalt cement used in this mixture was a 60- to 70-penetration grade steam and vacuum refined material. The material had a specific gravity (at 77 F) of 1.005 and a softening point of 118 F. The aggregates were sized on U. S. standard sieves and then recombined according to the Oklahoma Department of Highways' specifications for a type C surface course mixture (5). The asphalt and aggregate were combined by using standard mixing procedures to produce a uniform mix. Figure 1 shows the combined grading of the aggregate mixture and the type C specification.

The compacted asphalt concrete specimens were 4 in. in diameter and 2 in. high. These Hveem-gyratory specimens were molded by using a motorized gyratory-shear compactor in which the compactive effort is applied by hydraulic pressure and gyration of the compaction mold. This method of compacting test specimens of bituminous mixtures has been standardized by the Texas Highway Department (Test Method Tex-206-F, Part II) (6).

Hveem specimens were made with asphalt contents varying from 4 to 8 percent by total weight of the mixture. Specimens at 5 percent asphalt content were compacted at void contents ranging from 1 to 11 percent by volume. Different densities, i.e., void contents in the compacted specimens, were achieved by varying the compactive effort expended in the molding process.

TESTING PROCEDURE

The inherent nonhomogeneity of asphalt concrete and the high attenuation of ultrasonic waves passing through this material, as well as the self-imposed restriction of testing specimens compacted by standard methods to standard sizes, necessitated techniques

that differed from the standard procedures used with other, more homogeneous materials. The large grain sizes of some of the aggregate in the specimen required longer wave lengths than are usually employed. The scattering caused by the large aggregate grains and the viscous nature of the asphalt binder required a wave of relatively large amplitude to overcome the attenuation tendencies of the material. The longer wave length, in turn, does not allow sharply collimated sound beams as is customary in metal testing. In addition, all three types of wave modes (compression, shear, and surface) are excited regardless of the polarity of the source transducer. This occurs because of the elastic nature of the piezoelectric crystal and the surface irregularities at the transducer-specimen interface. Because of the high attenuation and scatter in the material, identical source and receiver transducers were used. The receiving transducer was placed directly opposite to the source transducer (direct transmission method) on the top and bottom faces of the test specimen (Fig. 2).

The ultrasonic compressional wave travels with a greater velocity than any of the other wave modes. If an ultrasonic wave is input at one face of the test specimen, the first motion detected by the receiver on the diametrically opposite face will be the arrival of the compressional wave. Other wave modes, as well as reflected and refracted compressional waves, will arrive later in time than the original wave traveling a direct path between the two transducers. This is because of their longer path lengths and/or slower characteristic velocities. Figure 2 shows the test setup and the first pulses of different waves. The reception of the direct path longitudinal wave, L_1, is followed by the reception of the transverse wave, T_1, and surface wave, S_1. These waves may be distorted by the reflected and refracted longitudinal waves (L_2, L_3, etc.). The numerous large aggregate grains further complicate the output pattern because of multiple-wave reflections and refractions at their boundaries.

The sample is supported such that the two faces are essentially free; therefore, the primary wave will be reflected at the material-air interfaces. The wave will travel back and forth between the interfaces, arriving at the receiver in odd multiples of the direct path travel time. Reflection continues in this manner until the wave source is shut down and the wave itself is damped to zero amplitude.

Two separate types of wave velocity determinations were made in this study. The first type employed the longitudinally poled transducers to generate a relatively high-amplitude compressional wave and lesser amplitude waves of other modes. The second type of test used the transversely poled transducers to input primarily a shearing mode wave form.

The operation of the test equipment in recording the travel time of the ultrasonic pulse was basically quite simple. The test specimen was placed on a holding device with its bottom face resting on the source transducer, and the receiver transducer was positioned on the top or opposite face of the specimen. The pulse generator activated both the source transducer and the horizontal trace of the oscilloscope simultaneously. When a signal was perceived by the receiver, it generated a small voltage that was preamplified and fed to the vertical plates of the oscilloscope, which caused a vertical deflection of the trace. A measurement of the time lapse between the activiation of the source transducer and the vertical deflection of the trace on the oscilloscope screen yielded the travel time. The velocity of the wave was simply the known specimen height divided by the observed travel time.

Longitudinal Wave Velocity Measurements

Figure 3 shows the oscilloscope trace of a wave transmitted through a 4 percent asphalt concrete specimen using the compressional transducers. The major particle motion occurs in the longitudinal mode due to the crystal polarity; hence, the compressional wave travels through the test material with a relatively large amplitude. Therefore, the receiver, also poled longitudinally, detects the longitudinal wave not only as the initial particle motion but also as a large-amplitude disturbance. By this reasoning, point A on Figure 3 is the point in time when the direct path compressional wave arrives at the receiver, t_{L1}. As previously discussed, the wave reflects between the two parallel surfaces. Consequently, points D and E in Figure 3 correspond to 3 times t_{L1} and 5 times t_{L1} respectively.

Figure 1. Combined aggregate grading chart.

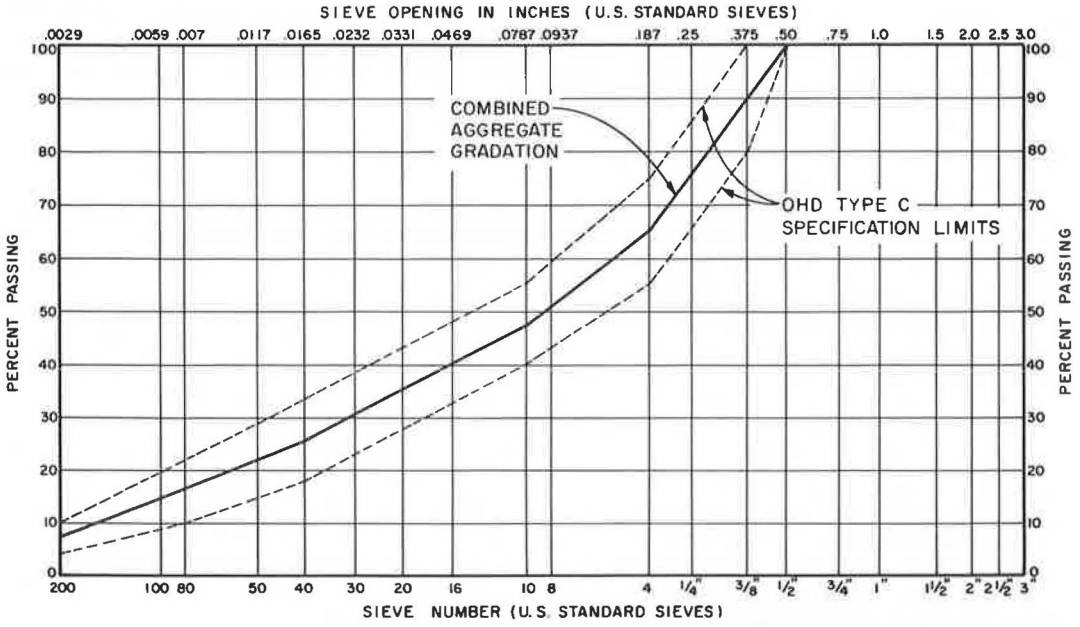

Figure 2. Ultrasonic wave paths and trace indication of their reception.

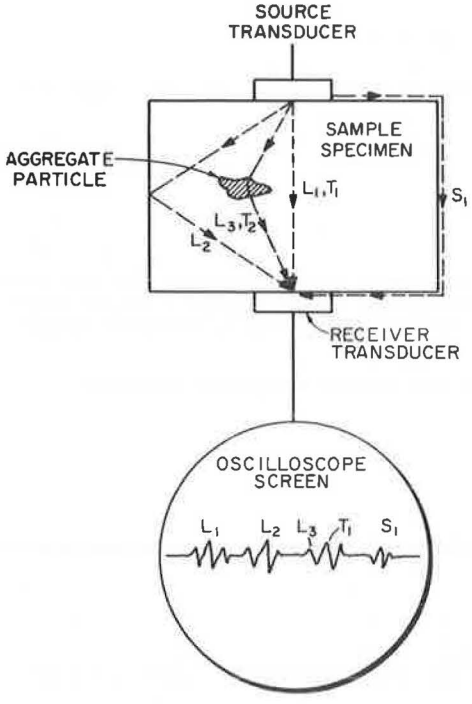

Figure 3. Oscilloscope trace of transverse wave, 4 percent asphalt content specimen.

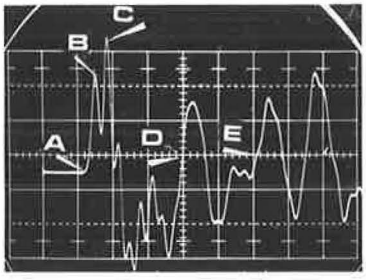

Because of the length of the driving pulse, the source crystal is resonating simultaneously with the longitudinal reflections in the material. This behavior inputs a low-amplitude wave with a frequency approximately equal to the resonant frequency of the crystal. The period of the high-frequency wave as measured from point B to point C (Fig. 3) is approximately 3.3×10^{-6}. This corresponds to a frequency of 303 kc/sec. This frequency agrees well with the calculated resonant frequency for the transducers of 308 kc/sec. During this time, both reflected and refracted waves of different modes, as well as the direct path shear wave, are striking the receiver. However, the arrival of the direct path shear wave was sufficiently masked by the extraneous indications so that it was not definitely distinguishable on the trace.

Transverse Wave Velocity Measurements

Shear wave velocities were more difficult to determine than were the compressional wave velocities. The basic problem in the measurement of shear wave velocity stems from the high attenuation of the shear wave in asphalt concrete, the consequent necessity of inputting a high-amplitude wave, and the difficulty of securing good transducer-test specimen coupling. Therefore, piezoelectric transducers operating in primarily a shear mode were needed to enable generation and detection of the shear wave.

Unlike the compressional wave reception, the first particle motion to arrive at the receiver will not be the same mode as the major input. Although the major input mode is shear, Poisson's effect will also cause small-amplitude compressional waves to be introduced into the specimen. These waves, traveling with a greater velocity, will arrive at the receiver before the larger amplitude shear wave. Other compressional waves, originating through mode conversion as the shear wave impinges on materials having different acoustic impedences, will also arrive ahead of the shear wave. If the original shear wave amplitude is not great enough, its arrival at the receiver will be masked by the other extraneous indications.

Figure 4 shows an oscilloscope trace output from an asphalt concrete specimen tested with the shear transducers. The low-amplitude, high-frequency precursor displayed in the initial portion of the trace is not fully understood at this time. The precursor remained constant throughout the various tests and was not noticeably affected by temperature or the physical makeup of the specimen.

Because the major input wave particle motion occurs transversely and the receiver is poled to be most sensitive to the shearing mode, the direct transmission transverse wave appears on the output trace with a relatively large amplitude. While the direct transmission longitudinal wave precedes in time the arrival of the transverse wave because of its higher characteristic velocity, the amplitude of the longitudinal wave is smaller compared to that of the transverse wave. Point A on the trace (Fig. 4) is considered to be the point in time of the arrival of the longitudinal wave. Peaks B and C define a period of 6.0×10^{-6} sec, corresponding to a frequency of 166 kc/sec. This frequency compares favorably with the resonant frequency of the transducers (172 kc/sec) indicating that these signals are caused by the reasonating of the shear transducers. At first observation, point C appears to be a likely choice for the arrival of the transverse wave. However, it was found that increasing the test specimen temperature resulted in variations in this point. The point in time where the trace crossed the zero axis (point D) was selected to be the time of arrival of the transverse wave (t_{T1}). This point was easily identifiable throughout the testing procedure. To determine if this point actually indicated the transverse wave arrival, we conducted tests on specimens of steel, Lucite, and concrete and compared the results with results published by other investigators. Table 1 shows that the procedure outlined above provided excellent agreement with published results.

Reflection of the transverse wave from the test material-air interface occurred in a manner similar to the reflection of the longitudinal wave. The amplitude of the reflected wave was much reduced because of the attenuation of the shear wave in the test media. Point E in Figure 4 is believed to be the arrival of the first reflected shear wave (3 times t_{T1}).

TEST RESULTS AND DISCUSSION

General

The testing technique employed in this study would be advantageous only if it yielded results indicative of the actual dynamic properties of the material being tested. It was believed that, if test results obtained in the manner previously described were compatible with the expected or predictable behavioral tendencies, and if they were consistent with the results obtained by other investigators using different testing procedures, the usefulness of this technique would be confirmed.

Admittedly, asphalt concrete can be thought of as an elastic material only under certain conditions. Primarily, these conditions are low temperature of the material, where the plastic properties of the matrix are reduced, and low magnitudes of loading. The assumption of homogeneity, also necessary for elastic theory, can be made only in the generalization that the matrix is equally nonhomogeneous in all directions. However, most engineers are so familiar with such material parameters as Poisson's ratio, Young's modulus, and the shear modulus that there does seem to be some value in determining these or similar parameters, i.e., dynamic E-modulus, G-modulus, and Poisson's ratio from wave velocity measurements. Such values should characterize a material and its behavior under varying conditions as well as the more fundamental factors rooted in the classical theory of elasticity.

The effects of variations in temperature and asphalt content on the dynamic E-modulus, G-modulus, and Poisson's ratio in a specific asphalt-aggregate mixture were investigated. The relations between the ultrasonic wave velocities and both the specimen asphalt content and specimen void content were also determined.

Ten specimens, two each with asphalt contents of 4, 5, 6, 7, and 8 percent by total weight, were continuously tested for both ultrasonic compressional wave velocity and ultrasonic shear wave velocity as their temperature was increased from -15 to 160 F. Internal specimen temperatures were monitored via the implanted thermistors, and velocity readings were made at increments of 5 F.

"Elastic" Constants

Plots of E-modulus (psi) and G-modulus (psi) values versus temperature of the respective asphalt content mixtures are shown in Figures 5 and 6 respectively. The values were calculated by using the equations presented earlier. For clarity, the actual data points are not shown, but the uneven nature of the plots indicates a certain amount of scatter in the readings. This data scatter can be attributed to several factors. Nonhomogeneity of the aggregate particle sizes, shape, and orientation in the compacted specimens is, perhaps, the most obvious source of error. Random errors inherent in the measurement procedure, i.e., those related to the instrumentation and those pertaining to operator techniques, could also be responsible for or have some influence on the scatter.

Despite the scatter, specimens at each of the asphalt contents exhibited the same general trend. As shown in the figures, both moduli values decreased with increasing temperature. The rate of decrease in both plots also increased as the specimen temperature was raised. The moduli values increased with asphalt content up to 6 percent. Above this limit the moduli decrease. E-modulus values ranged from a high of 5.03×10^6 psi for the 6 percent asphalt content specimens at -15 F to a low of 0.35×10^6 psi for the 8 percent asphalt content specimen at 160 F. The amount of decrease in the E-modulus values between -15 F and 160 F was in the range of 86 percent. The decrease in E-modulus with temperature was an expected occurrence. Similar findings have been reported by Goetz (1), Kallas and Riley (9), and Kingham and Reseigh (10).

The G-modulus values ranged from a maximum of 1.81×10^6 psi for the 6 percent asphalt content specimen at -15 F to 0.117×10^6 psi for the 8 percent asphalt content specimen at 160 F. The average decrease in G-modulus exhibited by the respective mixtures was approximately 87 percent of the maximum (low-temperature) modulus. As with the E-modulus plots, the G-modulus is a maximum throughout the temperature range for the 6 percent asphalt content mix.

Figure 4. Oscilloscope trace of transverse wave, 6 percent asphalt content specimen.

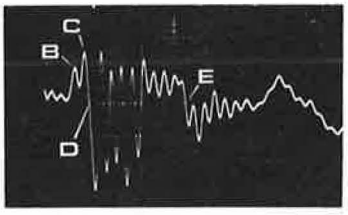

Table 1. Comparison of transverse wave velocity measurements.

Source	Transverse Wave Velocity (fps)		
	Steel	Lucite	Concrete
Krautkramer and Krautkramer (7)	10,600	4,700	7,500[a]
Filipczynski et al. (8)	10,600	3,700	7,000[a]
Stephenson and Manke	9,500	4,200	7,200

[a]The transverse velocity in concrete equals approximately one-half of the published values of longitudinal velocity.

Figure 5. Effect of temperature on E-modulus.

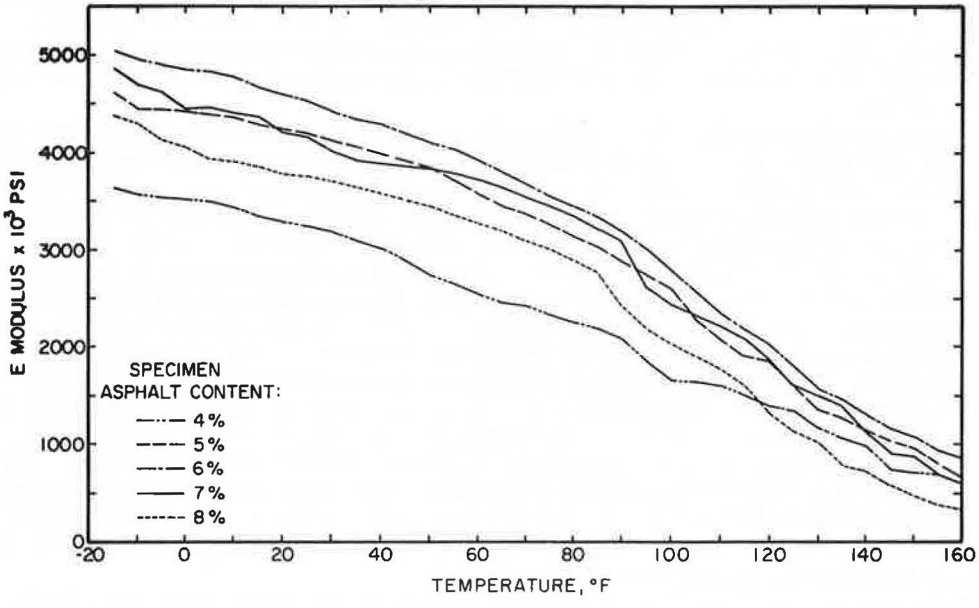

Figure 6. Effect of temperature on G-modulus.

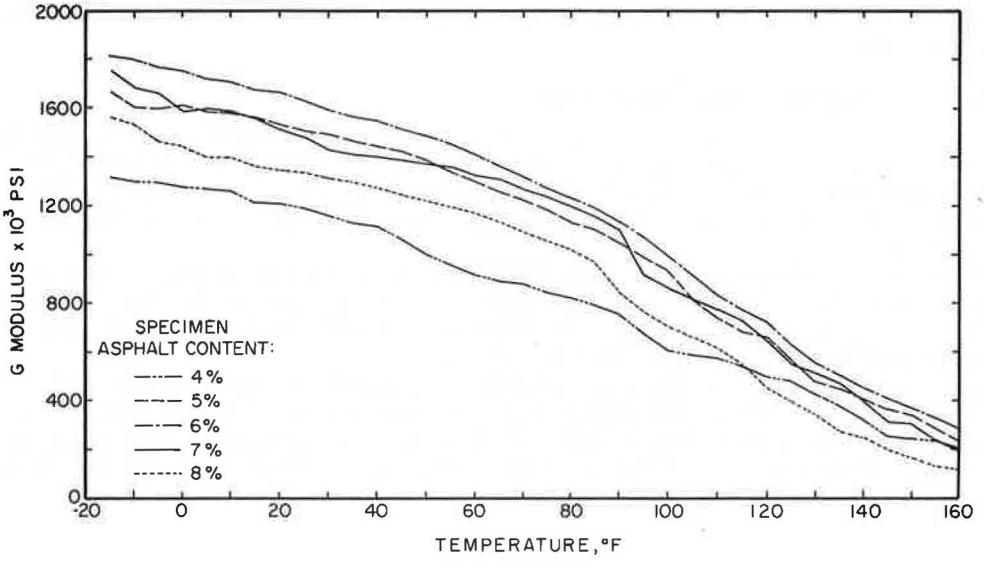

It was expected that at some low temperature the moduli would attain a limiting value. Although the curves do indicate a leveling off at lower temperatures, limitations of the temperature-monitoring equipment prevented examinations below -15 F.

At the other temperature extreme some minimum moduli value was also expected. However, beyond the temperature of 160 F the specimens softened to such an extent that they fractured and spalled during the testing operation. Consequently, velocity measurements and therefore moduli determinations could not be made above this temperature.

Various investigators (9, 11) have demonstrated the relationship of the so-called E-modulus to both the frequency of loading and the loading stress for asphalt concrete material. They have shown that the E-modulus values vary directly with frequency and inversely with loading stress. The values of the E-modulus presented here are in excellent agreement with the sonic modulus values reported by Goetz (1). Monismith et al. (11), using repeated-load compression tests, reported values of the modulus of resilient deformation (E_s) in the range of 8×10^5 psi. Their tests used a deviator stress of 20 to 40 psi; however, a much greater level was used in the ultrasonic technique. Gregg et al. (12), utilizing a triaxial testing method with low-frequency repetition, reported moduli of resilient deformation for bituminous stabilized sand bases in the range of 2.2×10^5 psi.

Because, in this procedure, both moduli are determined from evaluation of the compressional and shear wave velocities, any factor influencing these velocities are mirrored in the moduli values. The behavior of an asphalt-aggregate mixture is complicated by the material deformation characteristics at various temperatures related to the consistency of the asphalt binder. At relatively high temperatures, the mixture may be a highly plastic (tending to viscous) material and at lower temperatures the mixture may be considered as an elastic material. Between these temperature extremes the material will probably exhibit both elastic and plastic characteristics.

Figure 7 is a plot of Poisson's ratio versus temperature for the 5 percent and 8 percent specimens. The behavior is typical of the specimens at other asphalt contents. The plot shows that at low temperatures Poisson's ratio for the 5 percent specimen is approximately 0.385 whereas that for the 8 percent specimen is 0.405. Both values hold reasonably constant until a temperature of between 80 and 100 F is reached. Between 80 and 100 F, Poisson's ratio for both specimens begins to increase rapidly until a value of 0.449 and 0.477 is reached at 160 F for the 5 and 8 percent asphalt content specimens respectively. As would be expected, the ratios at the higher temperatures approach the theoretical maximum ratio of 0.50.

The figure also shows the effect of asphalt content on Poisson's ratio; i.e., Poisson's ratio increased monotonically with increasing asphalt content of the specimens. This further reflects the behavioral dependency of the material on the visoelastic nature of the binder. When the test specimen was heated to the point at which the asphalt binder began to soften, the change in asphalt consistency caused a significant loss of rigidity in the material.

Temperature Effects on Wave Velocities

Figure 8 shows compressional wave traces for a 4 percent asphalt content specimen. It is easily seen in these photographs that the arrival of the initial vertical deflection takes almost twice as long in the hotter specimen than in the colder specimen. The amplitude of the received wave is greatly reduced when the specimen is at the higher temperature.

Figure 9 shows three photographs of shear wave traces for a 6 percent asphalt content specimen. The arrival time of the large-amplitude shear wave is readily seen to increase as temperature increases. Another unique feature is the increased wave amplitude at 90 F in relation to the other two traces.

As temperature is increased, the viscosity of an asphalt cement will decrease. The material characteristics change from a brittle solid to a semisolid and, finally, to a viscous liquid. In an asphalt-aggregate mixture, the films of asphalt surrounding the aggregate particles serve as a binder or cementing agent. As the nature of the films

Figure 7. Effect of temperature on Poisson's ratio.

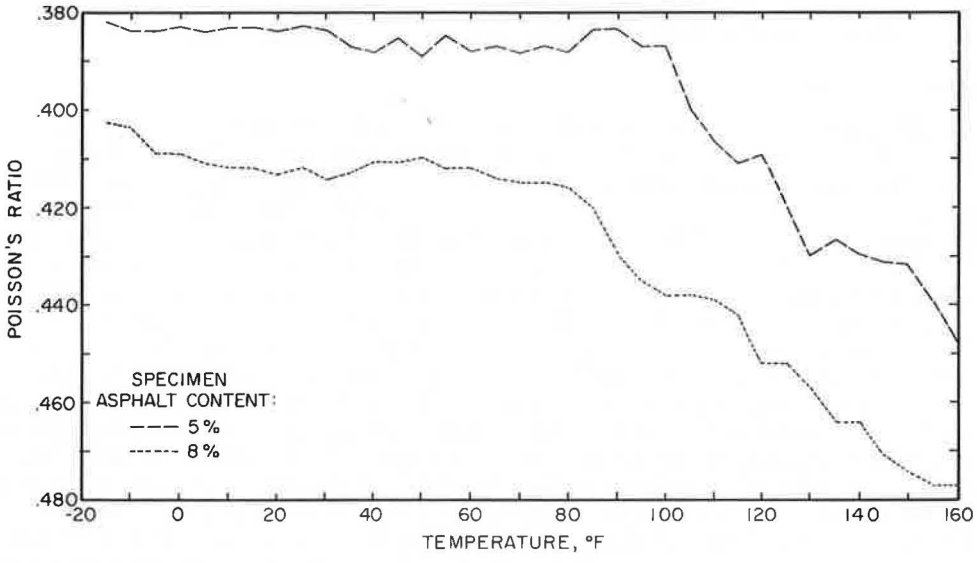

Figure 8. Effect of temperature on longitudinal wave, 4 percent asphalt content specimen.

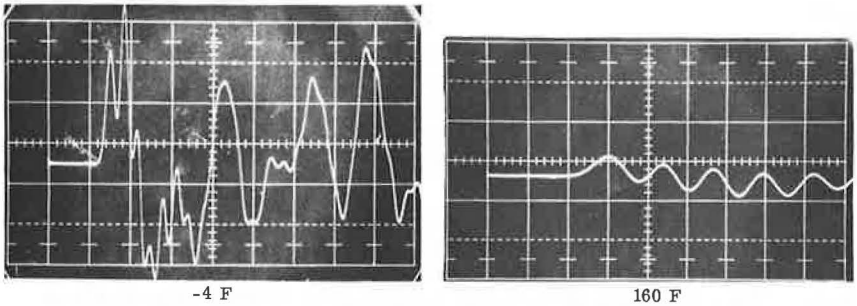

Figure 9. Effect of temperature on transverse wave, 6 percent asphalt content specimen.

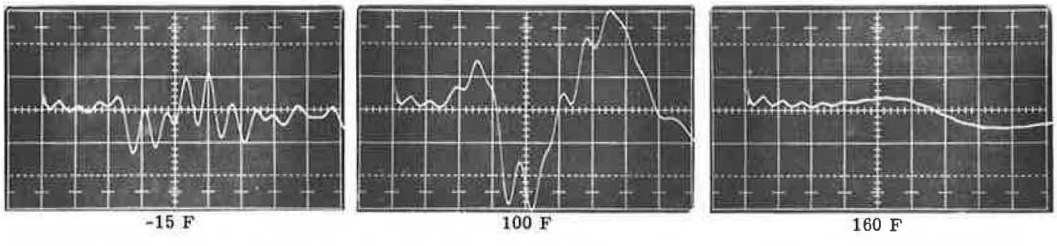

changes with increasing temperature, the aggregate matrix is less tightly bound together; i.e., it becomes less rigid. Consequently, the mixture is unable to transmit the compressional wave at as high a velocity as it can at low temperatures.

Asphalt Content Effects

Figures 10 and 11 show both compressional wave velocity and shear wave velocity versus percentage of asphalt content at temperatures of 0, 80, and 160 F. In all of the plots, the velocities increased with asphalt content up to a limiting value of either 6 or 7 percent. For the aggregate mixture used in this study, optimum asphalt content was 6.2 percent. However, no direct correlation of optimum asphalt content and maximum wave velocity could be made. These curves, although not conclusive for defining optimum asphalt content as determined by a standard test procedure, do give an indication of the percentage of asphalt that yields the best conditions of interparticle contact and minimum path length for the transmission of the wave. In a series of specimens compacted from a design mixture, conditions should exist where there is a sufficient quantity of asphalt cement to achieve optimum particle orientation and reduction of void content so that the pulsed wave can travel from aggregate particle to aggregate particle with only minimal travel distance through the acoustically slower asphalt binder. The use of lesser quantities of the asphalt binder should result in lower densities, increased voids, and more random particle orientation—all of which combine to reduce the velocity of the mechanical wave. Asphalt contents above this "optimum" will tend to force the aggregate particles apart, reduce interparticle contact, and force the wave to travel through the acoustically slower asphalt cement for longer periods. This will increase the travel time of the wave and greatly reduce its velocity.

Void Content Effects

In an attempt to define the relation between the percentage of voids in the test material and the velocity of an ultrasonic wave through it, 15 specimens were compacted by using the Hveem-gyratory technique. The void contents ranging from 0.84 to 11.22 percent by volume were obtained by varying the total compactive effort applied to the specimen. Compressional wave and shear wave velocity measurements were then made at -15 and 80 F.

Figure 12 shows both compressional wave velocity and shear wave velocity versus void content. Although a considerable amount of data scatter is evident, the apparent linear relationship between the variables prompted computation of the linear regression line for the data sets. The low slopes of both the compressional and shear plots at -15 F indicate a negligible effect of the voids contained in the test material on the wave velocities at that temperature. However, the linear regression line slope of both wave types at 80 F was considerably greater than those at the lower temperature. This, of course, indicates that an increase in the amount of voids in a specimen at 80 F caused a decrease in the rates of transmission of the ultrasonic waves through the material.

The data scatter in both the compression and the shear wave tests is probably attributable to the fact that the size of the aggregate particles as well as their orientation in the asphalt-aggregate mixture has a large influence on the rate of transmission of an elastic wave through the material. The aggregate used in the mix had a tip size of ½ in. Orientation of several of these larger particles such that most of the travel path (± 2.0 in.) of the elastic wave was through these particles would result in high velocities. The velocities of waves having travel paths through more of the asphalt cement rather than the aggregate constituent would have slower travel velocities.

Figure 12 shows that the amount of voids in a material specimen at low temperature had little, if any, effect on the rate of transmission of the ultrasonic wave. The increased viscosity of the asphalt binder at these temperatures seems to be a primary influence. At the higher temperatures, where the asphalt viscosity and the asphalt volume are greater, the amount of voids included in the matrix is relatively more important. This indicates that the nature of the binder has a smaller influence on interparticle contact in the more dense specimens than in the less dense specimens. That is, the better aggregate-to-aggregate contact in the denser or more highly compacted material results in a relatively higher rate of transmission of the acoustic wave.

Figure 10. Effect of asphalt content on compressional wave velocity.

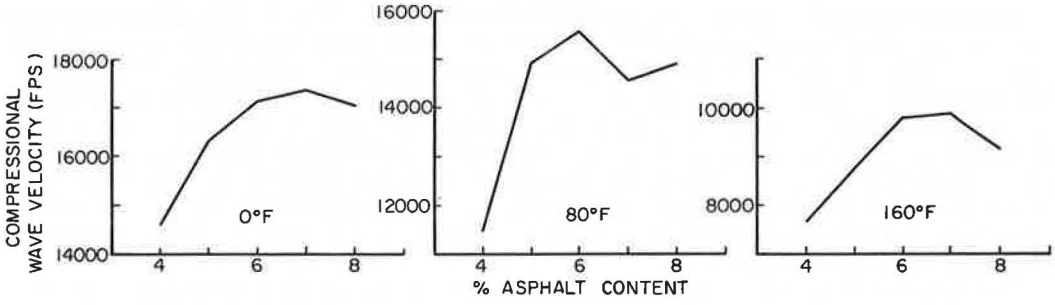

Figure 11. Effect of asphalt content on shear wave velocity.

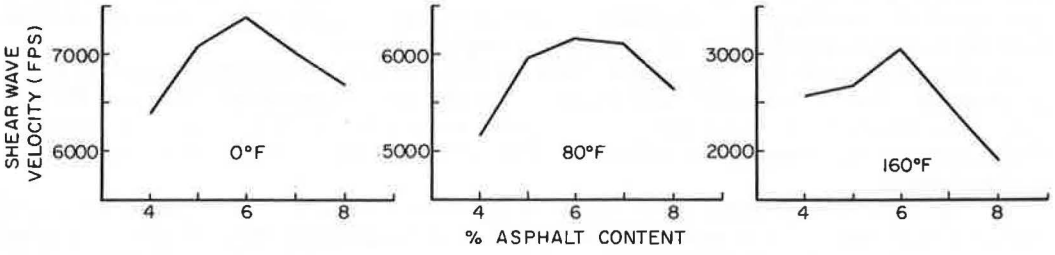

Figure 12. Effect of void content on wave velocities.

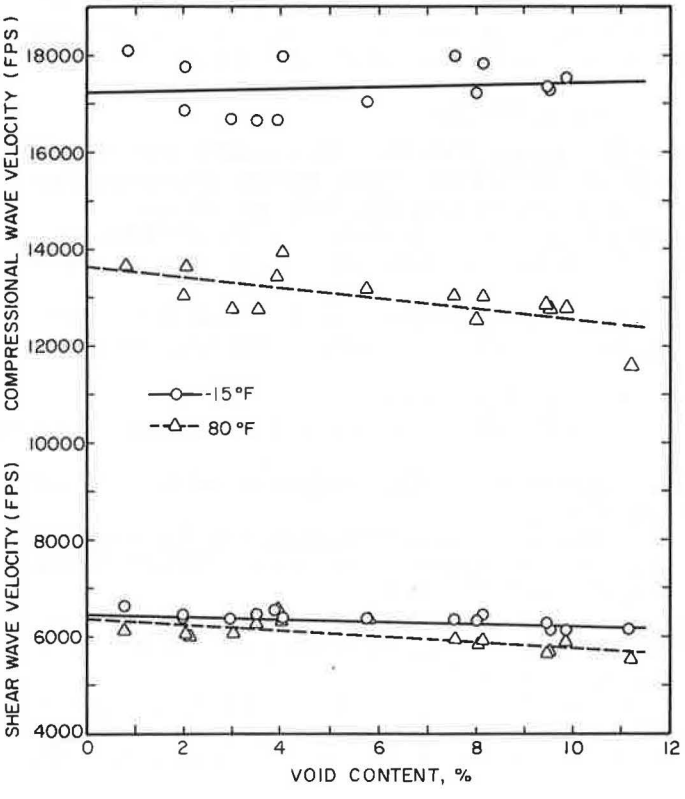

CONCLUSIONS

It can be concluded from these preliminary tests that it is possible to directly measure ultrasonic shear wave velocities through standard-sized specimens of compacted asphalt-aggregate material at temperatures representative of in-service conditions. In addition, the study has demonstrated that ultrasonic testing procedures can yield useful information regarding the dynamic properties of asphalt concrete. This nondestructive testing procedure shows great promise for determining the behavioral characteristics of other types of pavement construction materials as well. The possibility also exists that material parameters determined by this or similar techniques will have some application in the area of design, control, and subsequent in situ evaluation of flexible pavement components.

A brief, nonstatistical study of a single asphalt-aggregate mixture resulted in the following observations concerning the behavior of the material.

1. The temperature of the asphalt-aggregate test material had a great influence on both the dynamic E- and G-moduli calculated from the wave velocity measurements. Both moduli decreased with increasing temperature. The rate of decrease of the moduli increased with increasing temperature. The maximum moduli values were associated with the test specimens containing 6 percent asphalt cement.
2. Poisson's ratio increased monotonically with increasing asphalt content of the specimens. The values were essentially constant until a temperature between 80 and 100 F was reached. Beyond this limit, Poisson's ratio increased to approximately 0.50. This behavior was considered indicative of the influence of the viscous properties of the asphalt binder.
3. Maximum wave velocities occurred in specimens compacted with asphalt contents of 6 and 7 percent. An increase above 7 percent or a decrease below 6 percent asphalt content resulted in reduced velocities throughout the range of test temperatures. Thus, an "optimum" asphalt content for wave transmission existed at or between these limits.
4. At -15 F, the amount of voids contained in a compacted asphalt-aggregate specimen had little or no effect on either the compressional or shear wave velocity. At laboratory temperature (80 F), however, an increase in voids resulted in a decrease in wave velocity. This trend was most evident for the compressional wave.

REFERENCES

1. Goetz, W. H. Sonic Testing of Bituminous Mixtures. Proc. AAPT, Vol. 24, 1955.
2. Manke, P. G., and Gallaway, B. M. Pulse Velocities in Flexible Pavement Construction Materials. Highway Research Record, 131, 1966, pp. 128-153.
3. Stephenson, R. W. Temperature Effects on the Compressional Wave Velocities of Asphalt-Aggregate Mixtures. Oklahoma State University, M. Sc. thesis, July 1968 (unpublished).
4. Kolsky, H. Stress Waves in Solids. Dover Publications, Inc., New York, 1963.
5. Standard Specifications for Highway Construction. Oklahoma Dept. of Highways, 1967.
6. Manual of Testing Procedures. Texas Highway Dept., Vol. 1.
7. Krautkramer, J., and Krautkramer, H. Ultrasonic Testing of Materials. Springer-Verlag, New York, 1969.
8. Filipczynski, L., Pawlowski, Z., and Wehr, J. Ultrasonic Methods of Testing Materials. Butterworth, London, 1966.
9. Kallas, B. F., and Riley, J. C. Mechanical Properties of Asphalt Pavement Materials. Proc. Second Internat. Conf. on Structural Design of Asphalt Pavements, Univ. of Michigan, Ann Arbor, August 7-11, 1967.
10. Kingham, R. I., and Reseigh, T. C. A Field Study of Asphalt-Treated Bases in Colorado. Proc. Second Internat. Conf. on Structural Design of Asphalt Pavements, Univ. of Michigan, Ann Arbor, August 7-11, 1967.
11. Monismith, C. L., Terrel, R. L., and Chan, C. K. Load Transmission Characteristics of Asphalt-Treated Base Courses. Proc. Second Internat. Conf. on Structural Design of Asphalt Pavements, Univ. of Michigan, Ann Arbor, August 7-11, 1967.

12. Gregg, J. S., Dehlen, G. L., and Rigden, P. J. On the Properties, Behavior and Design of Bituminuous Stabilized Sand Bases. Proc. Second Internat. Conf. on Structural Design of Asphalt Pavements, Univ. of Michigan, Ann Arbor, August 7-11, 1967.

A PRACTICAL METHOD FOR MEASURING THE RESILIENT MODULUS OF ASPHALT-TREATED MIXES

R. J. Schmidt, Chevron Research Company

• ONE of the most needed highway engineering developments is a method of designing asphalt pavements, which is theoretically sound and, at the same time, practical. Attainment of this objective now seems feasible with the availability of improved procedures (both 5- and 15-layer programs are available from Chevron Asphalt Company in FORTRAN IV/OS) for the analysis of stresses and deformations in pavement structures using either multilayer elastic (1-5) or finite element design methods (6).

Essential to both the multilayer elastic and the finite element design methods are the various values of the resilient modulus, M_R, and Poisson's ratio, ν, of the materials used in the pavement structure. Test methods currently available to measure the M_R of mixes are practical enough to be used for important projects. However, the methods appear to be too complicated or expensive for routine control or mix design purposes. For these reasons, a need still exists for a method that can give a sufficiently accurate M_R with no more effort or expense than is required by the current Hveem or Marshall methods. This paper describes a method that is rapid and economical and appears adequate for use in pavement structural design calculations. Also, the same specimen can first be used to determine the M_R and subsequently be used to determine other properties such as the Hveem or Marshall stabilities.

THEORETICAL BASIS OF THE TEST

An indirect test for measuring the tensile strength of portland cement concrete (PCC) was described in 1953 by Carniero and Barcellus in Brazil (7) and independently by Akazawa (8) in Japan. In this test, cylinders of PCC were crushed by applying uniformly distributed loads along two opposite generatrices. It was shown by mathematical analyses (9, 10) (assuming plane stress) that a uniform compressive load applied perpendicularly to the horizontal diametral plane of a thin disk gives rise to a uniform tensile stress over the vertical diametral plane containing the applied load. A simplified mathematical treatment was given by Frocht (9) who supported his mathematics by photoelastic analyses of plastic disks.

When this approach is applied to dynamically loaded disks or cylinders, it is possible to determine the elastic modulus of the material. This is accomplished by measuring the elastic deformation across the horizontal diameter resulting from the application of a load along the vertical diameter. An expression (11) for the elastic modulus, E, can be developed as follows.

Frocht (9) gives expressions for the stresses, σ_x and σ_y, across the diameter, d, perpendicular to the applied load, P.

$$\sigma_x = [2P/\pi td\ (d^2 - 4x^2)/(d^2 + 4x^2)]^2$$

$$\sigma_y = -2P/\pi td\ [4d^4/(d^2 + 4x^2)^2 - 1]$$

where t is the thickness of the disks, and x is the distance from the origin along the abscissa. A typical distribution of these stresses is shown in Figure 1 (taken from

Sponsored by Committee on Mechanical Properties of Bituminous Paving Mixtures.

Frocht, 9). If we assume plane stress and elastic behavior, the expression for the strain, ϵ_x, across the diameter is

$$\epsilon_x = 1/E \left[\sigma_x - \nu(\sigma_y + \sigma_z^\circ)\right]$$

where ν is the Poisson's ratio.

By substituting in the preceding expression for σ_x and σ_y, we derive

$$\epsilon_x = 2P/E\pi td \left[(4d^4\nu - 16d^2x^2)/(d^2 + 4x^2)^2 + (1 - \nu)\right]$$

The total deformation is given by integrating the strain between $\pm d/2$:

$$\Delta = \int_{-d/2}^{d/2} \epsilon_x dx$$

where Δ = total deformation across the specimen.

By substituting for ϵ_x and integrating between the limits $\pm d/2$, we derive

$$\Delta = P/tE \left[(4/\pi) + \nu - 1\right]$$

By simplifying and solving for E, we get

$$E = P(\nu + 0.2732)/t\Delta \qquad (1)$$

Thus, if the horizontal deformation across a cylinder resulting from an applied vertical load is known, the modulus of elasticity can be calculated.

For purely elastic materials, Eq. 1 should apply for either static or dynamic loadings. For viscoelastic materials, such as asphalt concrete, Eq. 1 should apply reasonably well if the loading time is short enough so that viscous effects are small. Under short-duration dynamic loads on a viscoelastic material, the apparent Young's modulus, E, is frequently defined as the M_R, the material property useful to multilayer elastic or finite element structural design calculations.

EXPERIMENTAL PROCEDURE

In our procedure, a light pulsating load was applied through a load cell across the vertical diameter of a specimen, which caused a corresponding elastic deformation across its horizontal diameter. This dynamic deformation was measured with sensitive transducers requiring only a few grams of activating force. No appreciable restraining force was applied by the transducers. Air pulses were supplied to the pneumatic cylinder from an electrically activated solenoid or a fluidally operated valve.

The assembly is shown in Figure 2, and details of the equipment and procedures are given in the Appendix. The transducers are mounted directly on the specimen so that they ride with any vertical movement. Also, the twin transducers are additive in effect; consequently, horizontal movements or vibrations are automatically canceled. Output from the transducers and load cell are amplified and recorded on a strip chart recorder. An appropriate oscilloscope can also be used. Figure 3 shows a typical trace obtained on an asphalt concrete specimen loaded at 75-lb peak pulse load.

A load duration of 0.1 sec repeated 20 times a minute was chosen because this loading corresponded to the duration used by a number of investigators (12-21). Their various studies included relating laboratory-measured M_R to field behavior within the framework of multilayer elastic design theory. A load duration of 0.1 sec is about the same duration as is obtained with the Benkleman beam method of measuring pavement deflections. Also, nearly 3-sec pauses between load applications permit substantially complete viscoelastic recovery of the specimen.

Figure 1. Stress distribution.

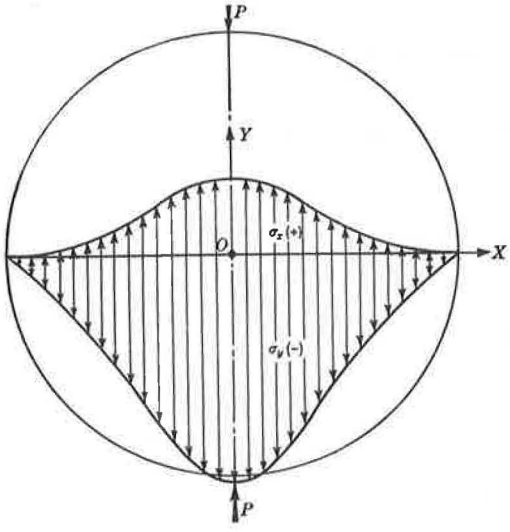

Figure 2. Diametral resilient modulus device.

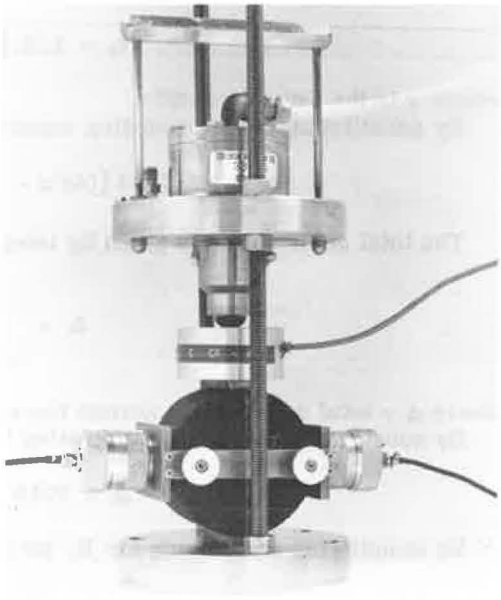

Figure 3. Typical trace of resilient modulus from diametral measurement.

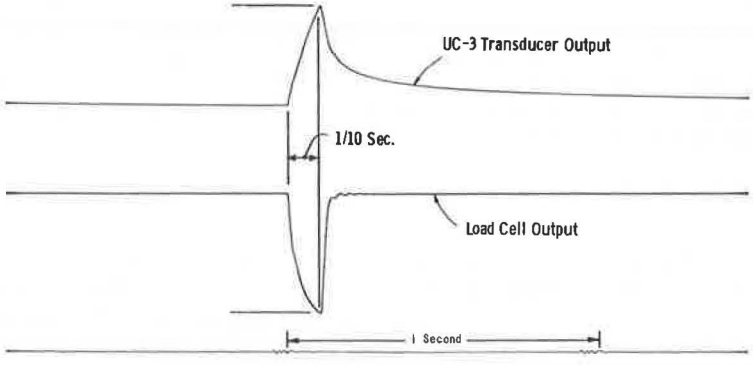

CALCULATION OF M_R FROM DYNAMIC DIAMETRAL MEASUREMENTS

Both the dynamic load, P, and the total deformation, Δ, are taken from recorded traces shown in Figure 3. These values are entered in Eq. 1, where M_R is assumed equal to E.

$$M_R = P(\nu + 0.2732)/t\Delta \quad (2)$$

A range of values for Poisson's ratio can be assumed without excessive error in the calculated M_R. Sayegh (22), using sonic experiments, showed that the ν of asphalt concrete ranges from 0.2 at a strain of 10 μin./in. to 0.5 at strain levels of 300 μin./in. Dehlen (20) demonstrated that the ν for asphalt concrete could vary from 0.35 to 0.5 depending on temperature and deformation. Cragg and Pell (23) found that at room temperature a ν of 0.35 is a reasonable value to assume. As will be shown later, 0.35 for an asphalt concrete gives a reasonable agreement among M_R values as determined by the diametral method when compared with direct tension or compression methods or with flexural methods, which use a temperature of 73 F.

COMPARISON OF M_R VALUES OF POLYMER SPECIMENS USING DIRECT TENSION AND DIAMETRAL METHODS

Both the ν and M_R of three different polymers [Lucite, high molecular weight polyethylene (HMW-PE), and Teflon] were determined by subjecting suitable specimens to 0.1-sec duration repeated direct tensile loads at several levels. The stress on the cross section was monitored by a load cell, while the axial and normal strains were sensed by two pairs of ½-in. strain gauges cemented to opposite sides of the tensile specimens. The M_R values obtained at various stress levels are shown in Figure 4. Poisson's ratios, calculated from the output ratio of strain gauges mounted at right angles to one another, are noted on the figure next to each data point.

Four-in. diameter cylindrical specimens were made from the same block of polymer as were the respective tensile specimens. The M_R of the cylindrical specimens was determined over a range of loadings by using the diametral method previously described. M_R values were calculated from their diametral deformation together with the ν determined on the tensile specimens. M_R values determined by both methods over a range of stress levels are shown in Figure 4. Both the Lucite and the HMW-PE are shown to give nearly identical values by the two methods at the same stress levels. The values for the Teflon agree within about 12 percent.

COMPARISON OF M_R VALUES OF AC SPECIMENS USING DIRECT TENSION, COMPRESSION, AND DIAMETRAL METHODS

Four-in. diameter by 8-in. tall asphalt concrete (AC) specimens were made from Cache Creek gravel and also from crushed Watsonville granite. Both mixes had the gradation shown in Figure 5, curve I. These mixes contained 5 percent by weight of 85- to 100-penetration asphalt and were compacted by the Hveem kneading compactor. After fabrication, two ½-in. wide slices were removed by a diamond saw from the opposite sides of the cylinder. Two-in. long strain gauges were cemented to these freshly sawed surfaces. Also, about ¼ in. of each end of these cylinders was removed; ½-in. thick brass disks were adhered with epoxy cement to the exposed ends of the specimen. The specimens were then subjected to 0.1-sec tensile or compressive pulsating loads having the same characteristics as those shown in Figure 3. The loads were applied through a load cell fastened to the brass disk that had been cemented to the top of the specimen. The brass disk on the bottom of the specimen was bolted to the bottom plate of the loading device. The M_R at various stress levels was calculated directly from the strains shown by the strain gauges cemented to the sides of the specimens and from the loads shown by the load cell.

After testing by this direct method, a 2½-in. thick section was sliced from the center of each specimen. This section included the same area that had been spanned by the strain gauges in the previous tests. The M_R values of the 2½-in. thick, 4-in. diameter slices were then measured by the diametral method previously described.

Figure 4. Comparison of resilient modulus of polymers using direct tension and diametral methods.

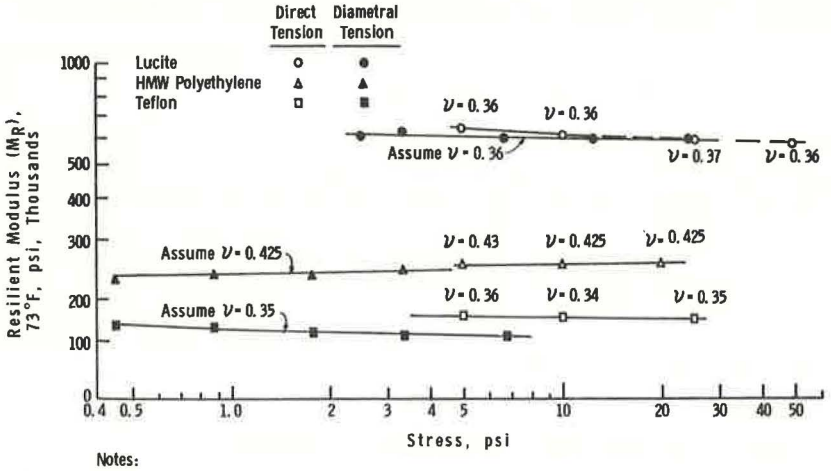

Notes:

1. Diametral tensile stress is average from center to edge, 42.9% of $\sigma_x = 2P/\pi tD$.
2. Poissons ratio, ν, shown on direct tension data points are measured values.

Figure 5. Gradations of aggregates used.

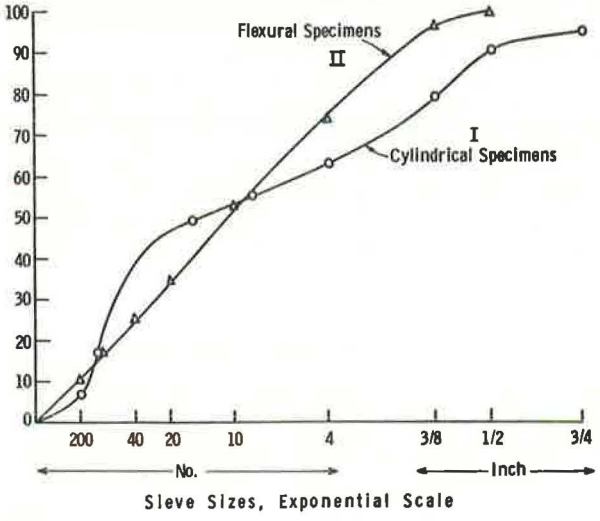

A typical comparison is shown in Figure 6. Both the direct tensile M_R and direct compressive M_R agree quite well over the range of stresses shown. M_R diametrally measured over a similar range of loading is also shown in Figure 6. These latter values were calculated by assuming three different values for ν: 0.2, 0.35, and 0.5. Good agreement is shown in M_R when a value of 0.35 is assumed for ν. Even when the extreme values of 0.2 and 0.5 are assumed, the calculated value varies only about ±25 percent from the value calculated by using a value of 0.35. Similar agreement was found for other asphalt concrete specimens prepared and tested in the same way.

COMPARISON OF M_R VALUES USING DIAMETRAL AND FLEXURAL METHODS

Bar-shaped asphalt concrete specimens, 1½ by 1½ by 15 in. long, were made from Watsonville crushed granite. These mixes were graded according to curve II shown in Figure 5. They contained 6 percent by weight (dry aggregate basis) of 85- to 100-penetration asphalt. The procedure used for preparing these specimens was described by Deacon (17), and the flexural M_R of these specimens was determined over a range of loadings by four-point loading by the method described also by Deacon (16).

At the same time that the flexural specimens were made, 4-in. diameter by 2½-in. thick cylindrical specimens were also made from this same mix. A comparison of the M_R values determined flexurally with those determined diametrally is shown in Figure 7. The stress levels plotted for the diametral samples are the maximum tensile stress existing in the specimen during the test. The stress values plotted on the flexural specimens are the maximum outer fiber stress. Equipment limitations prevented overlapping of the two stress levels obtained in the two methods. The data suggest that, in the case of the flexurally determined values, the outer fiber stress levels are so high that the response is nonlinear. The M_R values indicated by projection of these flexural values to the lower stress levels used in the diametral tests suggest that the agreement between flexurally determined M_R and diametrally determined M_R values is quite good at similar stress levels.

USE OF THE DIAMETRAL RESILIENT MODULUS DEVICE IN MIX DESIGN

Tests, such as the Marshall stability and Hveem stability, are widely used to design asphalt concrete mixes such that the mixes have stabilities adequate to prevent shear failures. These tests are augmented by the Marshall flow and Hveem cohesion tests. These latter tests attempt to prevent design of mixes that have high stabilities at the expense of adequate cohesion. The results of these tests are not necessarily related to the structural value of the mix, although Shook and Kallas (24) found a relation between the Marshall flow-stability ratio and M_R for some mixes. The diametral M_R of an asphalt concrete mix is a value that is directly related to the structural contribution of that layer of mix. The relation is shown by means of the multilayer elastic design or by finite element analysis. To this end, a mix should be designed and optimized for both shear strength and resilient modulus. Ideally, the mix design will also be optimized for fatigue resistance as well. An example of a mix design study on M_R (Fig. 8) shows the effect of the asphalt content on the M_R of the mix. This is the same mix as is shown in Figure 5, curve I. In this particular mix, the optimum plateau for the mix is shown to extend above 7 percent asphalt before it decreases. This test was also demonstrated by Schmidt (25) to be useful in investigating the influence of water on the the M_R.

CONCLUSIONS

A new method is presented for determining the resilient modulus of asphalt-treated mixes. It is low in cost and is more rapid than the currently used routine stability tests. Validity of the method is supported by its reasonable agreement with the M_R values determined by direct M_R tensile measurements on a variety of polymeric samples. Even when a relatively wide range of values is assumed for Poisson's ratio, the diametral method gives M_R values within 25 percent of the values found by direct measure-

Figure 6. Comparison of resilient modulus of AC specimens using direct tension, compression, and diametral methods.

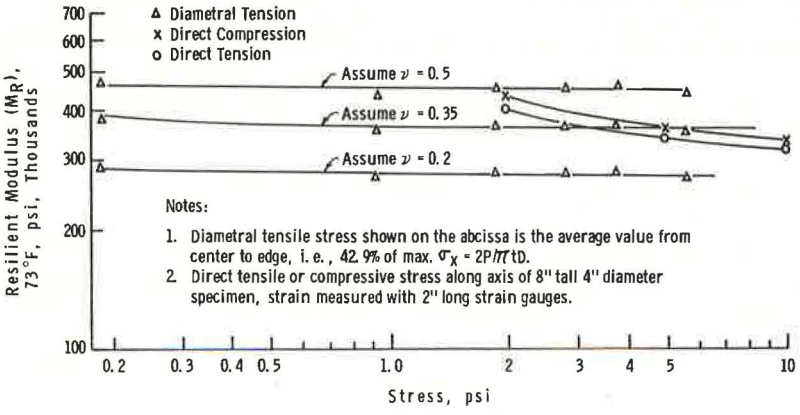

Figure 7. Comparison of resilient modulus using flexural and diametral methods.

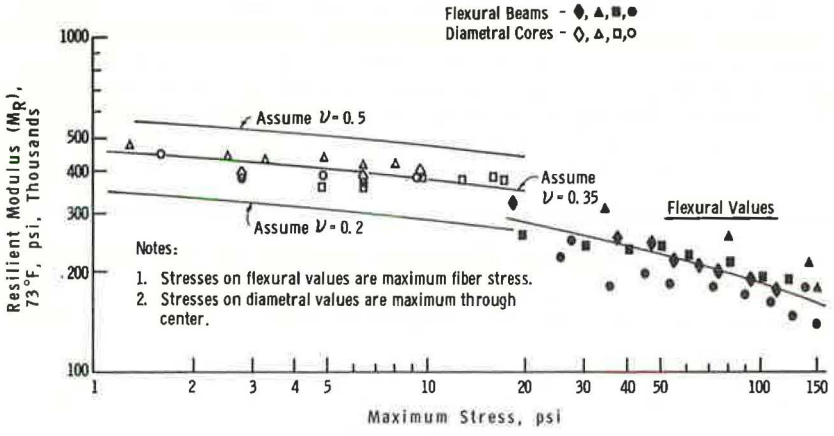

Figure 8. Influence of AC on resilient modulus.

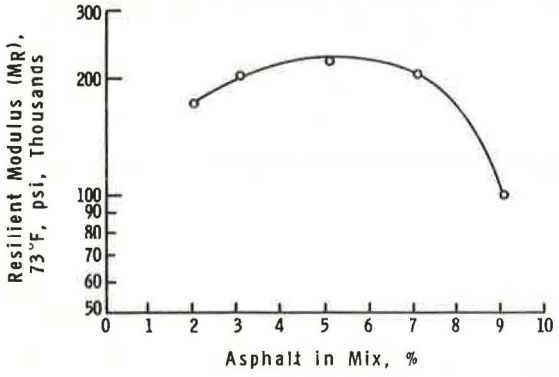

ment of the tensile or compressive M_R on asphalt concrete mixes. M_R values determined flexurally agree almost as well.

The usefulness of the method in designing asphalt-treated mixes for optimum M_R is shown by an example of a mix design relating asphalt content to the M_R.

ACKNOWLEDGMENT

Mathematical development of the expressions for the diametral deformation of disks (Eq. 1) from Frocht's expressions was done by P. H. Merz of the Mathematics Service Group, Chevron Research Company. Design of the transducer housing and the pre-preamplifier was done by V. C. Davis, Electronics Service Group of Chevron Research Company. The aid and consultation of these gentlemen are greatly appreciated by the author.

REFERENCES

1. Burmister, D. M. The Theory of Stresses and Displacements in Layered Systems and Applications to the Design of Airport Runways. HRB Proc., Vol. 23, 1943, pp. 126-144.
2. Fox, L. Road Res. Tech. Paper, No. 9, H.M.S.O., London, 1948.
3. Acum, W. E. A., and Fox, L. Geotechnique, Vol. 2, 1951, p. 293.
4. Warren, H., and Dieckmann, W. L. Chevron Research Company, unpublished rept.
5. Mehta, M. R., and Veletsos, A. S. Civil Eng. Studies, Struct. Res. Series, No. 178, Univ. of Illinois, Urbana, 1959.
6. Preterios, P. C., PhD thesis, Univ. of Calif., 1970.
7. Carniero, F. L. L. B., and Barcellus, A. Union of Testing and Res. Lab. for Materials and Structures, No. 13, 1953.
8. Akazawa, T., Union of Testing and Res. Lab. for Materials and Structures, No. 16, 1953.
9. Frocht, M. M. Photoelasticity, Vol. 2. John Wiley and Sons, New York, 1948.
10. Timoshenko, S., and Goodier, J. N. Theory of Elasticity, 2nd Ed. McGraw-Hill, New York, 1951.
11. Merz, P. H. Chevron Research Mathematics Group, 1971.
12. Monismith, C. L. Rept. TE 66-6, ITTE, Univ. of Calif., Berkeley, 1967.
13. Monismith, C. L., and Deacon, J. A. ASCE Trans. Eng. Jour., 1969, p. 317.
14. Monismith, C. L., Kasianchuk, D. A., and Epps, J. A. Rept. TE 67-4, ITTE, Univ. of Calif., Berkeley, 1967.
15. Vallerga, B. A., Finn, F. N., and Hicks, R. G. Proc. 2nd Internat. Conf. on Struct. Design of Asphalt Pavements, 1967, p. 595.
16. Deacon, J. A., and Monismith, C. L. Laboratory Flexural-Fatigue Testing of Asphalt-Concrete With Emphasis on Compound-Loading Tests. Highway Research Record 158, 1967, pp. 1-31.
17. Deacon, J. A. Univ. of Calif., Berkeley, PhD thesis, 1965.
18. Epps, J. A., and Monismith, C. L. Proc. AAPT, Vol. 38, 1969, p. 423.
19. Epps, J. A. Univ. of Calif., Berkeley, PhD thesis, 1968.
20. Dehlen, G. L. Univ. of Calif., Berkeley, PhD thesis, 1969.
21. Terrel, R. L. Univ. of Calif., Berkeley, PhD thesis, 1967.
22. Sayegh, G. Proc. 2nd Internat. Conf. on Struct. Design of Asphalt Pavements, 1967, p. 743.
23. Cragg, Z., and Pell, P. S. Proc. AAPT, Vol. 40, 1971, p. 126.
24. Shook, J. R., and Kallas, B. F. Proc. AAPT, Vol. 35, 1969, p. 140.
25. Schmidt, R. J. Presented at AAPT, 1972.

APPENDIX

TEST APPARATUS AND PROCEDURE

General Description

Equipment used for determining the M_R on asphalt-treated mixes consists first of a repetitive loading device that applies pulsating loads of 0.1-sec duration every 3 sec. Other pulse durations and frequencies may be preferred. This loading device has a pneumatic piston that operates when a pulse of air is supplied from an electrically timed solenoid valve. Alternatively, a fluidal valve can control the air pulses. Mechanical or electrical magnetic loading can also be used.

The pulsating load is sensed as it is transmitted to the specimen by a 150-lb capacity load cell. The cell is placed between the ram from the pneumatic piston and the loading strip on top of the specimen. Output from the load cell is recorded on a strip recorder. A typical recorder is a Hewlett-Packard Model 7702B coupled to a Hewlett-Packard Preamplifier Model 8805A.

The pulsating load, applied across the vertical diameter, results in a corresponding pulsating deformation across the horizontal diameter of the specimen. This horizontal deformation is sensed by a pair of Statham (UC-3) transducers. The two transducers are mounted in a yoke that is clamped to the specimen. (Fabrication details of the yoke and transducer housing assembly are available from Chevron Research Company as Drawing No. B-12828.) The tips of the transducers barely touch the specimen when operating. A horizontal displacement unbalances the bridges in the transducer strain gauges. A corresponding output voltage is pre-preamplified and fed to the input of a Hewlett-Packard Preamplifier Model 8802A. The circuit for the pre-preamplifier is shown in Figure 9. After amplification, the final output is sent to the second channel of the strip recorder. An appropriate oscilloscope can be used instead of the strip recorder. It is not, however, as convenient to use.

Calibration of the Transducers

Refer to Figure 9. With power switch S_2 on, no load on the transducers, and switch S_1 switched to ground the output of transducer, T_2, adjust R_1 to obtain an approximate zero output across the black and white leads of the ungrounded UC-3 transducer, T_1. Reverse switch S_1, and repeat adjustment with R_2 to obtain zero output from the other transducer, T_2. This adjustment is not critical and usually needs to be done only when new transducers are installed. Connect leads A, B, and D to appropriate Hewlett-Packard Model 8802A Preamplifier input terminals. Adjust and balance the Hewlett-Packard Preamplifier and recorder according to the manufacturer's instructions.

Mount one of the transducers in the calibrating jig shown in Figure 10. Turn the micrometer adjustment until the recorder just barely responds. Then, tighten the micrometer barrel to obtain 0.003-in. movement. (The total range of the transducer is only about 0.0045 in., so make certain that the calibrating movement is within the range of the transducer.) Note change in output of recorder. Repeat this on the second transducer, average the two outputs, and calculate the microinches for each millivolt reading on the Hewlett-Packard Recorder. This is the calibration factor to be used in subsequent calculations. A convenient way to quickly check the stability and proper operation of the transducer-amplifier-recorder combination is to test a 2-in. thick by 4-in. diameter Lucite disk. The M_R of this material is quite stable and, once determined, can be used as a reference.

Sample Insertion and Preliminary Adjustment

Refer to Figure 11. Place the yoke containing both transducers onto holder E; release locknuts A and A′; and retract both transducer housings, B and B′, by sliding them until the tips, C and C′, of the transducers are protected by being withdrawn inside the faces of the yoke. Loosen all four clamping screws, D, and gently insert the 4-in. diameter sample into the center of the yoke. Put sample onto the bottom centering strip, F. Gently tighten all four rubber-faced clamping screws so that the specimen is

Figure 9. Pre-preamplifier circuit for UC-3 transducer.

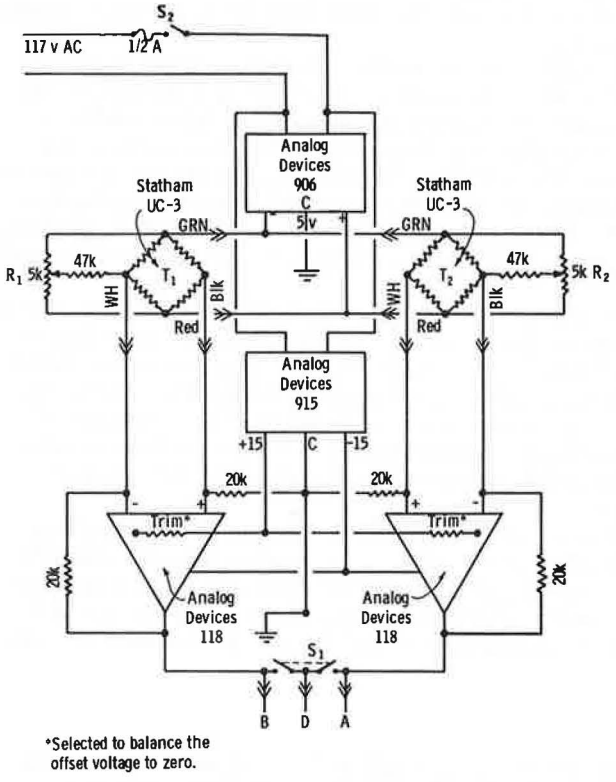

Figure 10. Micrometer and jig for calibrating UC-3 transducers.

Figure 11. Diametral resilient modulus device, yoke and holder.

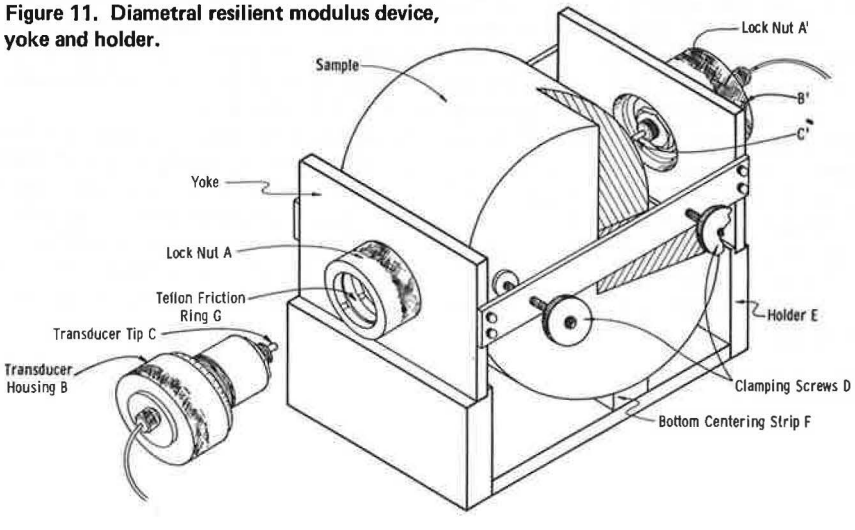

centered and square with respect to the yoke. Remove the specimen and yoke from the holder by lifting the specimen. Do not lift by the yoke. Place into the loading device as shown in Figure 11.

Place the top loading strip on top of the specimen, 180 deg from the bottom loading strip. Place the load cell on top of this top strip, and push shaft from pneumatic piston down until it firmly contacts with load cell.

With locknuts A and A′ loosened, slide transducer housings toward the specimen until the tips are within about 0.005 in. of the specimen. Tighten the locknuts to contract the Teflon friction ring, G, around the micrometer threads on the transducer housing. Set the attenuator on the preamplifier at 50, and advance one of the transducers toward the specimen by rotating the housing. Rotate until the pen on the recorder advances 50 mV (about 200 μin.). Rezero the recorder pen and repeat micrometer adjustment on the second transducer. Both transducers should now be in firm contact with the specimen without having been run in far enough to take up an appreciable part of their range.

In the case of very open mixes or irregular specimens, it may be necessary to form small seating pads on the specimen with plaster of paris. These seating pads may be needed under the clamps, transducer tips, and loading strips. Small $\frac{1}{4}$-in. diameter seat pads can also be fastened to the tips of the transducers to bridge the opening in specimens made from open mixes. Cores cut from pavements with 4-in. diameter diamond drills usually are only about $3\frac{1}{2}$ in. in diameter, in which case it is necessary to shim up the centering strip in the holder until the transducers are aligned across the diameter of the specimen.

It is most convenient to conduct the testing procedure in a constant-temperature room or chamber. However, the transducers can be waterproofed; and the assembly, including the bottom of the repetitive loading device, can be immersed in a constant-temperature water bath. Mixes frequently react with water and rapidly change their M_R. When held in a water bath to obtain temperature equilibrium, they should be placed in sealed plastic bags.

Operation

Turn on the electric timer and the air to the solenoid valve. Adjust air pressure until desired peak loads are indicated by the load cell on the recorder. Adjust preamplifier attenuation switch until the output from the transducers is within range. Operate the system for 100 cycles at low chart speed, at which time switch the chart speed to 100 mm/sec, and record one or more pulses of the load and deformation. Check the load pulse duration for the desired shape and duration. Adjust timer if necessary. Calculate the deformation from the peak pulse output recorded at the fast chart speed. Use the calibrating factor previously established to calculate the M_R.

Remove the specimen and yoke from the repetitive loading device, replace in holder, retract transducers, and rotate the specimen 90 deg. Reset the transducers and repeat the test with the specimen in this position. The two results obtained on the same specimen rotated 90 deg should be within 10 percent. Mixes made from certain aggregates may vary 20 percent. If the differences are greater than these values, rotate the sample to the original position and repeat. If exceptionally large differences are confirmed, then the particular sample is nonisotropic. Report the average M_R value obtained from the two readings.

A LABORATORY AND FIELD STUDY ON THE USE OF ELASTOMERS IN HOT-MIX EMULSIFIED ASPHALTS

Charles R. Gannon, Ashland Oil, Inc.; and
Kamran Majidzadeh, Ohio State University

•ASPHALTIC materials used as paving mixtures are selected with respect to stability and durability design criteria. The stability design criteria require paving mixtures to have sufficient initial stability to withstand the applied traffic loads. The durability design criteria, however, are concerned with the performance of paving mixtures under the traffic and environmental factors to which pavements are exposed during their service lives. Not all paving mixtures fulfill these two design requirements. In recent years, researchers have explored various means of improving qualities of paving mixtures, among which is the use of rubber additives in the asphaltic systems.

Historically many asphalt-rubber pavements have been constructed throughout the world. Various types of latices such as butyl, styrene-butadiene, acrylonitrile butadiene, and neoprene have been used, and different means of incorporating these materials into the hot-mix process have been employed. Two popular methods are (a) rubberizing the asphalt cement before the pug mill and (b) injecting the rubber latex directly into the pug mill.

A test pavement was constructed by using the hot-mix emulsion approach because (a) it has proved very successful, especially in Indiana; (b) latex, commonly anionic, is readily compatible in an anionic asphalt-emulsion system; (c) the homogeneity of the latex asphalt-emulsion and the immediate release of steam when the emulsion contacts the hot aggregate facilitate the coating of the aggregate, ensure complete dispersion throughout the mix, and inhibit thin film oxidation; (d) storage characteristics are excellent; (e) rubberized emulsion is easily pumped at temperatures slightly above ambient; and (f) depolymerization of the rubber can be held to a minimum (thus the maximum effect of the polymer in the mix can be used because of the cooling effect of the steam released from the mix).

A test pavement was constructed at Ashland Chemical's new Carbon Black Plant under construction at Belpre, Ohio. This site was chosen to permit an accurate traffic count of the number of vehicles and the weight per axle load. Traffic control and accurate vehicle weight are difficult to control on a public road (1, 2).

Figure 1 shows the top view and lateral cross section of the test pavement. All of the sections were laid on a prepared subgrade using the Ohio Department of Highways' 402 mix specifications.

Sections A, B, and C were constructed using MS-2h emulsion having an asphalt content of 70 percent. Control section A is without additive. Section B contains 1½ percent by weight and section C 3.0 percent by weight of SBR solids based on the asphalt content of the MS-2h emulsion. The SBR rubber was added in the form of latex. Control section D was constructed with conventional 85- to 100-penetration asphalt cement. The MS-2h emulsion base was identical to the 85- to 100-penetration asphalt cement. Asphalt or rubberized asphalt containing 5.6 percent by weight of SBR solids was used in each of the test sections.

Four-in. core specimens and slab specimens were removed from the pavement immediately after construction and at 1- and 2-year intervals. The rheological, strength,

Sponsored by Committee on Mechanical Properties of Bituminous Paving Mixtures.

and flexural fatigue characteristics of the asphalt-rubber mixtures were compared with control samples without additives at 0, 1, and 2 years to determine their relative durability under traffic loads and changing environmental conditions.

METHOD OF ANALYSIS

To investigate the engineering properties of the paving mixture, we sawed the cylindrical cores obtained from the pavement into samples 4 in. in diameter by 5 in. in length, which were used for compressive strength and compressive creep experiments. In addition, cylindrical specimens 4 in. in diameter and 2½ in. in length were prepared for Marshall stability evaluation. The unconfined compressive strength tests were conducted according to ASTM D 1074-60 at temperatures of 41, 77, 100, and 140 F. For such mixtures, a minimum of three samples were used at each temperature.

The compressive creep experiments were carried out on triplicate samples at 41, 77, 100, and 140 F and at stresses of 12, 6, 2, and 1 psi respectively. The specimens were preconditioned by applying and removing each stress twice. In the third cycle the load was maintained for a period of 1,500 sec during which creep deformation was recorded on a two-channel Sanborn recorder (3, 4).

The Marshall stability experiments were conducted on 4- by 2½-in. specimens according to ASTM D 1559, and the stability and flow were determined at 77, 100, and 140 F (5).

The beam specimens of 1½ by 1½ by 15 in., which were prepared from pavement slabs, were subjected to flexural fatigue and flexural strength measurements. In the flexural fatigue experiments, a deflection of 0.035 in. was imposed on the beams at a rate of 15 cpm, and the stiffness modulus was determined for various cycles of load repetition. The flexural strength tests (modulus of rupture) were conducted according to ASTM C 293-64 (5, 6, 7, 8).

In addition to determining the engineering properties of the pavement cores, we analyzed the asphaltic binder extracted from the pavement. The Immerex Method of extraction (ASTM D 2172) with a solvent system especially developed by Ashland Asphalt Research and the Abson method of recovery (ASTM D 1856) were used in this process. Physical and rheological experiments such as penetration (ASTM D 5), softening point (ASTM D 36), and viscosity were conducted on the extracted binder (5).

ANALYSIS AND DISCUSSION OF RESULTS

Strength Evaluation

To investigate the effect of rubber additives on the strength characteristics of paving mixtures, we used two independent methods of testing in this study: unconfined compressive strength and Marshall stability tests. These tests were conducted on four mixtures at various testing temperatures.

The results of unconfined compressive strength of asphaltic mixtures at 0, 1, and 2 years in service are given in Table 1. The comparison of these experimental data indicates that the phenomena of age-hardening and age-softening have taken place in the paving mixtures. Control mixture D, after 1 year in service, exhibited age-hardening at all test temperatures. Age-hardening is also evident from the strength data of the other three mixtures at 140 F. The decrease in the strength of mixtures A(1), B(1), and C(1) at temperatures of 41, 77, and 100 F after 1 year in service is the evidence of the age-softening phenomenon.

The strength of the paving mixtures after 2 years in service exhibits a somewhat different trend. At 140 F there is a reverse trend of age-softening for the four mixtures studied. At 41 F, the age-softening trend for mixtures A(2), B(2), and C(2) is reversed. A similar reversal of age-softening is apparent for these mixtures at the other test temperatures. The age-hardening trend is continued for material D(2) at temperatures of 41, 77, and 100 F.

The comparison of the Marshall stability data at various test temperatures for materials A, B, C, and D at ages of 0, 1, and 2 years indicates a very similar trend. These data are given in Table 2. It is interesting to note that the percentage of increase

in the Marshall stability of mixture D due to aging is substantially higher than the percentage of change in the other mixtures. The age dependency of the compressive strength and Marshall stability of these four mixtures is indicated by the strength-ratio service-life relations shown in Figures 2, 3, 4, and 5. The similarity between Marshall stability data and compressive strength is quite apparent.

In summary, the observed trend of the variation of mixture strength (compressive strength and Marshall stability) with age indicates that control mixtures D(0), D(1), and D(2) have substantially age hardened. This age-hardening may eventually lead to brittleness and could cause cracking of the pavement. Mixtures B and C, which contain the rubber additives, first exhibit age-softening after 1 year in service and then, in a reversal trend, appear to be approaching initial strength characteristics. That is, for all practical purposes, age-hardening has been retarded in these mixtures. Mixture A (control mixture with 0 percent additive) appears to be exhibiting a continuous trend of age-softening.

Flexural Response

The results of the flexural fatigue experiments conducted on asphaltic beams confirm the previously described phenomena of age-hardening and age-softening. Control mixture D with 85- to 100-penetration asphalt cement exhibits a substantial age-hardening characteristic. On the other hand, mixture A, with 0 percent additive, follows an age-softening trend (Fig. 6). The rubberized mixtures B and C, which exhibited an age-softening after the first year in service, have slightly age hardened in the second year and are approaching the initial flexural fatigue characteristics. However, a comparison of the stiffness modulus as calculated from fatigue equations (Table 3) indicates that mixture C(2), even after 2 years in service, has remained superior to the other mixtures. Mixture B(2), with $1\frac{1}{2}$ percent rubber additive, exhibits better flexural fatigue characteristics than do mixtures A and D. Mixtures A(2) and D(2) appear to have similar characteristics after 2 years in service.

The result of flexural strength as measured by the modulus of rupture indicates that (Fig. 6) the rubberized mixtures B(2) and C(2) are superior to the other mixtures. With respect to age-hardening phenomena, again it is noted that mixture D(2) has substantially age hardened, whereas the relative changes in the other mixtures are negligible.

Rheological Response

In this study, asphaltic specimens were subjected to uniaxial compressive creep experiments at temperatures of 41, 77, 100, and 140 F. The creep stresses were respectively 12, 6, 2, and 1 psi for these temperatures. After two cycles of preconditioning, the deformation of specimens for the third loading cycle was recorded, and the creep compliance J(t), which is strain per unit stress, was determined. Figures 7 and 8 show two typical creep curves after 1 and 2 years in service.

The comparison of creep compliance of four mixtures indicates that, after 1 year in service, age-softening (corresponding to higher creep deformation) has taken place in mixture C(1). Age-hardening, corresponding to the reduction in creep deformation, has occurred in mixture D(1). After 2 years in service, however, the change in the creep compliance of mixtures A(2), B(2), and C(2) is insignificant as compared to the change in the creep compliance of D(2). Mixture D(2) has continued to age harden. This observation is in agreement with the age-hardening and age-softening phenomena discussed previously.

It is well known that rheological behavior of asphaltic mixtures similar to other viscoelastic materials depends on two parameters: time and temperature. In this study, the creep data after 1 year in service were subjected to time-temperature superposition principles, and the temperature-dependent function a_T was determined. The a_T-T relation for four mixtures is shown in Figure 9. Similarly, a typical master curve, developed after superimposing the rheological data, is shown in Figure 10. From the comparison of a_T-T relation for four mixtures, it is apparent that mixture C(1) is the least temperature-dependent material, whereas D(1) is the most dependent.

Figure 1. Test pavement.

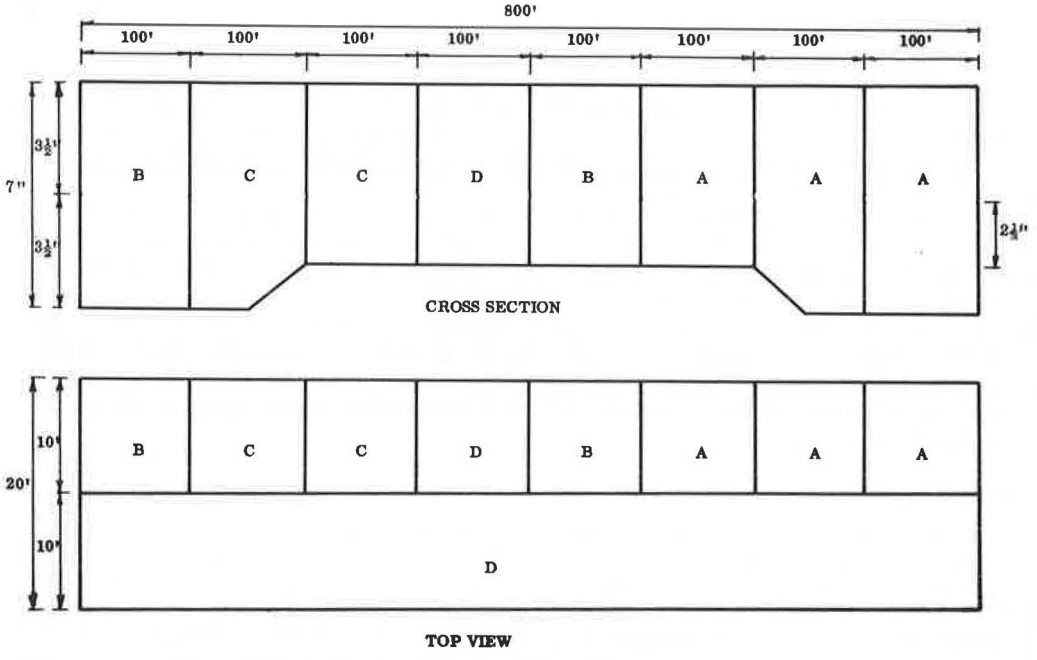

Table 1. Compressive strength of asphaltic mixtures.

Temperature (deg F)	Compressive Strength, psi											
	A(0)	A(1)	A(2)	B(0)	B(1)	B(2)	C(0)	C(1)	C(2)	D(0)	D(1)	D(2)
41	709.8	455	605	710.0	358	480	710.8	334	446	590	755	1,070
77	301	200	191	315.0	182	184	385.7	158	198	230	342	485
100	109.2	120	103	124.7	87.5	64.5	141.7	91	64	57.7	143	141
140	13.7	71.5	21.4	12.0	74.5	18.3	18.3	59.5	19	6.3	83.5	33.4

Table 2. Marshall stability of asphaltic mixtures.

Temperature (deg F)	Marshall Stability, lb											
	A(0)	A(1)	A(2)	B(0)	B(1)	B(2)	C(0)	C(1)	C(2)	D(0)	D(1)	D(2)
77	4,536	4,195	3,544	5,275	3,747	4,300	4,711	4,319	3,825	4,650	6,159	5,800
100	2,566	2,513	2,280	2,555	1,980	1,538	2,589	1,849	2,180	1,597	2,281	2,932
140	518	888	951	353	654	518	671	1,125	651	370	952	851

Figure 2. Age dependency of Marshall stability, mixture C.

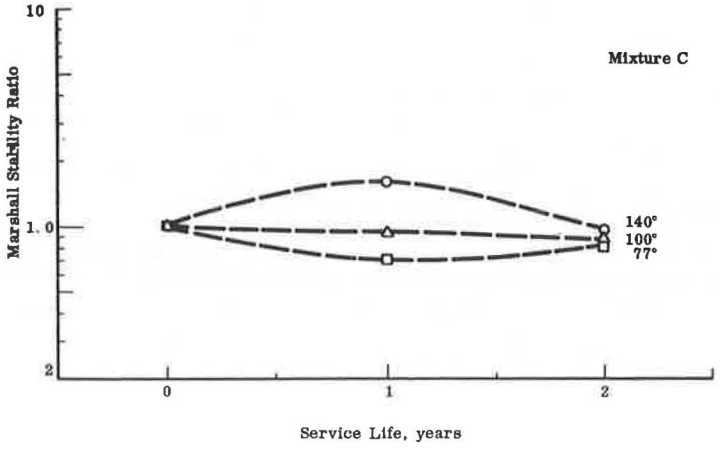

Figure 3. Age dependency of compressive strength, mixture C.

Figure 4. Age dependency of Marshall stability, mixture D.

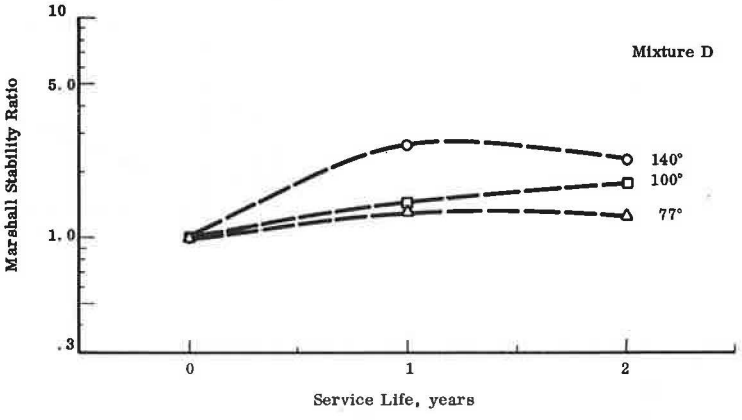

Figure 5. Age dependency of compressive strength, mixture D.

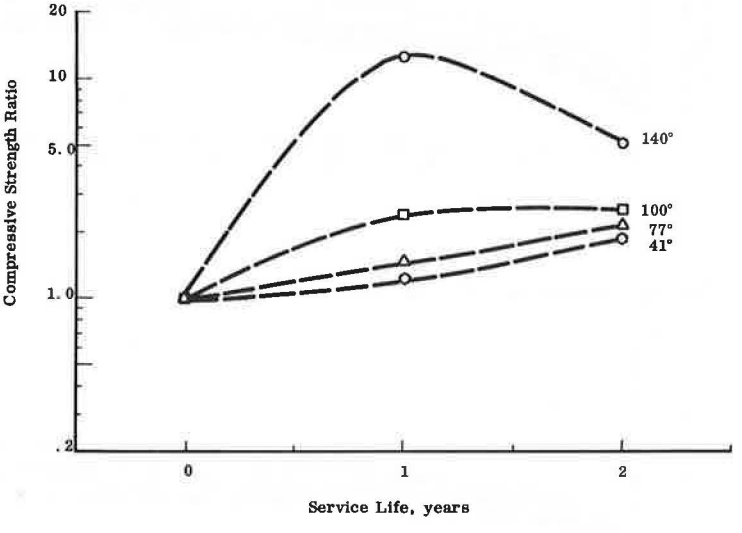

Table 3. Variation of stiffness modulus with age.

	Flexural Fatigue, Stiffness Modulus, psi × 10^3											
Cycles	A(0)	A(1)	A(2)	B(0)	B(1)	B(2)	C(0)	C(1)	C(2)	D(0)	D(1)	D(2)
10	87.7	76.2	72.0	106.6	70.2	94.0	108.2	75.6	96.0	29.7	54.2	67.0
100	72.1	55.2	46.0	85.0	50.0	71.0	91.0	56.5	73.0	24.0	39.5	51.0
1,000	63.7	42.0	37.8	65.3	38.5	54.8	69.1	37.5	51.0	22.5	33.0	39.8
5,000	51.2	33.0	27.0	53.5	32.0	43.5	51.0	28.5	35.5	18.2	28.7	30.0

Figure 6. Flexural fatigue characteristics of mixtures.

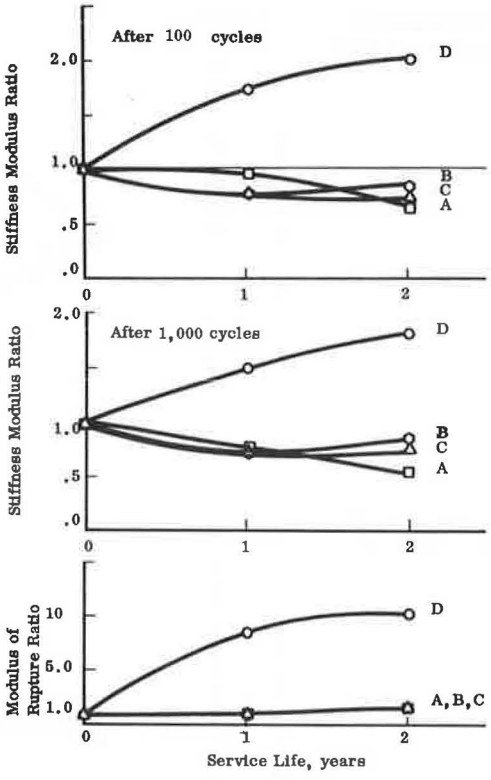

Figure 7. Typical creep curve, mixture 1 year in service.

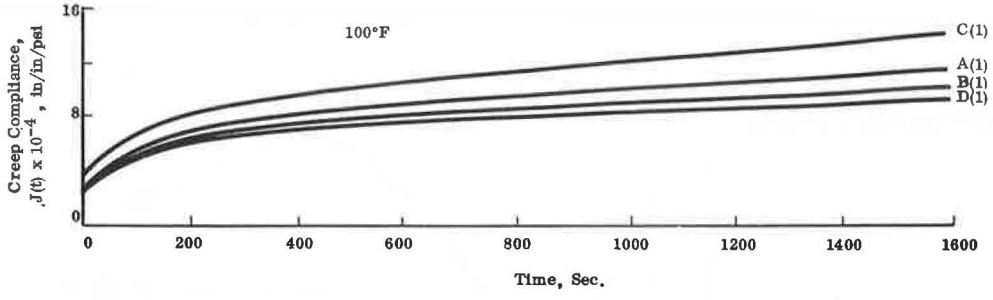

Figure 8. Typical creep curve, mixture 2 years in service.

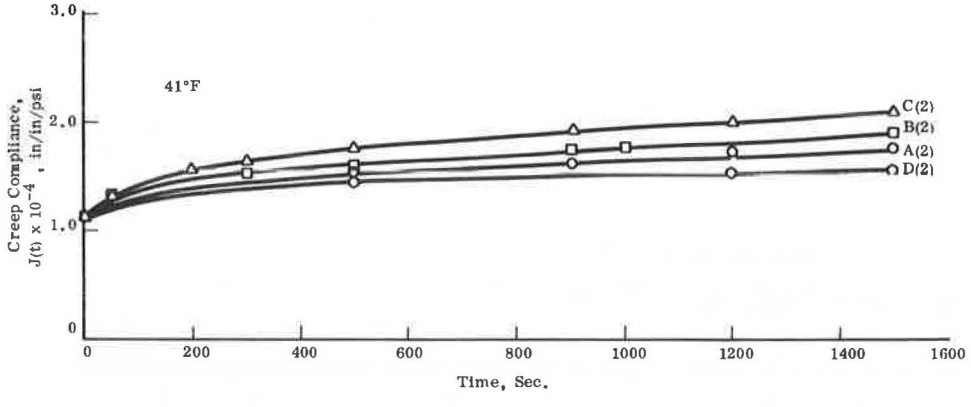

Figure 9. a_T-T relation for four mixtures.

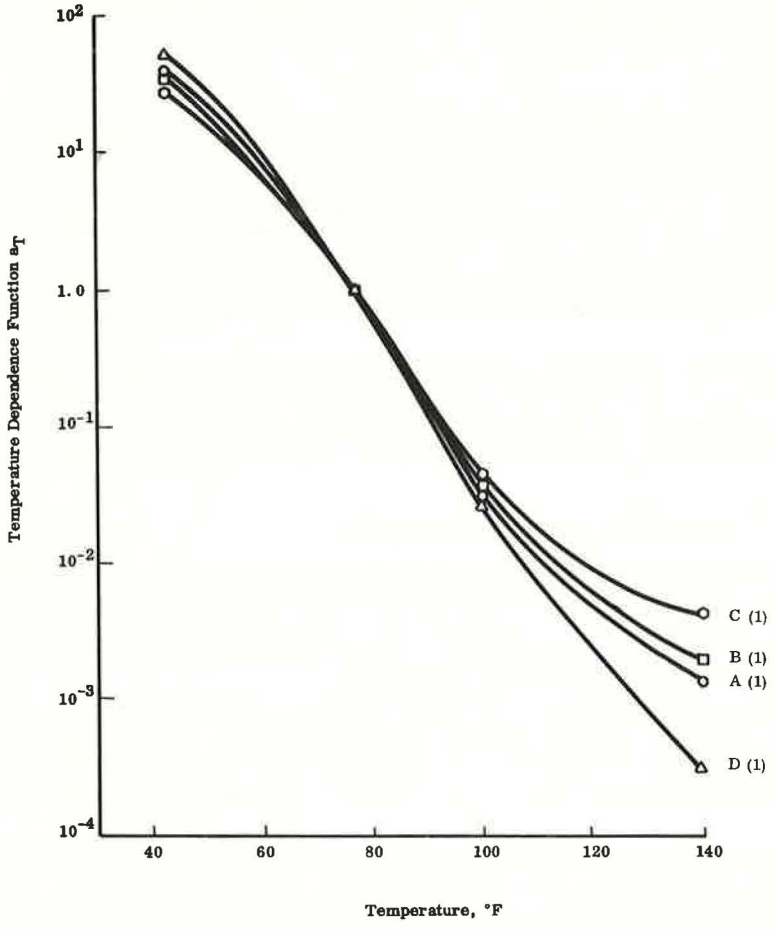

Figure 10. Master curve.

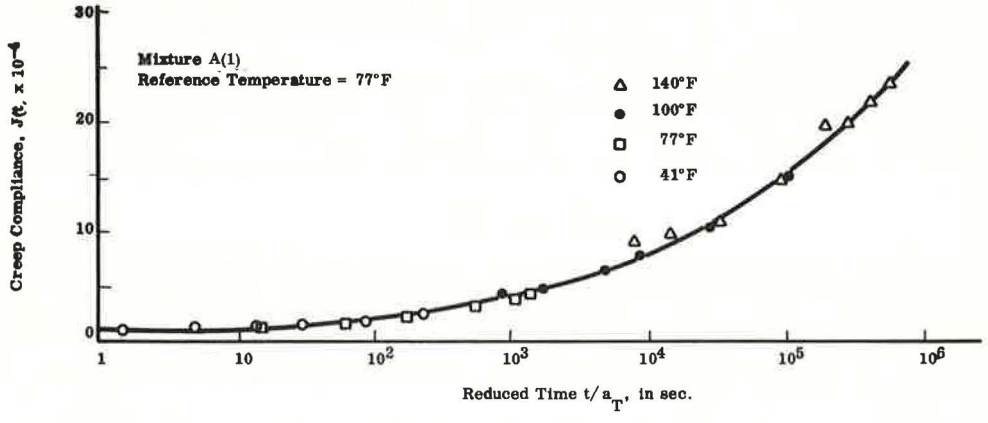

The comparison of creep compliance after 2 years in service at various loading times and test temperatures also indicates that the temperature dependency of mixture C(2) differs from that of the other three mixtures.

Properties of Asphaltic Binder

As was indicated previously, the asphaltic binders, extracted and recovered from the paving mixtures, were subjected to standard physical and rheological experiments. In this report, the results of penetration and softening point tests are examined. It is noted that the softening point of the control mixture D has increased with age, indicating an age-hardening trend. The age-softening trend, however, is observed in the other three mixtures. The greatest softening effect is observed in mixture A(2). The examination of penetration data also indicates that penetration of material is reduced with age, whereas there is a trend for increase in penetration for the other three mixtures.

In brief, the data on physical properties of asphaltic binders such as softening point, penetration, and ductility confirm the previous observations on the strength and rheological behavior of these mixtures. A comparison of viscosity data on extracted asphalts is in progress at the present time and appears to be supporting the previous conclusions.

SUMMARY AND CONCLUSIONS

In this report, the experimental data on four paving mixtures after 0, 1, and 2 years in service are examined. Mixture A is an emulsified hot-mixed asphaltic mixture with 0 percent latex additive. Mixtures B and C are emulsified hot-mixed asphaltic mixtures with 1½ percent and 3 percent rubber additive. An 85- to 100-penetration asphalt cement with no additives was used in the control mixture D.

The significance of rubber additives in the mixture behavior was investigated by performing compressive strength, creep, flexural fatigue, flexural strength, and Marshall stability tests on asphaltic mixtures. The extracted and recovered binders were also treated for physical characteristics. The following are conclusions reached from this study.

1. The evaluation of engineering properties of mixtures at 0 year in service indicates that mixture C with 3 percent additive is superior to the other mixtures.
2. The evaluation of engineering properties after 1 year in service indicates an age-hardening trend for mixture D. Mixtures A, B, and C show slight age-softening effects.
3. The evaluation of engineering properties after 2 years in service indicates that mixture D has continued its age-hardening trend. Mixture A with 0 percent additive follows an age-softening trend. Rubberized materials B and C appear to be approaching their initial engineering characteristics.
4. Mixture C, with 3 percent rubber additive, has remained superior to the other mixtures as related to temperature susceptibility. This mixture is the least temperature susceptible, and mixture D is the most temperature dependent. The superiority of mixture C is also apparent from flexural strength and flexural fatigue data.

REFERENCES

1. Beddoe, G. H. A Proposed Laboratory and Field Study on the Use of Elastomers and Carbon Black in Hot-Mix Emulsified Pavements, Part I. Sept. 1968.
2. Gannon, C. R. A Laboratory and Field Study on the Use of Elastomers in Hot-Mix Emulsified Asphalts, Part II. Dec. 1968.
3. Pagen, C. A. Rheological and Compressive Strength Properties of the Belpre, Ohio, Test Pavement. July 1969.
4. Majidzadeh, K. Rheological and Compressive Strength Properties of the Belpre, Ohio, Test Pavement Field Cores (After 1-Year Service). April 1970.
5. Gannon, C. R. A Laboratory and Field Study on the Use of Elastomers in Hot-Mix Emulsified Asphalts, Part III. Oct. 1969.

6. Deacon, J. A., and Monismith, C. L. Laboratory Flexural-Fatigue Testing of Asphalt-Concrete With Emphasis on Compound-Loading Tests. Highway Research Record 158, 1967, pp. 1-31.
7. Deacon, J. A. Fatigue of Asphalt Concrete. Univ. of California, D.Eng. thesis, 1965.
8. Kallas, B. F., and Riley, J. C. Mechanical Properties of Asphalt Pavement Materials. The Asphalt Institute, Res. Rept. 67-1, Jan. 1967.

INFLUENCE OF AGGREGATE SHAPE ON ENGINEERING PROPERTIES OF ASPHALTIC PAVING MIXTURES

M. Livneh and J. Greenstein, Bruner Institute of Transportation, Haifa, Israel

The following properties characterize flaky aggregates as opposed to cubical aggregates: (a) tendency to stratify (lowest energy level), (b) low compactibility, (c) larger specific surface area for the same fraction, and (d) higher breakage value (lower moment of inertia). These properties may be expected to produce the following characteristics in asphaltic mixtures: (a) weakness planes, which favor a low load-carrying capacity and strength anisotropy; (b) low density; (c) high optimal bitumen content; and (d) high breakage value, which distorts the original grading and causes the formation of voids free of bitumen or fines, thereby reducing the load-carrying capacity still further. The subject was investigated with the aid of a literature survey on the influence of aggregate sphericity on the engineering properties of asphaltic mixtures and laboratory tests designed to give a reliable picture of aggregate behavior in pavements. The influence of aggregate sphericity in the extreme cases of asphaltic mixtures is characterized by dense and open gradings, i.e., a solid mass and minimum void percentage respectively. The conclusion, which occasionally contradicts the findings of others, is that flaky aggregates (specifically the hard, crushed type used in laboratory studies) may be regarded as a conventional material from the engineering viewpoint, i.e., that they may be used for producing asphaltic mixtures.

•QUARRY aggregates frequently contain a high proportion of noncubical material, mainly as a result of the mineralogical composition of the rock and the type of quarrying equipment. The use of these aggregates in asphaltic paving mixtures is somewhat problematic. The uncertainty over this is reflected in the discrepancies between the various standard specifications and the results of various studies.

A comprehensive, up-to-date survey (1) established that "aggregate shape is discussed in literature primarily in terms of differences between natural aggregates (gravels and sands) and crushed aggregates (crushed gravel or crushed stone)." Crushed material has a higher angularity and roughness than does natural aggregate; therefore, the sphericity of the aggregate (proximity of the particle to the sphere or cube) is not eliminated when comparing the engineering properties of mixtures consisting of both types. Studies on such asphaltic mixtures are found in the literature (2-12). A quantitative study that can claim to have eliminated sphericity was conducted by Li and Kett (13), which consisted of Marshall and Hveem tests on specimens made with dense-graded aggregate and covered a wide range of sphericity. The conclusions of this study were as follows: (a) Shapes with a/c > 3 (Appendix, Fig. 21) are critical; and (b) the maximum proportion of critically shaped flaky material that may be used without detriment to stability is about 40 percent. The latter conclusion is controversial because the obtained stability values of both cubical and flaky aggregates are far above the accepted level. Moreover, when using unconventional materials, the tests performed serve as partial criteria for field conditions.

Sponsored by Committee on Characteristics of Aggregates and Fillers for Bituminous Construction.

STUDY OBJECTIVE

In order to reach engineering conclusions concerning the use of flaky aggregates for the preparation of asphaltic mixtures, we compared, under actual road condition and in conjunction with a series of laboratory tests, the engineering properties of flaky aggregates with those of cubical aggregates (routine particles). The scope of this paper is confined to laboratory tests whose object was to approximate actual road conditions.

Flaky aggregates may be attributed with the following properties as compared with cubical aggregates: (a) tendency to stratify (lowest energy level), (b) low compactibility, (c) larger specific surface area for the same fraction, and (d) a higher breakage value (lower moment of inertia).

The preceding properties may be expected to produce the following characteristics in aggregate mixtures: (a) weakness planes, which favor a low load-carrying capacity and strength anisotropy; (b) low density; (c) high optimal bitumen content; and (d) high breakage value, which distorts the original grading and results in the formation of voids free of bitumen or fines, thereby reducing the load-carrying capacity still further.

Some of the preceding properties have been found in the single-sized flaky aggregate. For example, findings given elsewhere (14, 15) demonstrate that flaky aggregates have a higher void percentage (low compactibility) than similar mixtures containing cubical aggregates.

In asphaltic mixtures, the grading may tend to mask or eliminate the properties of the flaky aggregate. Stratification is likely to be prevented, interparticle contact intensified, and breakage reduced. In addition, the overall surface area of the aggregate is likely to be increased so that variation due to shape would be negligible. Insofar as these assumptions are confirmed in practice, flakiness does not disqualify the aggregate as a conventional ingredient for asphaltic mixtures.

In this study, two gradings were investigated: (a) dense grading, percentage passing $^3/_4$ in., 100 percent; No. 4, 61 percent; and No. 200, 6.5 percent; and (b) open grading, percentage passing $^3/_4$ in., 100 percent; No. 4, 28 percent; and No. 200, 2 percent. These gradings represent the two extreme cases of the influence of sphericity. The study consisted of a series of laboratory tests designed to give a reliable picture of flaky aggregate behavior in road pavements.

The study objective necessitates a knowledge of the following.

1. Marshall test: The influence of aggregate shape on the rates of stability and flow is measured in the Marshall tests. This is a routine test that enables one to determine strength indexes (stability and flow) for the design of asphaltic mixtures. However, because this test does not enable one to determine all the properties of aggregates under road conditions, the influence of aggregate shape on the engineering properties of asphaltic mixtures was investigated with the aid of the following laboratory tests.
2. Triaxial shear test: In this test, part of the specimens were compacted parallel to the direction of the maximum principal stress σ_1 and the other part perpendicular to this direction. The results of this test enable one to determine the following: (a) the load-carrying capacity under conditions simulating the wheel load on the road surface (namely, compacting parallel to the maximum principal stress); (b) the cohesion coefficient and the internal angle of friction, which is a representative parameter of the aggregate matrix (3); and (c) the influence of shape on anisotropic properties.
3. Moving-wheel test: This test enables one to determine the influence of shape on the grooving effect and is the most approximate to actual road conditions. It is carried out by means of a wheel traveling on an asphaltic concrete slab on a single track at a specified load and number of cycles. It provides information mostly on the fatigue and on horizontal surface resistance.
4. Breakage value test: Flaky aggregates have poorer mechanical properties than do cubical aggregates of the same category (Appendix). Therefore, a higher breaking percentage may be expected in asphaltic mixtures containing flaky aggregates. This breakage favors the formation of voids free of bitumen and fine, which causes the specimen to weaken. The breakage value and its influence on the mechanical properties of asphaltic mixtures were investigated on specimens compacted by common laboratory methods—dynamic compaction (Marshall), kneading compaction, and static compaction

(triaxial shear and moving wheel)—and with the aid of a moving steel wheel. The latter method is the most approximate to road conditions.

5. Splitting test: The load-carrying capacity of asphaltic mixtures is governed, among other things, by its ability to withstand tensile stresses. Because the air pockets that form as a result of breakage of the aggregates are liable to decrease the tensile strength, the splitting test is used to determine this property.

6. Weight-volume ratio test: Standards and specifications establish definite values of void percentage in asphaltic mixtures. A high void percentage may give rise to oxidation of the bitumen, and a low void percentage may cause it to rise to the surface. For this reason, it is important to investigate the influence of shape on the compactibility of asphaltic mixtures. This property was tested by using various compaction methods (dynamic, kneading, and static) to eliminate the effect of the mode of compaction. Another reason for employing several methods was to investigate the possibility of arranging the flaky particles in a stratification pattern. Theoretically, such a pattern would produce higher densification rates in asphaltic mixtures containing flaky particles.

ASPHALT TESTS

Marshall Test

Specimens were compacted with 50 blows on each side. The test results (Marshall stability and flow versus bitumen content, shape being the parameter) are shown in Figures 1 and 2. The bitumen content throughout this paper refers to the weight of the aggregates. For dense grading, Figure 2 shows that flaky particles produce a somewhat lower Marshall stability (15 to 20 percent), but the absolute value for both shapes is higher than normal. The latter is due to the extra hardness of the aggregate in question (Appendix). Figure 1 also shows that sphericity does not influence flow values.

In the case of open grading, Figure 1 shows that the stability of specimens containing flaky aggregates is 500 to 600 lb (about 55 percent) lower than specimens containing cubical aggregates and that sphericity has no influence on the flow values. The decrease of stability values in specimens containing flaky aggregates is mainly attributable to the considerably higher breakage of these particles as compared with cubical particles and, to a negligible extent, to their shape.

As for optimal bitumen content, Figures 1 and 2 show that, in both dense and open gradings, the particle shape has no influence on this property. From this, the following may be concluded: (a) An increase in specific surface area is negligible in comparison with the specific surface area of the total mass of the particles (particularly of the fine fraction), and (b) the optimal bitumen content is not increased by the breakage of the aggregates because of the relatively insignificant increase in specific surface area of the aggregates. As is known, even a greater increase in the specific surface area of the aggregates brings about a relatively small increase in the optimal bitumen content as shown in Figure 3 (16).

It should be noted that a decrease in the difference between the breakage percentages of cubical and flaky particles will decrease the difference between stability values: dense grading, from 600 lb (about 20 percent) to 150 lb (10 to 15 percent); and open grading, from 500 lb (about 55 percent) to 180 lb (about 35 percent) (Fig. 4). In the case of open grading, if identical densities are used as a basis of comparison, the stability values of specimens containing cubical aggregates are similar to the values of specimens containing flaky aggregates (Fig. 5). This result may be attributed to the somewhat low compactibility of the flaky particles as compared with that of the cubical particles in this grading. Therefore, to achieve identical densities, we used a higher compaction energy in specimens containing flaky aggregates. This additional energy compensates for the decrease in the stability values resulting from the greater breakage of these particles.

The results prove that in dense mixtures the flaky particles are prevented from assuming a stratification pattern perpendicular to the direction of compaction (lowest energy level) as a result of laboratory compaction techniques. This is confirmed by the data shown in Figure 6 (dense grading), which shows that the orientation angle is

Figure 1. Marshall stability versus bitumen content, dynamic compaction.

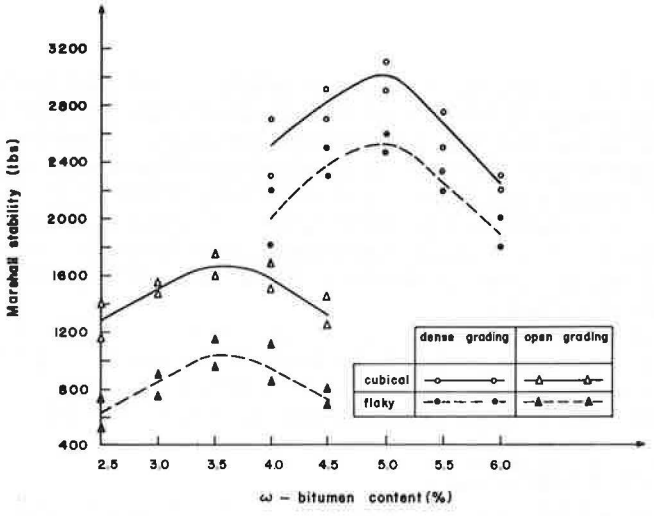

Figure 2. Marshall flow versus bitumen content, dynamic compaction.

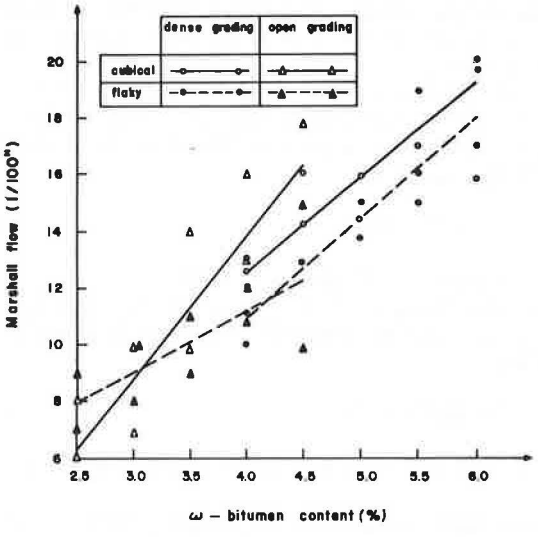

Figure 3. Optimal bitumen content versus specific surface area.

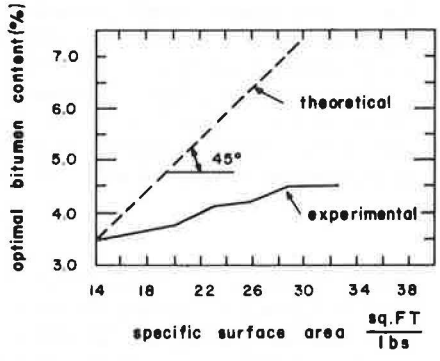

Figure 4. Marshall stability versus compaction energy.

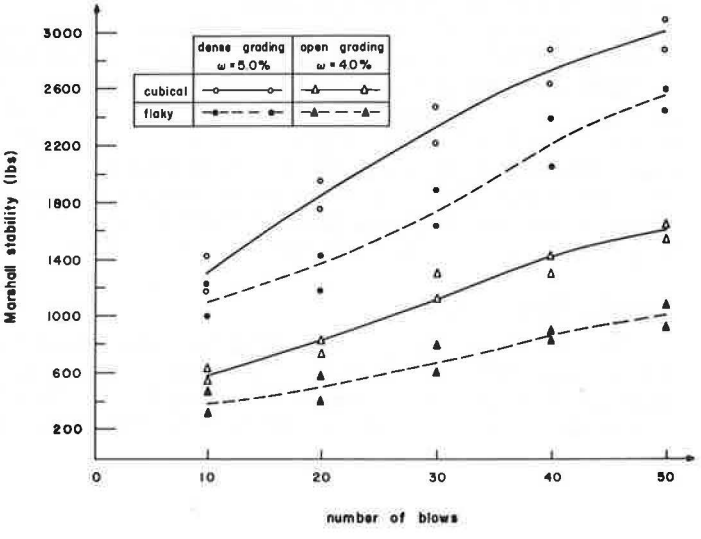

less than 45 deg (the axis of symmetry with respect to the perpendicular) but is still large enough to prevent the formation of weakness planes. This finding does not conform to the observations of Puzinauskas (5). As for the influence of sphericity, he concluded that elongated or flattened particles accentuate the anisotropy as compared with rounded particles. In other words, the structure index (load-carrying capacity ratio of parallel and perpendicularly compacted variants) is higher in the former case. However, Puzinauskas' conclusions were based on a comparison of crushed aggregate with natural gravel; therefore, it may be stated that the sphericity factor in this case was not isolated.

In conclusion, the Marshall test results indicate that the stability of the flaky specimens for dense grading is higher than is usual for asphaltic mixtures. This result was obtained with flaky aggregates corresponding to the B.S. classification of "100 percent flaky," which has a high crushing value of 31 percent for the fraction of -½ in. +⅜ in.

Triaxial Shear Test

Dense Grading—The tests were carried out on statically compacted 4- by 8-in. specimens having a uniform bitumen content of 5 percent by weight (which is optimal according to the Marshall stability test). Part of the specimens were compacted parallel to the direction of loading (double-plunger method) and the other part perpendicular to this direction. The test was immediately preceded by immersion in water at 60 C for ½ hour and was carried out at the same temperature. The basis used for comparing compressive strengths—equal density—is justified in the case of dense grading because of the similar compactibility of both shapes.

As can be seen from Figures 7 and 8, the sphericity influences neither the deviatoric stress, regardless of the direction of loading, nor the anisotropy. The implication of the relation between the deviatoric and lateral stresses as shown in the figures is an isotropic internal angle of friction Φ (18), given by

$$\sin \Phi = \tan\gamma/(\tan\gamma + 2) \quad (1)$$

where γ denotes the slope of the straight line shown in Figures 7 and 8.

The figures indicate that the cohesion is anisotropic. In this case, a strength factor D should be considered, which is defined by the intersection of the tangent to Mohr's circle and the axis $\sigma = 0$ and is expressed by

$$D = d\,(1 - \sin \Phi)/2\cos \Phi \quad (2)$$

where d denotes the deviatoric stress for $\sigma_3 = 0$. D differs from conventional cohesion (18).

Thus it is seen that sphericity has no influence on the strength factor either. The preceding results are attributable to the low breakage of the flaky particles at the center (shear zone) of the specimen.

Open Grading—Specimens were prepared, tested, and compacted as in the case of dense grading. The optimal bitumen content used was 3.5 percent.

Analysis of the grading after compaction revealed a segregation effect that resulted in a higher concentration of fines at the bottom of the specimen; however, because this effect is common to both shapes, it may be assumed that it does not distort the situation. Results (Figs. 9 and 10) show that sphericity has no influence on the compressive strength regardless of the direction of compaction and that the shape has no influence on the anisotropy or on the strength parameters. Unlike in dense-graded mixtures, in this case both the angle of internal friction and the cohesion are anisotropic.

Moving-Wheel Test

The series of moving-wheel tests (6), carried out on 38.0- by 18.0- by 4.5-cm specimens compacted under a 40-ton load, was designed to determine the influence of sphericity on the grooving resistance, the fatigue behavior of the asphaltic mixture under simultaneous vertical load and impact, and the fatigue behavior of the mixture under

Figure 5. Marshall stability versus density, open grading.

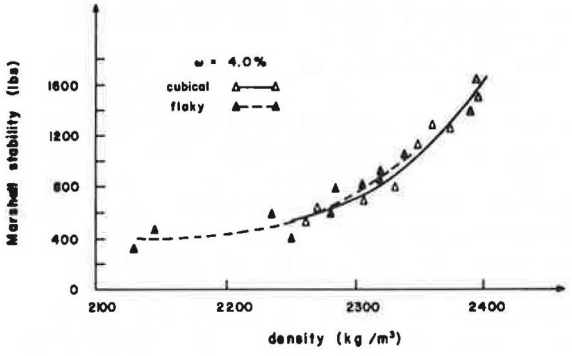

Figure 6. Specimen cross sections (dynamic compaction).

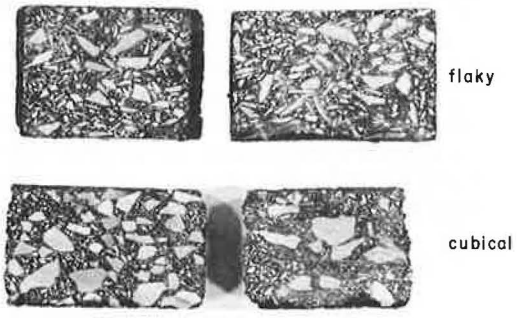

Figure 7. Deviatoric stress at failure versus lateral pressure, parallel compaction (dense grading, bitumen content 5.0 percent).

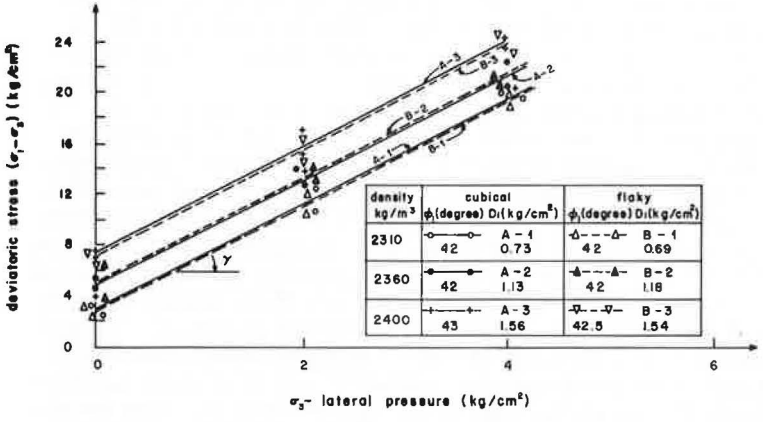

Figure 8. Deviatoric stress at failure versus lateral pressure, perpendicular compaction (dense grading, bitumen content 5.0 percent).

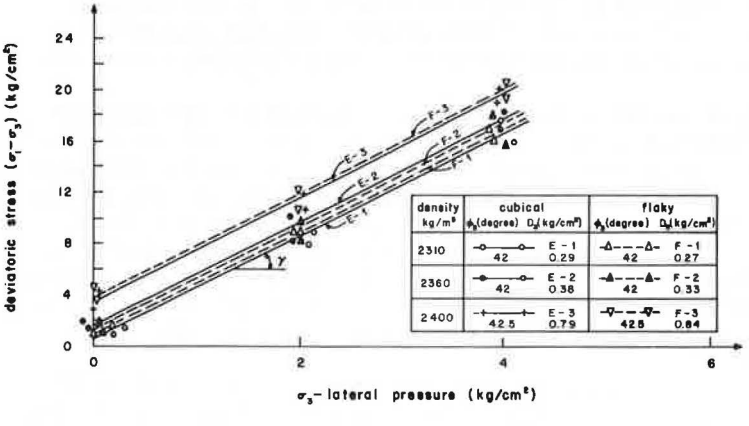

repeated loading. Some of the specimens were tested at room temperature (20 to 25 C); the vertical pressure was about 90 psi. Other specimens were tested under water at 60 C; the vertical pressure was about 60 psi. Figures 11 and 12 show the apparatus used in this test and also a specimen after the test was performed.

The influence of aggregate sphericity in both dense and open gradings under the conditions of these tests (room temperature of 20 to 25 C, water at 60 C) is shown in Figures 13, 14, and 15. From these figures, it may be concluded that sphericity has no significant effect on the grooving rate, whereas a rise in test temperature from 20 to 60 C causes the grooving rate to rise sharply. In the moving-wheel test, the elimination of the differences in the load-carrying properties between specimens containing cubical aggregates and specimens containing flaky aggregates, as compared with the Marshall test, may be attributed to the decrease in the breakage percentage of flaky particles.

It is noteworthy that, on a semilogarithmic scale, the curve that describes the relation between the degree of grooving and the number of cycles per second has the form of a straight line.

Breakage Value Test

Flaky aggregates, as compared with cubical aggregates of the same category, have poor mechanical properties (Appendix). Therefore, the breakage value of flaky particles in asphaltic mixtures may be expected to be higher. This is confirmed by the grading test performed after the compaction of laboratory specimens. It was found that the chief cause of breakage is not shear but is compaction. In the coarse fraction (-¾ in. +½ in.), the following breakage values were determined for flaky particles in dynamically compacted specimens (50 blows each side): (a) dense grading, approximately 60 percent as compared to almost 0 percent for cubical particles; and (b) open grading, approximately 80 percent as compared with 30 percent for cubical particles. The higher breakage of flaky particles in dense grading does not cause any significant change to take place in the grading. On the other hand, this breakage gives rise to the formation of air pockets that are free of bitumen and that reduce the stability values by some 15 percent (Fig. 1). In open grading, as may be expected, the breakage percentage of flaky particles is more significant as compared with cubical particles. Therefore, the number of air pockets is greater (and the change in the grading accordingly more significant), which results in a sharp decrease (about 55 percent) in the stability value as compared with specimens containing cubical aggregates (Fig. 1). The breakage of flaky particles changes their shape to cubical and to cubical-flaky (a shape in between cubical and flaky). In dense gradings, at a compaction energy of 50 blows, approximately 40 percent of flaky particles change in shape and become cubical-flaky. In open grading, 40 to 50 percent and 10 to 15 percent of flaky particles change shape to cubical-flaky and cubical respectively. From these results, it can be concluded that, in both dense and open gradings, after breakage there remains a quantitative difference between cubical aggregates (whose breakage does not alter their shape) and flaky aggregates.

To decrease the breakage value, we reduced the dynamic compaction energy from 50 to 10 blows (at a rate of 10 blows at a time). This in turn decreased the difference in the breakage values between flaky and cubical particles and increased the difference between the various shapes. The decrease in the breakage percentage of flaky particles (-¾ in. +½ in.) resulting from the decrease in the compaction energy from 50 to 10 blows was as follows: dense grading, from 60 to 40 percent; open grading, from 80 to 50 percent; and cubical particles, from 30 to 20 percent. The decrease of the difference in breakage percentages may be attributed to the decrease of the difference in the stability rates between specimens containing cubical aggregates and specimens containing flaky aggregates (Fig. 4).

Other attempts to reduce the breakage percentage of the particles, such as the adoption of the kneading compaction method (17), failed to yield the desired result. On the other hand, the following results were found: (a) In the center of the specimens (dense grading) examined in the triaxial shear test, the breakage rate of flaky particles

Figure 9. Deviatoric stress at failure versus lateral pressure, parallel compaction (open grading, bitumen content 3.5 percent).

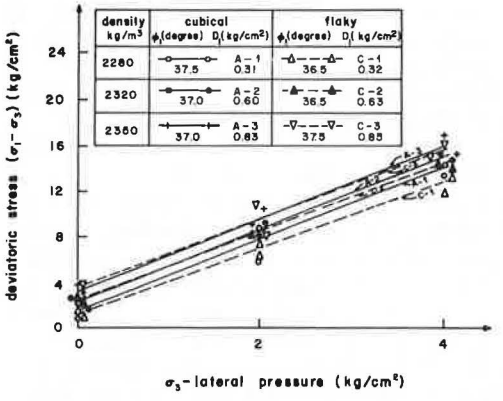

Figure 10. Deviatoric stress at failure versus lateral pressure, perpendicular compaction (open grading, bitumen content 3.5 percent).

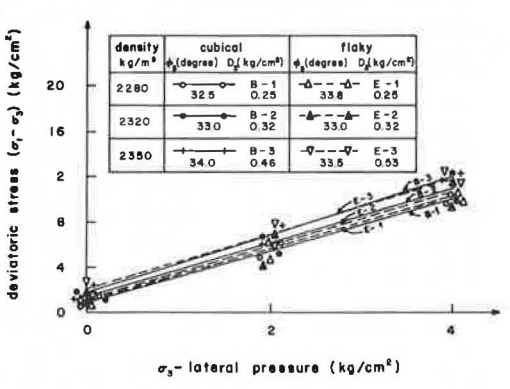

Figure 11. Wheel test apparatus.

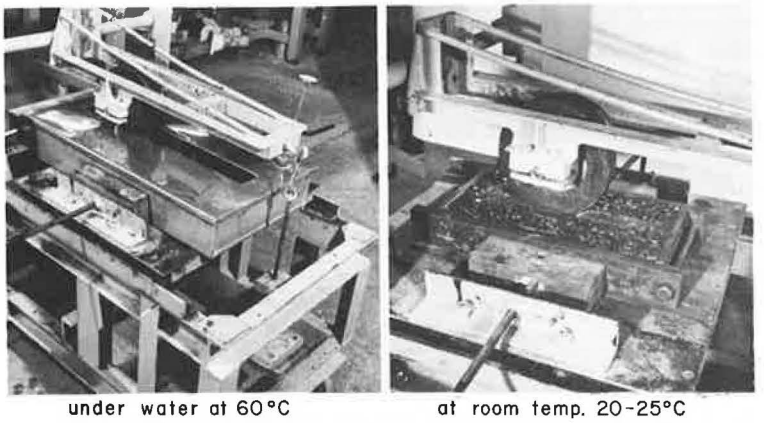

Figure 12. Wheel test specimen (60 C, 3,000 cycles).

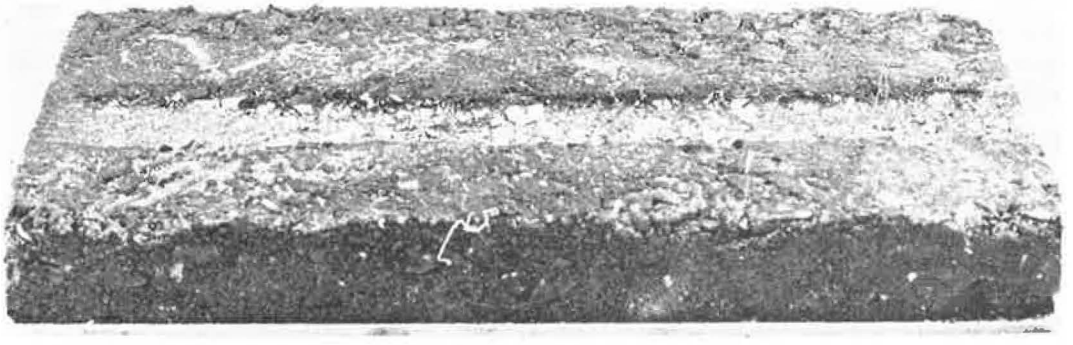

was approximately 25 percent, whereas the breakage of cubical particles was relatively negligible; and (b) in the loading-wheel test, the breakage value of flaky particles was approximately 30 percent in dense grading and 50 percent in open grading, whereas the breakage fraction of cubical particles was about 25 percent. Because the triaxial shear and moving-wheel tests showed that aggregate sphericity has no influence on load-carrying capacity (as opposed to the difference obtained in the Marshall test), it is reasonable to assume that the reduction of the difference in the breakage values between flaky and cubical particles, which was obtained in these tests as compared with the Marshall test, contributes to this result. In other words, the difference in load-carrying capacities decreases as the breakage fraction of flaky particles decreases.

These results give rise to the following questions: (a) What is the breakage value of hard flaky particles in road pavements; and (b) What is the influence of breakage on the decrease in tensile strength of asphaltic mixtures? The answer to the second question is discussed in the next section. To obtain an answer to the first question, we used a steel wheel to compact the specimens (Fig. 16). This method, which may be compared to the method employed on site, involves compacting the specimen for 24 min with a steel wheel 20 cm in diameter and 10 cm in width. The load applied on the specimen is 100 kg. It was found that in using this compaction method the breakage percentage of flaky particles is smaller than that obtained with specimens compacted by common laboratory methods. In dense grading, the breakage percentage of flaky particles (-¾ in. +½ in.) is about 15 percent and in open grading about 30 percent. The breakage value of cubical particles was negligible in dense grading and was about 15 percent in open grading. This relatively small breakage value will give rise to a negligible change in the shape of flaky particles. In dense grading, about 15 percent change shape to cubical-flaky; in open grading, about 30 and 10 percent change shape to cubical-flaky and cubical respectively. From these results, it may be concluded that hard flaky particles may be expected to have a lower breakage value on the road than in laboratory specimens.

Another contribution of the mobile steel-wheel compaction method is that it enables one to determine the pattern of flaky particles in road pavements. From Figure 17 it may be concluded that the use of flaky particles does not produce a stratification pattern in the aggregates. In other words, the use of flaky particles in road pavements does not create weakness planes perpendicular to the direction of compaction.

Splitting Test

The splitting test can be used to determine the tensile strength (23) of asphaltic mixtures and to examine the influence of breakage on tensile strength. In this test, cubical specimens with 10-cm sides were used. Dense grading and a bitumen content of 5 percent were used in all the specimens, which were statically compacted at a pressure of 15 tons. Before splitting, the specimens were immersed in water at a temperature of 60 C.

The results of the splitting test are given in Table 1. This table shows that the use of hard flaky aggregates, as compared with cubical aggregates of the same category, does not decrease the tensile strength of the specimen and does not affect its anisotropic properties.

Weight-Volume Ratio Test

Single-size unstabilized flaky mixtures are less compactible than their cubical counterparts (20, 21). Because open-graded asphaltic mixtures also contain aggregates of various sizes, there is a possibility of eliminating, or at least of reducing, the influence of sphericity on compactibility.

A flaky mixture cannot be expected to have a lower void percentage as compared with a cubical mixture because this is only possible if the flaky particles assume a stratification pattern, which was proved to be impossible. This conclusion was confirmed by investigating the influence of sphericity on density by using the three compaction methods: dynamic, kneading, and static. The void percentage in asphaltic mixtures containing flaky aggregates was never smaller than that of mixtures containing

Figure 13. Grooving versus bitumen content with number of cycles (N) as parameter, dense grading at 24 C.

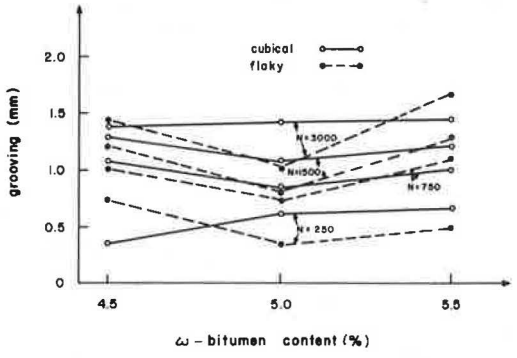

Figure 14. Grooving versus bitumen content with number of cycles (N) as parameter, open grading at 23 C.

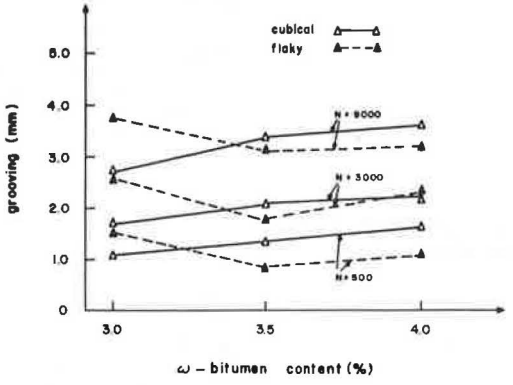

Figure 15. Grooving versus bitumen content with number of cycles (N) as parameter, dense grading at 60 C.

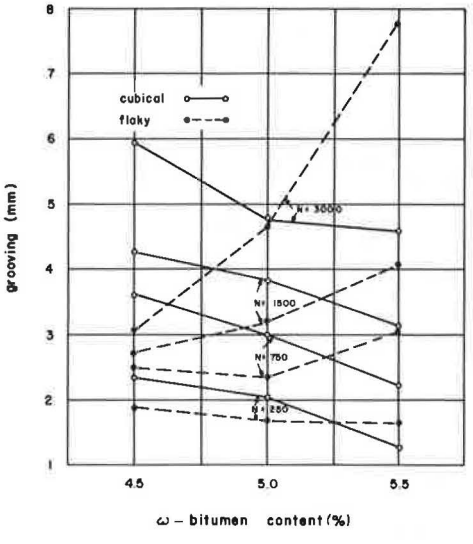

Figure 16. Steel wheel, compaction apparatus.

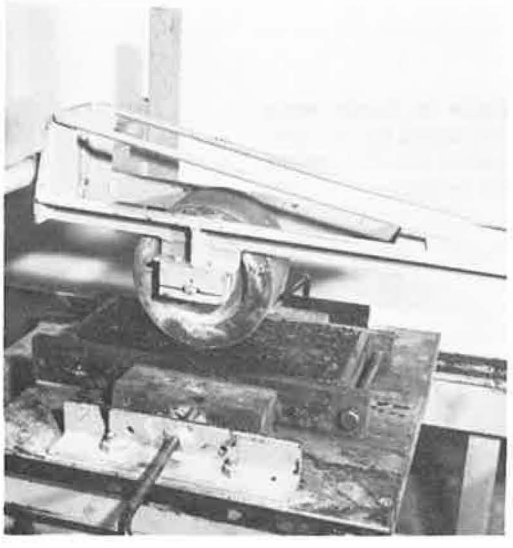

Figure 17. Sections of steel wheel, compacted specimens.

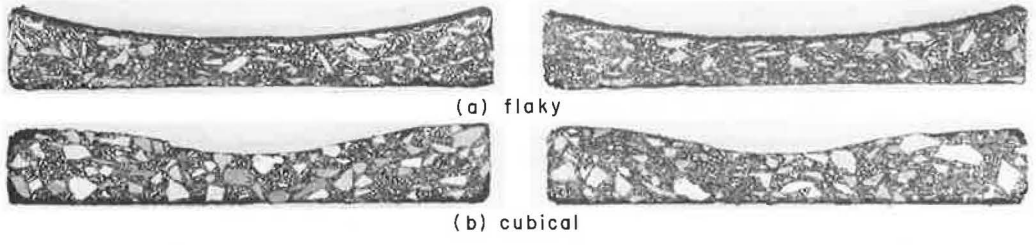

Table 1. Splitting test results.

Aggregate	Density (kg/m³)	Compaction Direction[a]	$q_{parallel}$ (kg/cm²)	$q_{perpendicular}$ (kg/cm²)	$q_{parallel}/q_{perpendicular}$
Cubical	2,310	Parallel	27.1	—	1.6
	2,310	Perpendicular	—	16.9	1.6
Flaky	2,295	Parallel	24.2	—	1.5
	2,300	Parallel	32.9	—	1.5
	2,300	Perpendicular	—	19.2	1.5

[a]In relation to direction of load.

Figure 18. Density versus bitumen content.

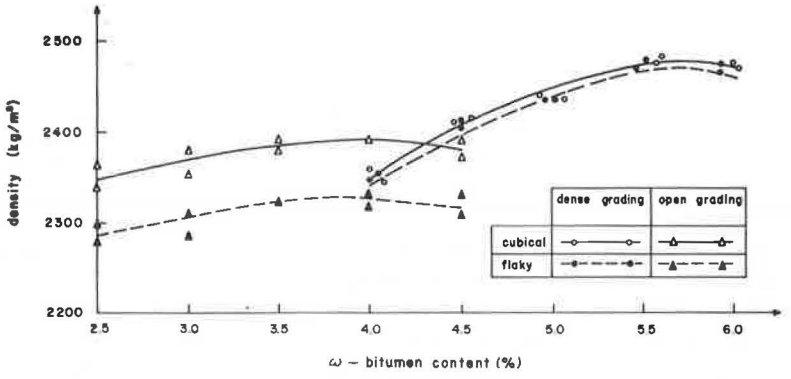

Figure 19. Density versus compaction energy, open grading (bitumen content 4.0 percent).

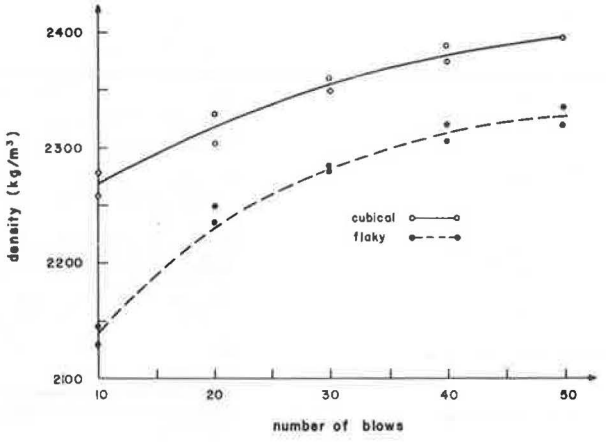

Table 2. Summary of findings.

Mixture Property[a]	Dense Grading	Open Grading
Marshall stability	No influence of shape; stability (reduced by 15 to 20 percent) in flaky mixtures in the case of higher breakage due to mode of compaction; stability higher than average for all shapes	Stability similarly reduced (by 55 percent); reduction of breakage narrows stability gap to 35 percent
Breakage value	Typical for laboratory compaction techniques used; lower in the case of wheel compaction and simulated field conditions	Typical for laboratory compaction techniques used; lower in the case of wheel compaction and simulated field conditions
Density	No influence of shape	Lower density in flaky mixtures (by 3.5 to 5.5 percent)

[a]There was no influence of shape in the following properties: Marshall flow, load-carrying capacity (triaxial shear test), optimal bitumen content, strength parameters D and Φ, grooving, and splitting test.

cubical aggregates. In the case of dense grading, the values of the void percentage were identical (Fig. 18), regardless of the compaction method. In open grading, the flaky specimens had a density of about 3.5 percent lower than the cubical specimens. Reduction of the compaction energy by the dynamic method increased the difference to about 5.5 percent (Fig. 19). In other words, the influence of sphericity was limited even here. It is noteworthy that, in the case of dynamic and kneading specimens, the density was determined by using the wax method (22). The excessively high results obtained—especially in the open-graded material—are apparently due to the penetration of the wax into the voids. In the case of the statically compacted specimens used in the wheel test, the density was determined by direct measurement. These results prove that, in both open and dense gradings, the flaky particles (like cubical particles) are arranged in a random pattern.

SUMMARY AND CONCLUSIONS

The data given in Table 2 lead to the conclusion, which occasionally contradicts the findings of others, that flaky aggregates (specifically the hard, crushed type used in the laboratory study) may be regarded as a conventional material from the engineering viewpoint, i.e., that they may be used for producing asphaltic mixtures for pavement layers.

In view of the difference in crushing values between the shapes (cubical, 21 percent, and flaky, 31 percent) on the one hand and their identical mode of production and mineralogical composition on the other, it was found that the crushing value is shape-dependent and that flaky material should thus be rejected. This, however, conflicts with the laboratory findings previously mentioned. Hence, it can be concluded that abrasion and crushing value are not always reliable criteria for determining the engineering quality of aggregates in road pavements and should thus be investigated further.

ACKNOWLEDGMENT

This paper is partially based on Greenstein's research work for the M.Sc. degree, under the supervision of Livneh, and is published by permission of the Graduate School of the Technion, Israel Institute of Technology, Haifa, Israel.

REFERENCES

1. Effects of Aggregate Size, Shape, and Surface Texture on Properties of Bituminous Mixtures. HRB Spec. Rept. 109, 1970, 41 pp.
2. Griffith, J. M., and Kallas, B. F. Aggregate Voids Characteristics in Asphalt Paving Mixes. HRB Proc., Vol. 36, 1957, pp. 382-387.
3. Griffith, J. M., and Kallas, B. F. Influence of Fine Aggregates on Asphaltic Concrete Paving Mixtures. HRB Proc., Vol. 37, 1958, pp. 219-255.
4. Lottman, R. P., and Goetz, W. H. Effect of Crushed Gravel Fine Aggregate on the Strength of Asphaltic Surfacing Mixtures. Nat. Sand and Gravel Assn., Washington, D.C., Circular 63, 1956.
5. Puzinauskas, V. P. Influence of Mineral Aggregate Structure on Properties of Asphalt Paving Mixtures. Highway Research Record 51, 1964, pp. 1-18.
6. Shklarsky, E., and Livneh, M. The Use of Gravels for Bituminous Paving Mixtures. Proc. AAPT, Vol. 33, 1964, pp. 584-610.
7. Wedding, P. A., and Gaynor, R. D. The Effects of Using Gravel as the Coarse and Fine Aggregate in Dense-Graded Bituminous Mixtures. Proc. AAPT, Vol. 30, 1961.
8. Field, F. The Importance of Percent Crushed in Coarse Aggregate as Applied to Bituminous Pavements. Proc. AAPT, Vol. 27, 1958.
9. Lefebvre, J. Recent Investigations of Design of Asphalt Paving Mixtures. Proc. AAPT, Vol. 26, 1957.
10. Chapel, K. F. The Use of Sand and Gravel in Bituminous Mixtures. Proc. AAPT, Vol. 25, 1956.
11. Campen, W. H., and Smith, J. R. A Study of the Role of Angular Aggregates in the Development of Stability in Bituminous Mixtures. Proc. AAPT, Vol. 17, 1948.

12. Herrin, M., and Goetz, W. H. Effect of Aggregate Shape on Stability of Bituminous Mixes. HRB Proc., Vol. 33, 1954, pp. 293-307.
13. Li, M. C., and Kett, I. Influence of Coarse Aggregate Shape on the Strength of Asphalt Concrete Mixtures. Highway Research Record 178, 1967, pp. 93-106.
14. Huang, E. Y., Squier, L. R., and Triffo, R. P. Effect of Geometric Characteristics of Coarse Aggregates on Compaction Characteristics of Soil-Aggregate Mixtures. Highway Research Record 22, 1963, pp. 38-47.
15. Huang, E. Y., Auer, A., and Triffo, R. P. Effect of Geometric Characteristics of Coarse Aggregates on Strength of Soil Aggregate Mixtures. Proc. ASTM, Vol. 64, 1964.
16. Campen, W. H., Smith, J. R., Erickson, L. G., and Mertz, L. R. The Relationship Between Voids, Surface Area, Film Thickness and Stability in Bituminous Paving Mixtures. Proc. AAPT, Vol. 21, 1952.
17. Preparation of Test Specimens of Bituminous Mixtures by Means of California Kneading Compactor. Tentative, ASTM D1561-627, Oct. 1962.
18. Livneh, M., and Greenstein, J. State of Failure Stress in a Medium With Anisotropic Cohesion and Isotropic Internal Friction Angle. Israel Jour. of Tech., Vol. 9, No. 5, 1971.
19. Knight, B. H., and Knight, R. G. Road Aggregates—Their Uses and Testing. Edward Arnold Co., London, 1948.
20. Dallavalle, J. M. The Technology of Fine Particles, Micromeritics, 2nd Ed. Pitman Publishing Corp., London, 1948.
21. Huang, E. Y. A Test Evaluating the Geometric Characteristics of Coarse Aggregate Particles. Proc. ASTM, Vol. 62, 1962.
22. Specific Gravity of Compressed Bituminous Mixtures. ASTM D1188-56, Oct. 1962.
23. Livneh, M., and Shklarsky, E. The Splitting Test for Determination of Bituminous Concrete Strength. Proc. AAPT, Vol. 31, 1962.

APPENDIX

STUDY MATERIALS

Both coarse and fine aggregates (plus and minus sieve No. 4 respectively) were prepared from the same stone. Mineralogically, both consist of two forms of dolomite: One is yellowish, dense, hard, and fine-grained, and the other is whitish, slightly chalky, hard, and somewhat porous.

The coarse aggregate shape was classified in the three fractions (-¾ in. +½ in., -½ in. +⅜ in., and -⅜ in. + No. 4) by using special sieves with rectangular apertures, as is shown in Figure 20. The description of the cubical and flaky aggregates (thickness-to-width ratio, i.e., p = c/b, Fig. 21) is shown in Figures 22 and 23. It can be seen that, under the present definition, shape categories vary mainly according to flakiness (100 percent flaky and 0 percent flaky according to B.S. specifications on flaky and cubical aggregates respectively), whereas elongation is almost the same for each fraction.

Crushing and abrasion tests indicate that the breakage is lowest for cubical aggregates [21 percent in crushing (-½ in. +⅜ in.) fraction and 18 percent in abrasion (grading B in Los Angeles abrasion test)] and highest for flaky aggregates (31 percent in crushing and 27 percent in abrasion with the fractions remaining the same). These data for cubical aggregates also reflect the relatively high hardness of the aggregate used in this study. The reason for selecting this aggregate was the high percentage of flaky aggregates that are found in quarries containing hard stones.

The specific gravity of the coarse material (in all gradings and shapes) was found to be the same (2.66), which indicates uniformity in its mineralogical composition. A similar uniformity was observed for the percentage of water absorption (1.5 percent), which indicates that the surface area is mainly governed by roughness and angularity values, whereas the influence of sphericity is negligible. The specific gravity of the

Figure 20. Rectangular sieves versus standard sieves.

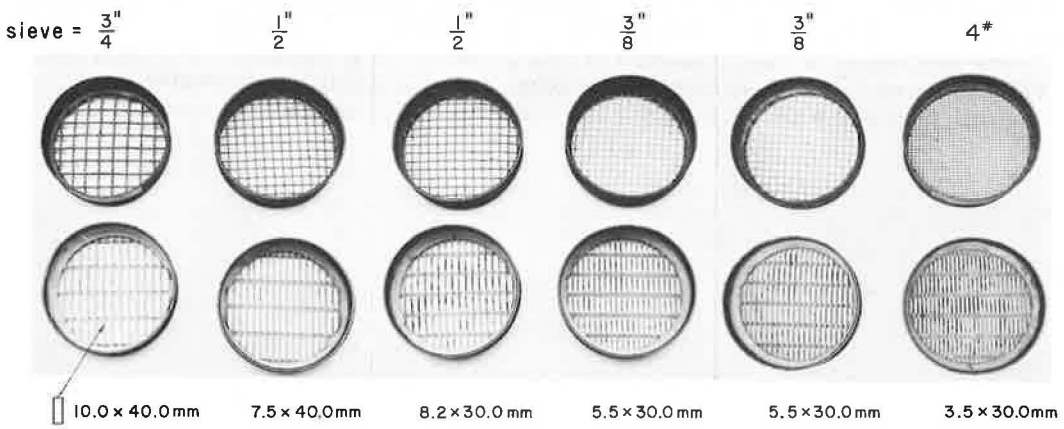

Figure 21. Aggregate dimensions.

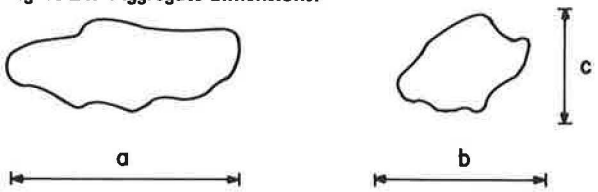

Figure 22. Aggregate shape.

Figure 23. Cumulative flakiness index.

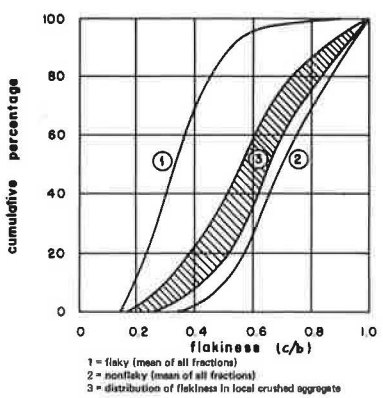

fine material was found to be higher in dense grading than in open grading (2.81 versus 2.78) probably because of the higher content of the fraction passing sieve No. 200 (6.5 percent versus 2 percent). The specific gravity of the latter is 2.88.

The fine material was nonplastic in both gradings. The values of sand equivalent were 58 percent and 73 percent for the dense and open gradings respectively.

A bitumen with a penetration of 80 to 100 was used throughout the study.

BEHAVIOR OF COLD MIXES UNDER REPEATED COMPRESSIVE LOADS

M. Fayek Howeedy, Ein-Shams University, Cairo, U.A.R.; and
Moreland Herrin, University of Illinois

• RECENT studies dealing with repeated loads have been concerned with the behavior of hot bituminous mixes. Cold mixes, however, have received limited interest. A cold bituminous mix is prepared by mixing the aggregates with a cutback asphalt. This mix may be spread and compacted at atmospheric temperature. Cold mixes remain workable for long time periods; hence, in addition to being suitable for immediate use, they may be transported for long distances and placed in stockpiles for future use. The advantages gained from such a bituminous mix that is not dependent on temperature for mixing, placing, and drying of the aggregates are mainly economic. The increasing use of cold mixes, because of their economic aspects, warrants research that will produce a better understanding of the behavior of cold mixes.

The objectives of this research are to study the behavior of bituminous-aggregate mixes (BAMs) under repeated compressive load (fatigue life) in unconfined conditions and to determine the modulus of resilience of these mixes under specific conditions. The study includes the influence of such variables as cutback content, aggregate gradation, type of cutback, curing time, and temperature on the fatigue life of BAMs.

The modulus of resilience is defined as the applied compressive stress divided by the resilient (recoverable) strain. It was introduced to the asphaltic material research by Hveem (2). Later, Seed et al. (5, 6) evaluated the modulus of resilience for compacted subgrade clayey soil and granular bases. Recently, Terrel and Monismith (7) determined the modulus of resilience of a BAM. Although Terrel and Monismith were primarily interested in the influence of curing time, they did indicate the influence of confining pressure and temperature on the modulus of resilience. The importance of the modulus of resilience as determined by experimental work is that it can be incorporated in elastic theories to determine the deflection or the stresses of a pavement when subjected to a specific loading.

MATERIAL

Two different types of cutback asphalt were used in this study. The first was rapid-curing asphalt (RC-800) obtained from Sinclair Refinery, Wood River, Illinois. The RC-800 contained 21.3 percent volatiles by total weight. The specific gravities of the solvent and residue were 0.77 and 1.02 respectively. The rapid-curing cutback was used to prepare 95 percent of the tested specimens. The second type of cutback was medium-curing asphalt (MC-250) obtained from the same source as RC-800. The MC-250 contained 21.3 percent volatiles by total weight. The specific gravities of the solvent and residue were 0.79 and 1.01 respectively.

Aggregates were obtained from Pontiac Gravel Co., Mohamet, Illinois. The origin of these aggregates is glacial outwash of Wisconsian age. The coarse aggregate, passing a $^3/_4$-in. sieve and retained on a No. 8 sieve, has a bulk specific gravity of 2.58. The fine aggregate, passing a No. 8 sieve and retained on a No. 200 sieve, has a specific gravity of 2.65. Two aggregate gradations were used: dense and open. The gradations of the aggregates are as follows:

Sponsored by Committee on Bituminous Aggregate Bases.

Aggregate Gradation	Sieve Size, Percent Passing							
	¾ in.	½ in.	⅜ in.	No. 4	No. 10	No. 40	No. 80	No. 200
Dense	100	85	76	61	46	24	13	6
Open	100	84	72	49	30	8	0	0

A pit-run gravel was simulated by passing a loess material through a No. 200 sieve. The clay fraction of the loess was approximately 10 percent, the liquid limit was 28 percent, the plastic limit was 25 percent, and the plasticity index was 3 percent.

MIX DESIGN

Methods for designing cold mixes are not thoroughly standardized, perhaps because cold mixes are not used as extensively as hot mixes. The existence of a large number of types and grades of cutback asphalts, which make them practically applicable to every condition of temperature, aggregate, and paving equipment, may be responsible for the lack of a rational design method.

Accordingly, a laboratory program was carried out to answer the following questions.

1. For a certain cutback content, what are the drying (between mixing and molding) and curing times (between molding and testing) that give the maximum stability?
2. For determined drying and curing times, what is the cutback content that gives the maximum density?

It is realized that maximum stability and maximum density are probably not the only criteria that should be considered in designing BAMs. However, because this investigation was not directed toward developing a design procedure, it was felt that these two criteria would produce a satisfactory mix. Laboratory results indicated that maximum stability (as measured in the Hveem stabilometer) of the dense mix can be achieved at a drying time of 4 hours in an oven adjusted to a temperature of 180 F and a curing time of 10 days at room temperature (approximately 75 F). The maximum density was obtained at a cutback content of 7 percent. These values were used as a guide for selecting the magnitude of the variables considered in the investigation.

VARIABLES

The variables in this study include (a) testing temperature (19, 22, and 25 C), (b) cutback content (6, 7, and 8 percent), (c) aggregate gradation (dense and open), (d) curing time (10 days and 300 days), and (e) type of cutback asphalt (RC-800 and MC-250).

TESTING PROCEDURES

Cylindrical specimens 3⅛ in. in diameter and 6 in. in height were fabricated in a steel double-plunger mold. Each group of specimens having the same properties and tested under similar conditions is defined as a series. The designation of the eight test series and their properties are given in Tables 1 and 2.

A testing machine of the constant-displacement type was used to apply repeated compressive stresses to the unconfined specimens. The displacement was produced by an adjustable motor-driven eccentric operating a series of levers. Figure 1 shows the testing machine. The loads applied to the specimen were equivalent to the force required to cause a deflection in a steel bar dynamometer equal to the vertical movement of the oscillating shaft of the machine. Necessary readjustments of the load during the course of the tests were accomplished by varying the length of the adjustable connecting rod, H.

The loads were applied at a rate of 730 cpm. The hand crank, O, was used only when the machine was stopped to allow the measurements of the total deformation experienced by the test specimen when subjected to a specific load through two dial indicators.

The testing machine was placed in a controlled-temperature environment. A minimum stress of ¼ psi was maintained on the specimen to avoid the dynamic effects

Table 1. Series designation of BAMs used in repeated load tests.

Series	Gradation	Top Size (in.)	Cutback Type	Cutback Percent	Curing Time (days)	Testing Temperature (deg C)
I	Dense	3/4	RC-800	7	10	25
II	Dense	3/4	RC-800	7	10	22
III	Dense	3/4	RC-800	7	10	19
IV	Dense	3/4	RC-800	8	10	22
V	Dense	3/4	RC-800	6	10	22
VI	Open	3/4	RC-800	7	10	22
VII	Dense	3/4	RC-800	7	300	22
VIII	Dense	3/4	MC-250	7	120	22

Table 2. BAM test results.

Series	Unit Weight Average pcf	Unit Weight c_v Percent	Unconfined Compressive Strength Average pcf	Unconfined Compressive Strength c_v Percent	Amount of Voids (percent)	Amount of Water (percent) Original	Amount of Water (percent) After 10 Days	Amount of Volatiles (percent) Original	Amount of Volatiles (percent) After 10 Days
I, II, III	139.4	0.59	61.5	6.07	6.1	4.8	0.07	1.49	0.04
IV	140.8	1.00	52.6	14.10	3.8	4.8	0.10	1.70	0.22
V	137.9	0.32	55.6	0.75	8.1	4.8	0.06	1.28	0.04
VI	136.9	1.13	35.1	11.05	7.8	—	—	—	—
VII	136.5	0.12	156.5	0.0	8.1	—	—	—	—
VIII	140.1	0.50	22.6	0.41	4.4	—	—	—	—

Notes: c_v defines the coefficient of variation. See Herrin (1) for procedures used to determine water and volatile contents.

Figure 1. Fatigue testing machine.

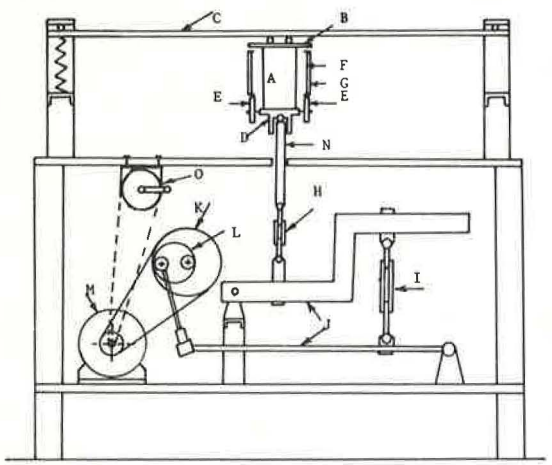

A - Test specimen
B - Loading head
C - Steel bar dynamometer
D - Steel base
E - Dial indicator
F - Extension rod
G - Clip
H - Adjustable connecting rod
I - Movable adjustable connecting rod
J - Load levers
K - Eccentric
L - Adjustable crank
M - Motor
N - Oscillating shaft
O - Hand crank

caused by complete stress removal and subsequent reloading. The machine was turned off to measure the deformation at a specified number of load applications. The hand crank was turned one cycle, causing the oscillating shaft to be displaced once. The maximum reading of one dial indicator (occurring when the shaft is at its highest position) represented the total deformation; the minimum reading (occurring when the shaft was at its lowest position) represented the residual deformations. At the same time, the second dial indicator was read. The average value of residual and total deformations at a specified number of load applications was determined, and the modulus of resilience was computed. The total number of test specimens was 117. The maximum number of test specimens per series was 28 (series II), the minimum was 6 (series VIII), and the average was 14.

FAILURE CRITERION

The variation in residual strain with number of stress applications at different stress levels for several specimens from series II is shown in Figure 2. The plotted data indicate that the relations between the residual strain and the logarithm of number of load applications could be divided into three portions: A, B, and C. Part A appeared to be a straight line, part B to be slightly curved, and part C to have a sharp curvature and probably could be defined as an excessive permanent deformation zone. This behavior was found to be true at different stress levels and for approximately 95 percent of the BAM specimens. A common factor among all the plots was that part B always encompassed 1 percent residual strain. A designer should certainly not use a mix when it is in the condition of part C. Part A was generally encountered at a low residual strain percentage. Thus, the number of load repetitions required to reach 1 percent residual strain was used as a failure criterion.

TEST RESULTS

The axial compressive strains (total and residual) were plotted against the logarithm of number of stress applications for each specimen. The number of stress applications at 1 percent residual strain was determined and is reported as N_f. The resilient strain was determined at 1 percent residual strain, and the corresponding modulus of resilience was calculated (applied stress divided by resilient strain at failure). In general, the value of the modulus of resilience appeared to be constant in the vicinity of 1 percent residual strain (Fig. 3).

The N_f and resilient strain at 1 percent residual strain were used to prepare two diagrams for each series: One was a plot of the axial compressive stress, σ, versus logarithm of number of stress applications to failure, σ - N_f diagram, and the other was a plot of the calculated modulus of resilience versus the axial compressive strength. The influence of the variables studied, temperature, cutback content, aggregate gradation, curing time, and type of cutback on the fatigue life and the resilience characteristics of BAM specimens is shown in Figures 4 through 9. The equations shown in Figures 4, 6, and 8 represent the best fitting line through the experimental data for a specific series.

DISCUSSION OF EXPERIMENTAL RESULTS

Influence of Testing Temperature

The effect of temperature on the fatigue life and resilience characteristics of BAM specimens was investigated by testing the specimens at 25, 22, and 19 C. The experimental results indicated that the resistance of the BAM specimens to fatigue failure increased with a decrease in the testing temperature (Fig. 4). Specimens tested at lower temperatures sustained a larger number of load applications to failure than those tested at higher temperatures.

The viscosity of the binder may be defined as the property that retards flow; therefore, when a force is applied to the binder, the higher is the viscosity, the slower is the deformation of the binder (8). The decrease in the temperature caused an increase in the binder's viscosity, which consequently produced greater resistance to deformation.

Figure 2. Residual strain versus number of stress applications at different stress levels for selected specimens, series II.

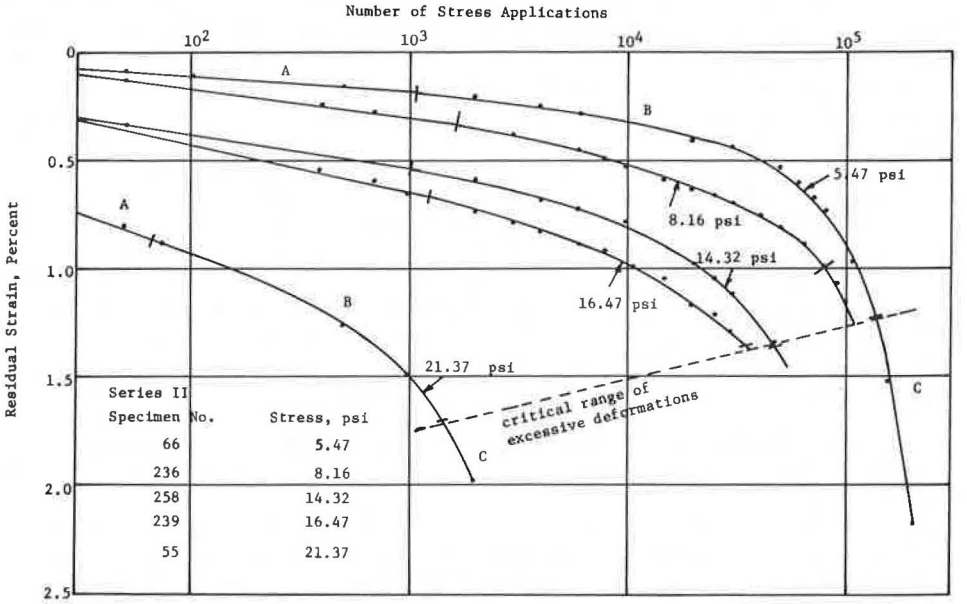

Figure 3. Variation of modulus of resilience with number of stress applications.

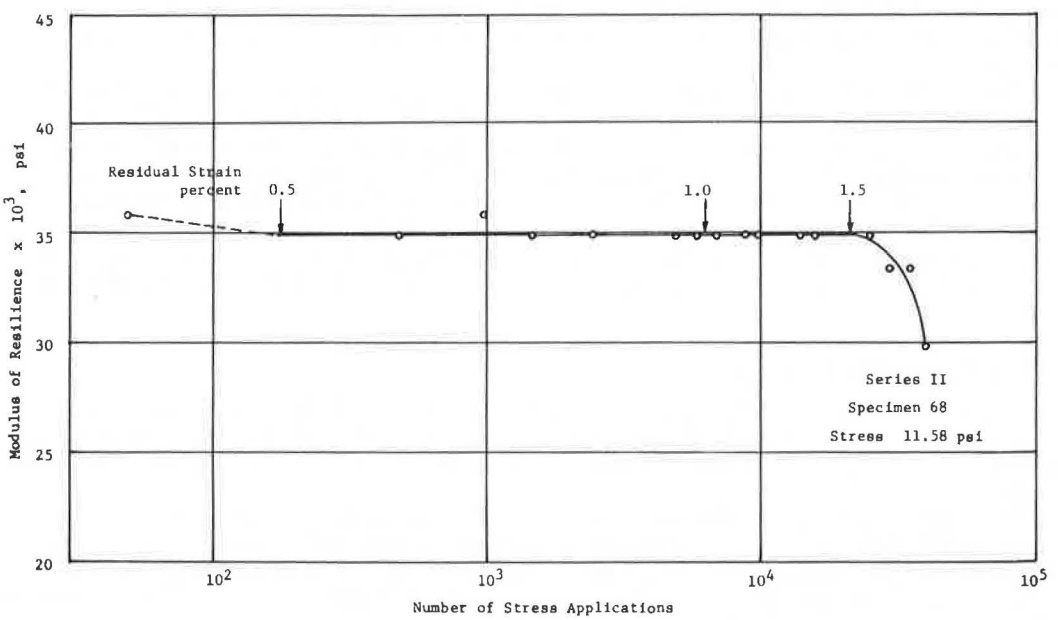

Thus, BAM specimens tested at relatively low temperatures need a larger number of repetitions to reach 1 percent residual strain than those tested at higher temperatures (until the glass transition point of the asphalt is about reached). At temperatures lower than the glass transition point, the asphaltic mix probably behaves brittlely because the binder changes from the liquid to the brittle condition. If the brittle condition is reached, the number of load applications to failure may decrease considerably.

Another explanation for the increase of fatigue life of BAMs with a decrease in temperature can be made in terms of the so-called molecular chain concept used by Marek (3). According to the molecular chain concept, asphalts are composed of a long, polymer-like molecular chain structure. The behavior of the asphalt is related to the response of the molecular chain acting by itself and in combination with applied stresses.

When the repeated compressive load is applied, a certain amount of stretching and untwisting of the polymer chains may result. This process is reflected by the gradual increase in permanent deformations of the specimens with an increase in the number of load applications as shown in Figure 2. Thus, at a relatively low temperature, the asphalt film needed a larger number of load applications to undergo a certain amount of stretching and untwisting. At higher temperatures, however, the molecular structure was relatively loose; consequently, the resistance to uncoiling and stretching of the chain decreased. Therefore, the same amount of stretching could be reached at higher temperatures by a relatively smaller number of load applications, as was reached at lower temperatures.

The variation of the modulus of resilience with the applied stress (Fig. 5) indicated that the modulus generally decreased rapidly with an increase in the applied stress. However, at stresses of about 15 psi, there was little change. At higher stresses, there was an increase in the modulus with further increase in applied stress (Fig. 5). The general shape of the modulus of resilience-normal stress relations of BAMs is similar to the shape of the same relation of compacted subgrade material tested in repeated load triaxial compression (5). However, the magnitude of the modulus of resilience of series II at stresses between about 10 to 20 psi was approximately 10 times that of the subgrade soil from the AASHO test road (tested at a confining pressure of 3.5 psi) (5).

The molecular chain concept can be used to explain the change in the modulus with temperature. Because the mobilization of the chain and/or segments of chains decreases at relatively low temperatures, the ability of the chains to deform is reduced. Not only will the total deformations be small, but also the ability of the film of the binder to recover after the load is removed will be greatly reduced because of the decrease in the mobilization of the chains. The result is relatively low resilient deformations and a high modulus of resilience. At high temperatures, however, the molecular structure will be relatively loose, and the reverse of the previous situation may occur.

Influence of Cutback Content

Figure 6 shows that the fatigue life of BAM specimens slightly increased with an increase in the RC-800 cutback content from 6 to 7 percent. An increase in the cutback content to 8 percent, increased the fatigue life of the BAM specimens at stresses above 9 psi.

It can be concluded that the increase in the cutback content above optimum (maximum density occurred at approximately 7 percent) caused an increase in the fatigue life of BAM specimens. This conclusion agrees with Pell's conclusion (4) that the fatigue life of the sandsheet specimen, tested under flexural repeated load, increases with an increase in the asphalt content up to optimum.

The increase in the fatigue life with an increase in the cutback content tends to support the idea that film thickness has considerable influence on fatigue behavior of BAMs. Such behavior tends to be in line with a hypothesis that states that the reduction in the film thickness during the application of the repeated load may govern the fatigue behavior of the BAM until zone C is reached (Fig. 2). Thicker films would tend to require a larger number of load repetitions in order to be reduced to a critical value at

Figure 4. Influence of testing temperature on fatigue life of BAMs.

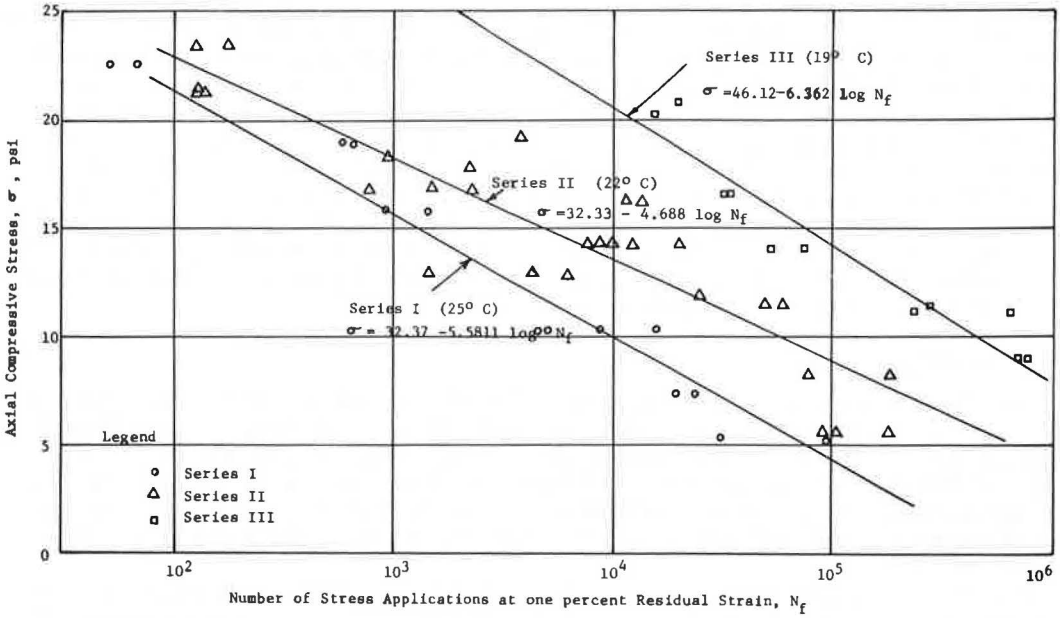

Figure 5. Influence of testing temperature on the modulus of resilience.

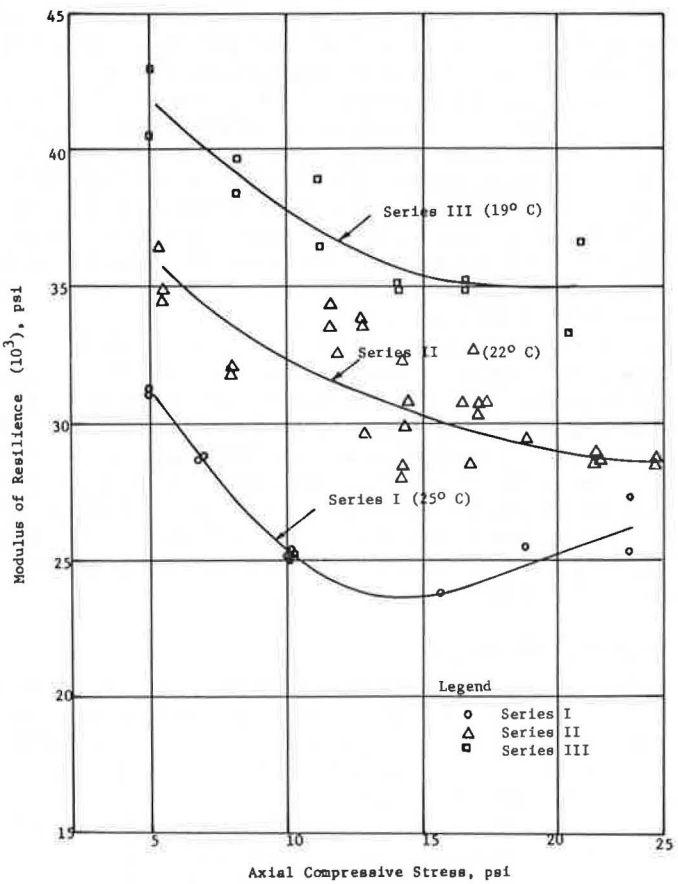

zone C when compared with thinner ones. When the film reaches a critical value, the specimen may give way in tension.

The variation in the modulus of resilience with the amount of cutback is shown in Figure 7. In general, there appears to be an optimum cutback content, as mixes with 7 percent cutback had greater modulus than mixes with 6 percent. Mixes with 8 percent cutback have a lower modulus than mixes with 6 percent cutback. This additional decrease in the modulus may be due to the curing process. According to the results given in Table 2, the amount of volatiles left in series IV (8 percent RC-800) after 10 days' curing was 12.9 percent (of the original value) compared to 2.7 percent and 3.1 percent for series II (7 percent RC-800) and series V (6 percent RC-800) respectively. It appears, therefore, that the binder in the specimens prepared with 8 percent RC-800 has a lower viscosity as compared to those prepared with 7 percent and 6 percent RC-800, which would produce a slightly lower modulus.

Influence of Gradation

Test results of the open- and dense-graded mixes are shown in Figure 8. The figure indicates that dense-graded mixes have more resistance to fatigue failure than do open-graded mixes. Because 7 percent cutback asphalt was used in both cases, it is expected that the open-graded mix would have a relatively larger number of voids than the dense-graded mix. Evidence of this is given in Table 2. The increase in the number of voids may have contributed toward the decrease of the fatigue life of the open-graded mixes.

The influence of gradation on resilience characteristics is shown in Figure 9. The open-graded mixes experienced a unique behavior with respect to the other mixes. The shape of the curve does not follow the general shape that was observed in the other seven series. For an open-graded mix, Figure 9 shows an increase in the values of the modulus of resilience up to about 12.5 psi, then a sharp decrease in the modulus with further increase in the axial compressive stress.

The curves representing series I (dense graded, 25 C) were plotted with those for series VI (Figs. 8 and 9) for purposes of comparison. Figure 9 indicates that the values of the modulus of resilience of series VI (open graded, 22 C) are higher than those of series I (dense graded, 25 C) within a range of axial compressive stress of about 9 to 19 psi. Statistical comparison between the fatigue response (slope of the regression lines) of the two series, however, indicated a significant difference between the two series (at 95 percent confidence level). However, series I (dense graded, 25 C) (Fig. 8) had better fatigue resistance than series VI (open graded, 22 C) even though it had less modulus of resilience.

This example should warn the engineer that one must not use the modulus of resilience alone when using a theoretical analysis (instead of the conventional modulus of elasticity) to evaluate a bituminous mix in the design of transportation structures. High modulus of resilience may appear to be the only factor to consider, but this is a misleading concept. The evaluation should also consider the fatigue resistance of the material. Therefore, it does not seem appropriate to use a material with a high modulus of resilience without taking a careful look at its fatigue characteristics. It appears, then, that two figures similar to the σ - N_f diagram and modulus of resilience-stress relation should go hand in hand when selection of a material for use in transportation structures is being made.

Influence of the Curing Time

The influence of curing time was studied by curing series II and VII for about 10 and 300 days respectively. It was not possible to obtain data concerning the fatigue life of series VII because of the very slow rate of residual deformations that was experienced by the test specimens. Consequently, comparison between the two series will be limited to the resilience characteristics.

Because a considerable time elapsed between the testing of the two series, it would be appropriate to explain first what could happen to the binder as time passed. Tests performed on representative specimens of series II indicated that the amounts of water

Figure 6. Influence of cutback content on fatigue life of BAMS.

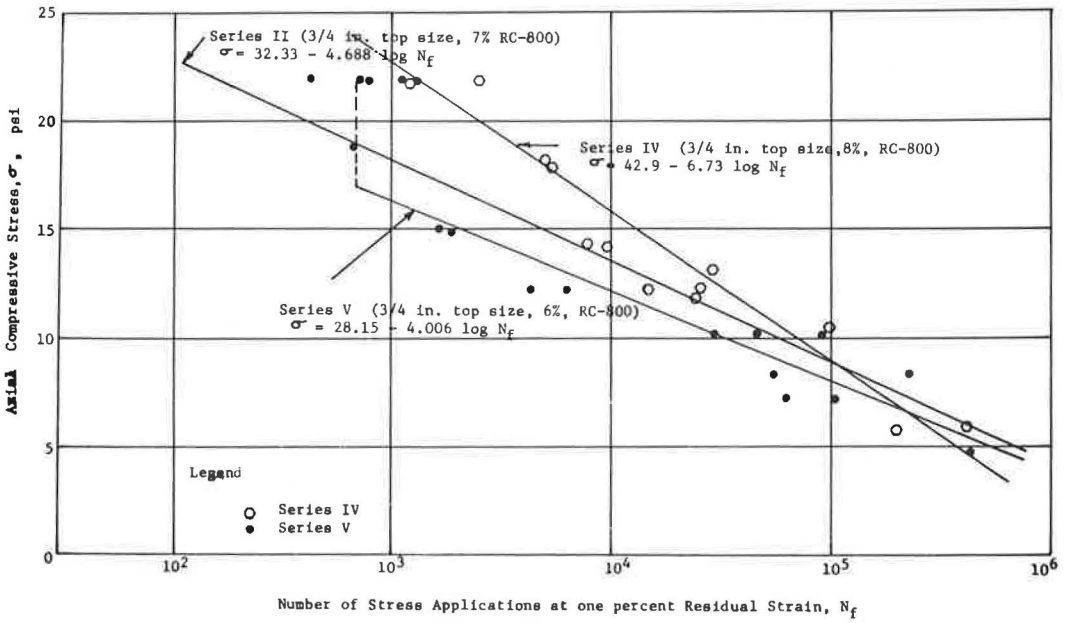

Figure 7. Influence of cutback content on the modulus of resilience.

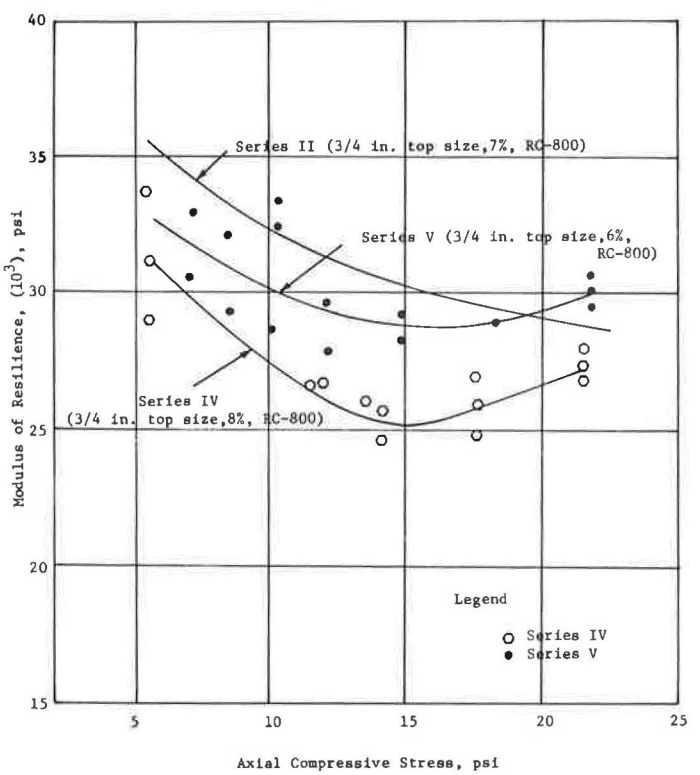

Figure 8. Influence of gradation on fatigue life of BAMs.

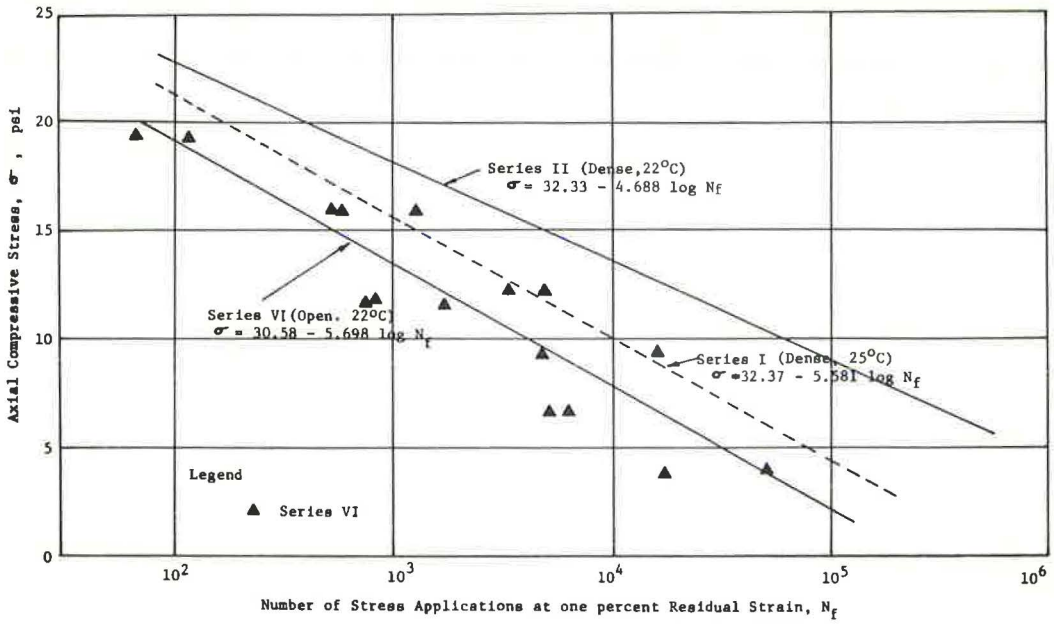

Figure 9. Influence of aggregate gradation on the modulus of resilience.

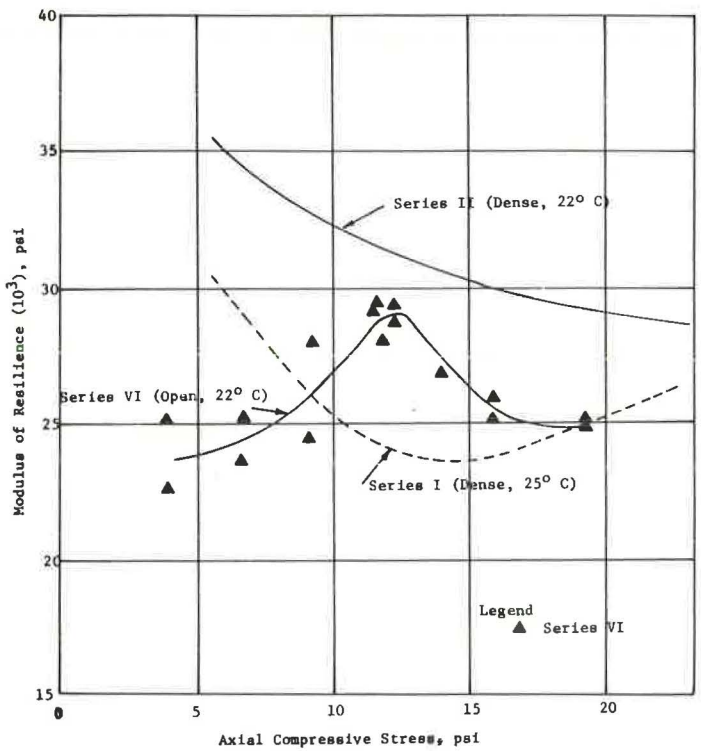

and the number of hydrocarbon volatiles left in the specimens after a curing period of 10 days were 1.5 percent and 2.7 percent (with respect to the original amount) respectively. Therefore, it is expected that the amount of water and the number of hydrocarbon volatiles left in specimens representing series VII (cured for about 300 days) would be close to zero before the curing period elapsed. In addition, an increase in the viscosity of the asphalt residue probably occurred because of the complete evaporation of the volatiles over the 300-day period. The increase in the viscosity of the residue means an increase in the molecular chain strength. In other words, the resistance to bond rotation and chain deformation might also have increased. Consequently, the application and removal of the repeated loads would result in relatively small and total resilient deformations. Thus, BAM specimens with higher binder viscosities are expected to have higher moduli of resilience than those with lower ones.

Figure 10 shows the influence of curing time on modulus of resilience. The figure indicates an average increase of about 80 percent in the modulus values, over a stress range from about 5 to 20 psi, because of an increase in the curing period from about 10 to 300 days. If the comparison is made with respect to the values of the modulus of resilience for compacted clay (tested in repeated-load triaxial compression at a confining pressure of 3.5 psi) reported by Seed et al. (5), then the modulus of BAM specimens (cured for about 300 days) would be about 19 times the modulus of the subgrade (over a stress range from about 10 to 20 psi). The increase of the modulus of resilience with curing time of BAM specimens prepared with MC-800 and tested in repeated-triaxial compression at confining pressures of 5 to 40 psi and a deviator stress of 10 psi was also reported by Terrel and Monismith (7).

Influence of Type of Cutback

The influence of type of cutback was studied by using an RC-800 cutback to prepare specimens of series II and an MC-250 to prepare those of series VIII. Test results

Figure 10. Influence of curing time on the modulus of resilience.

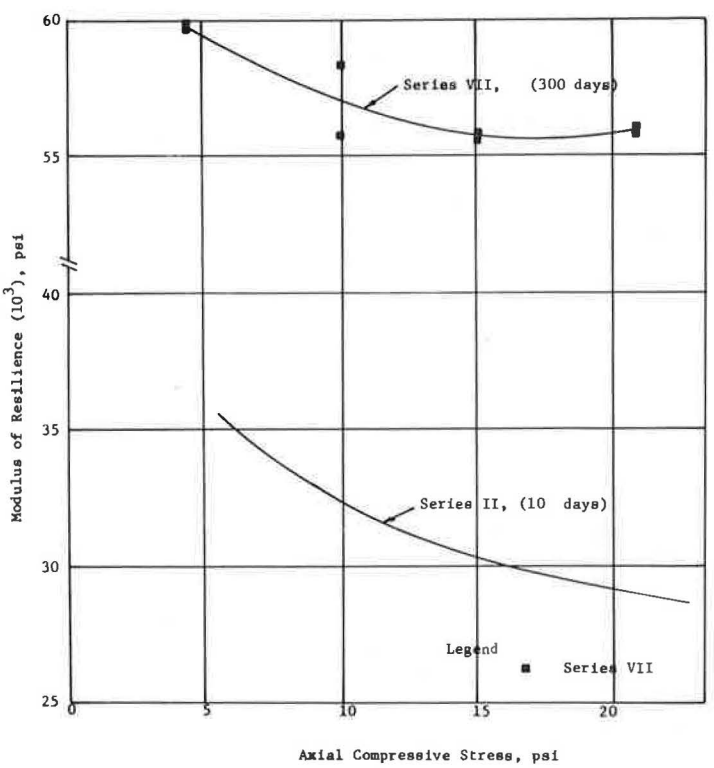

Figure 11. Influence of type of cutback asphalt on fatigue life of BAMS.

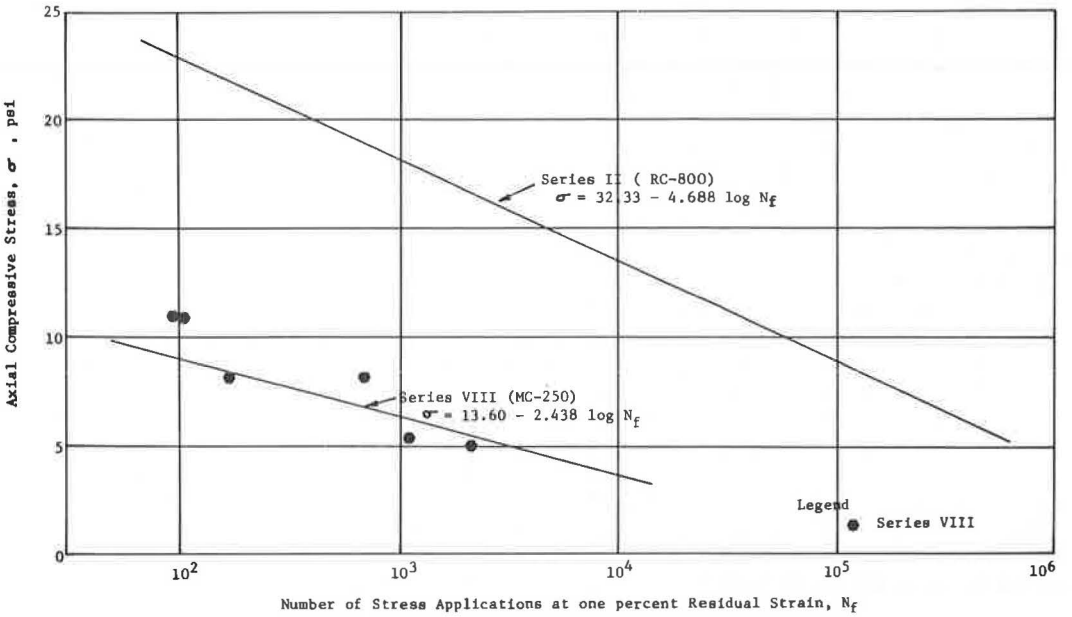

Figure 12. Influence of type of cutback asphalt on the modulus of resilience.

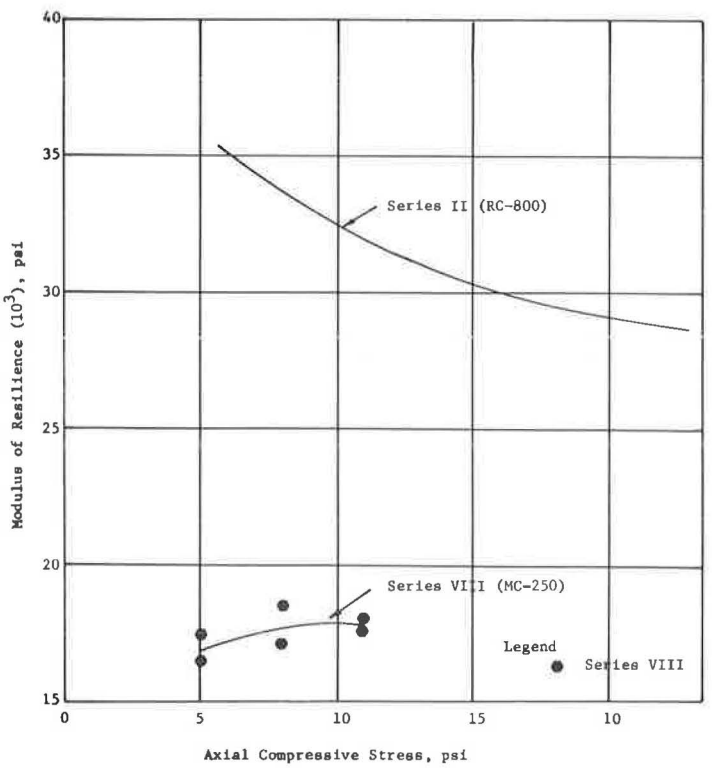

indicated that specimens prepared with the RC-800 cutback and cured for 10 days had better resistance to fatigue failure than those prepared with the MC-250 cutback and cured for 120 days (Fig. 11). Furthermore, specimens prepared with the MC-250 cutback had the shortest fatigue life among all of the other series investigated.

If the water and volatiles evaporated from the specimens of series II (RC-800) and series VIII (MC-250), the residue of the asphalt cement would govern the fatigue behavior of both series (other variables being similar). The major difference between the asphalt cement of the two types of cutback is the degree of viscosity. The RC-800 cutback is produced from an asphalt cement of a higher viscosity than that of the MC-250 cutback. The high-viscosity asphalt cement may resist shear stresses more than a softer one. As a result, specimens prepared with an RC-800 cutback have a higher resistance to the fatigue failure than those prepared with an MC-250 cutback (Fig. 11).

Figure 12 shows the influence of the type of cutback asphalt on the modulus of resilience. Because of the relatively low fatigue resistance of the specimens prepared with the MC-250 cutback, the maximum applied axial stress was about 11 psi. It does not seem that the modulus of resilience-stress relation of series VIII (MC-250) follows the general shape of the other series. The limited amount of experimental data of series VIII indicates that the modulus may increase with an increase in the axial stress from about 5 to about 9 psi and that it was constant from 9 to about 11 psi.

Figure 12 indicates also that the moduli of resilience of specimens prepared with the RC-800 cutback are much higher than those prepared with the MC-250 cutback. This increase is probably due to the high viscosity of the binder of the specimens prepared with the RC-800 cutback as compared to those prepared with the MC-250 cutback.

It can be concluded that specimens prepared with a high-viscosity asphalt cement tend to resist the fatigue failure much more than those prepared with a low-viscosity asphalt cement.

Endurance Limit

Repeated compressive tests performed in this investigation indicated no sign of the possibility of the existence of an endurance limit (Figs. 4, 6, 8, and 11) in the BAM specimens.

CONCLUSIONS

The following conclusions can be drawn from this study and are limited to the test materials and conditions.

1. Bituminous aggregate mixes exhibited progressive failure over a range of axial unconfined compressive stresses of about 4 to 24 psi.
2. Three distinct zones were observed on a plot of the residual strain versus the logarithm of number of repetitions. The zones had the following shapes: (a) straight line, (b) slight curvature, and (c) excessive curvature where the residual strain increased rapidly with little increase in the number of load applications. One percent residual strain always occurred at the slight curvature zone.
3. The fatigue life of BAMs tested under repeated compressive stresses are highly temperature dependent: Within the temperature range studied, the lower is the temperature, the longer is the life.
4. An increase in the cutback content from 6 to 8 percent increased the fatigue life of the BAM specimens. It should be noted that maximum density in a specimen does not necessarily result in maximum fatigue resistance because the maximum density occurred at a cutback content of 7 percent.
5. The viscosity of the binder has a significant influence on the fatigue life of BAMs. The higher is the viscosity, the longer is the life. BAM specimens prepared with MC-250 had the shortest fatigue life when compared with all series investigated.
6. In this investigation, there was no indication of the existence of an endurance limit for the BAMs.
7. In most cases, the modulus of resilience decreased with an increase of axial stresses to about 15 psi; it then leveled off and increased with further increase in the

stress up to about 24 psi. This behavior agrees with the relation of the modulus of resilience versus deviator stress for compacted subgrade soils (AASHO Road Test).

8. The moduli of resilience of BAMs are also temperature and viscosity dependent. The modulus increased with a decrease in the temperature, within the temperature range studied, and with an increase in the viscosity of the binder.

9. The magnitude of the modulus of resilience of dense-graded bituminous aggregate mix prepared with $^3/_4$-in. top size, 7 percent RC-800, cured for about 10 days, and tested at 22 C was found to be about 10 times as much as the modulus of resilience of subgrade AASHO Road Test (tested at a confining pressure of 3.5 psi) over a range of stress from 10 to 20 psi. When the curing time of BAM specimens increased to about 300 days, the previous ratio increased to about 19 over the same range of stresses.

10. The values of the modulus of resilience increased about 80 percent over a stress range from 5 to 20 psi when the curing time increased from 10 to about 300 days. Thus, curing has a very significant effect on the resilience characteristics of BAMs.

11. Both fatigue and resilience characteristics should be studied together when a selection of material for transportation structures is being made. Higher values of the modulus of resilience do not necessarily mean better fatigue resistance.

REFERENCES

1. Herrin, M. Drying Phase of Soil-Asphalt Construction. HRB Bull. 204, 1958, pp. 1-13.
2. Hveem, F. N. Pavement Deflections and Fatigue Failure. HRB Bull. 114, 1955, pp. 43-73.
3. Marek, C. R. Mechanism of Tensile Behavior and Failure of Asphalt Cement in Thin Films. Univ. of Illinois, PhD thesis, 1967.
4. Pell, P. S. Fatigue of Bituminous Materials in Flexible Pavements. Proc. Institution of Civil Engineers, Vol. 31, July 1955, pp. 283-314.
5. Seed, H. B., Chan, C. K., and Lee, C. E. Resilience Characteristics of Subgrade Soils and Their Relation to Fatigue Failures in Asphalt Pavements. Proc. Internat. Conf. of Struct. Design of Asphalt Pavements, 1962, pp. 611-636.
6. Seed, H. B., Mitry, F. G., Monismith, C. L., and Chan, C. K. Prediction of Flexible Pavement Deflections From Laboratory Repeated-Load Tests. NCHRP Rept. 35, 1967, 117 pp.
7. Terrel, R. L., and Monismith, C. L. Evaluation of Asphalt-Treated Base Course Materials. Proc. AAPT, Vol. 37, 1968, pp. 159-199.
8. Terrel, R. L., and Monismith, C. L. Bituminous Materials in Road Construction. H.M.S.O., London, 1962, Chapter 6, pp. 89-124.

ASPHALT PAVEMENT TEMPERATURES RELATED TO KUWAIT CLIMATE

Amir F. Bissada, Ministry of Public Works, Kuwait

This paper reports on the asphalt pavement temperatures measured in Kuwait, which vary from about 5 C to more than 75 C. The pavement temperatures recorded were summarized and related to important climate parameters including changes in air temperature and in the solar radiation received by the pavement. Data analysis shows that pavement temperatures and duration of these temperatures in Kuwait are relatively high compared to those in other hot areas. This led the author to consider the possible effects of high temperatures on the effective stiffness modulus of asphaltic layers and on the load-carrying capacity of the pavement. By applying the three-layer elastic system, we can show that the thickness of the asphaltic layer, for temperatures prevailing in Kuwait, is controlled by the value required to provide permissible vertical compressive strain on the underside of the asphalt layer.

•IN hot desert areas, such as Kuwait, it is the high temperatures and the duration of these temperatures that call for special attention and interest in research for developing procedures in design, analysis of performance, and laboratory testing that can account for the high temperatures.

The recent use of deflection measurements as an overlay design procedure for asphalt pavement and the application of thicker asphalt paving courses in heavy-duty roads in Kuwait have resulted in the need for more information concerning pavement temperatures.

Extensive research on temperature distribution in asphalt pavements has been carried out in many areas having different climates. In the United States, there was a need for knowledge of pavement temperatures representing cold, average, and hot climatic conditions (1, 2, 3).

The relatively high temperatures prevailing in Kuwait result in lowering the effective stiffness modulus of the asphaltic component of the pavement, which causes a decrease in its load-spreading properties and in the stability of the pavement as a whole. Much information is now available concerning the elastic as well as the viscoelastic properties and the stress-deflection relations of the asphalt pavement materials over a wide range of temperatures. This information could provide background for developing a procedure for pavement design at high temperatures.

The purpose of this paper is to present data on variations of asphalt pavement temperatures in Kuwait climatic conditions and to analyze the effect of these temperatures on asphalt pavements.

DATA COLLECTION

This study involved the collection of data on asphalt concrete pavement temperatures and air temperature and solar radiation.

The measurements of pavement temperatures took place during 1966-67 after the construction of an asphalt concrete pavement at the International Airport of Kuwait,

Sponsored by Committee on Mechanical Properties of Bituminous Paving Mixtures.

located at latitude 29 deg and 14 min north and longitude 47 deg and 59 min east at an approximate elevation of 55 m above sea level.

The asphaltic concrete laid was a dense-graded hot mix at a temperature of about 138 C. The mix met the local specification for base course (1½-in. maximum size) and surface course (½-in. maximum size). The asphalt cement was a locally produced type of grade 60 to 70 penetration. The spreading and compaction of the mix were carried out in layers 10, 10, 6, and 4 cm thick. Tests carried out on the core samples showed that the average bulk density of the asphalt concrete layers was 2.25 grams/cm^3. The subbase was a sandy soil containing calcareous material of 30 cm thickness compacted in 2 layers to about 95 percent AASHO T-180.

Holes about ¾ in. in diameter were bored in the asphalt concrete by using a special drill down to depths of 5, 10, 15, 20, and 25 cm from the surface. The holes were then filled with a light bituminous cutback. Laboratory glass thermometers with a temperature range of -10 to +110 C with an accuracy of ±1 C were inserted in these holes to the depth required. For the surface temperature measurements, the mercury bulb of the thermometer was painted with asphalt cement and laid on the surface and held there by a thin coat of asphalt cement.

Temperature readings were started for recording about 1 day after the thermometers had been fixed in position. Temperature measurements were taken at 6:00 a.m., 10:00 a.m., 2:00 p.m., and 6:00 p.m. on certain days of the year, which represent the range of various weather conditions that prevail in Kuwait.

Air temperature and solar radiation were recorded at 2-hour intervals during the data collection period at the meteorological station at Shuwaikh, located at latitude 29 deg and 20 min north and longitude 47 deg and 57 min east at an elevation of 11 m. Long-term meteorological records covering a 10-year period (from 1955 to 1965), which include the average maximum and minimum monthly change of air temperature, solar radiation received, and surface temperature, are given elsewhere (4, 5). The instruments used to obtain the readings were located and set up according to international standards.

DATA ANALYSIS

Air Temperature and Solar Radiation

It is known that both air temperature and solar radiation can add heat to the pavement to raise temperature. Straub, Schenck, and Przybycien (2) concluded that changes in solar radiation have a greater effect on pavement temperatures than does varying air temperature. In Kuwait, relatively high values of air temperatures and solar radiations have been recorded during the entire year and especially in the summer months. The maximum air temperature recorded in July and August was 49 C at a low-lying area in August 1957. The wind influences greatly the temperature in Kuwait. The hottest air temperatures occur on summer days during periods of calm or light northerly winds when there is no dust or humidity to block the sun's rays.

Frost is rare in Kuwait, although the air temperature near the ground may occasionally drop below the freezing point. The duration of freezing conditions is seldom long enough to cause ice to form. In no case have freezing conditions prevailed for more than a few hours.

Figure 1 shows the relative hot-weather condition that prevails in Kuwait. About 75 percent of the year, the air temperature exceeds 20 C up to an average maximum of 44 C.

Actinograph records of the solar radiation rate in kilowatt-hours received by one square meter of horizontal surface show that the maximum energy of solar radiation is equal to 1.08 kW/sq m/hr, which amounts to 9 kW-h/sq m daily in the summer. Figure 2 shows the average daily solar radiation and sunshine hours in each month. The average minimum solar radiation occurred in December and is 4 kW-h/sq m/day. The average maximum rate received from June to August is 8 kW-h/sq m/day.

Pavement Temperature Cycles

Daily pavement temperature cycles during the 1-year recording period are shown in Figures 3 through 7. The temperature cycles shown in these figures represent the different weather conditions that prevail in Kuwait. During a completely sunny summer day, the temperature cycle generally follows the pattern shown in Figure 8.

The surface pavement temperature reaches the highest value during the afternoon at about 2:00 p.m., as the solar radiation begins to decrease. Then it begins to fall and approaches the value of the air temperature during the night hours and becomes the lowest temperature for the entire pavement. The surface pavement has the greatest temperature extremes. As the depth of pavement increases, the wave of the temperature cycle becomes a flatter curve.

This pavement temperature pattern occurs during the winter on sunny days except that the temperature extremes are less marked because of the lower temperature effect of both air temperature and solar radiation (Fig. 9). However, the possibility of cloud cover during the winter season affects the surface pavement temperature greatly. On cloudy days, which generally do not represent more than 5 percent of the year in Kuwait, the difference in pavement temperatures measured at various depths approaches a minimum. The wave of the surface pavement temperature cycle becomes a flatter curve compared with that on a sunny winter day. However, in both cases the surface temperature remains always above the air temperature. This is similar to the case of hot climates (3) but differs from that indicated in cooler areas in the winter (6).

MAXIMUM AND MINIMUM PAVEMENT TEMPERATURES

Surface Pavement Temperature

The solar radiation temperature depends on the color, texture, and orientation of the pavement surface exposed. In Kuwait, the surface texture of asphalt concrete pavement under service gets rough because of weathering and stripping effects. It also changes in color from black to gray. This is the natural color of the exposed coarse aggregate and the dust or desert sand filling the surface voids. These changes in surface conditions cause a decrease in the absorbed amount of solar radiation. The temperatures measured on weathered or raveled asphalt concrete surface covered with dust were found to be about 8 C less than that of a clean black smooth-textured surface under the same weather conditions.

For surface pavement temperatures, a mercury thermometer was used with an asphalt-coated bulb resting on the surface. Half of the surface area of the bulb was touching the pavement surface, and the other half was exposed to the air. The temperatures recorded were considered representative of the amount of solar radiation absorbed by the asphalt-filler coating film and not that of the surface of the exposed coarse aggregate on the surface, which is of lower temperature. For purposes of evaluating the performance of the surface layer of asphalt concrete, the temperature of the asphalt coating film (and not that of the exposed coarse aggregate on the surface pavement) should be considered because of its thermoplastic characteristics.

The monthly changes in solar radiation, measured by means of the black-bulb thermometer in the meteorological station, show a good correlation with surface temperatures of asphalt pavement measured during the test period. The absolute and average maximum and minimum surface temperatures covering the years 1958 to 1967, recorded in the meteorological station in Kuwait, are shown in Figure 10. It shows that the absolute maximum temperature recorded was 84 C, and the average maximum temperature in July was 76 C. The absolute minimum surface temperature recorded was -4 C, and the average minimum temperature in January was 7 C. Figure 8 shows that the surface pavement in summer (July) experiences a daily temperature variation from 32 C to 74 C spread over daily 9-hour and 15-hour heating and cooling cycles respectively.

Figure 1. Average monthly air temperature.

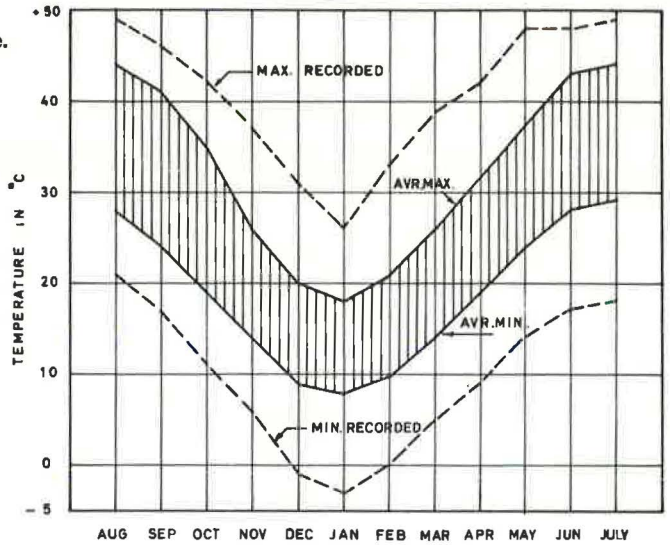

Figure 2. Average daily solar radiation and sunshine hours.

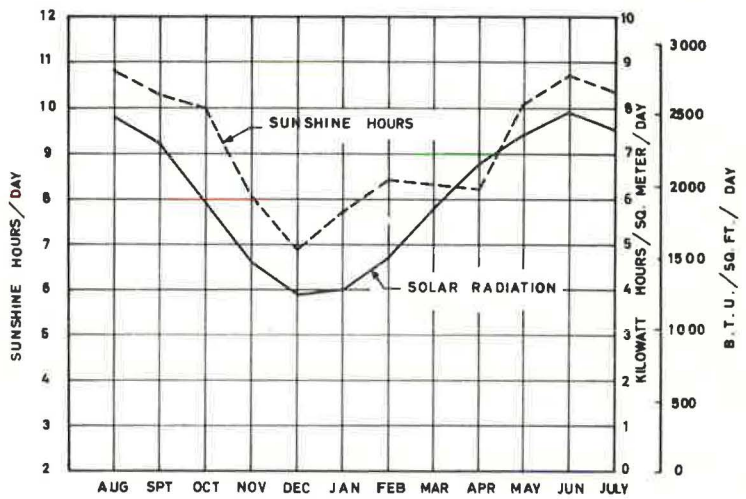

Figure 3. Typical pavement temperature cycle on a summer day.

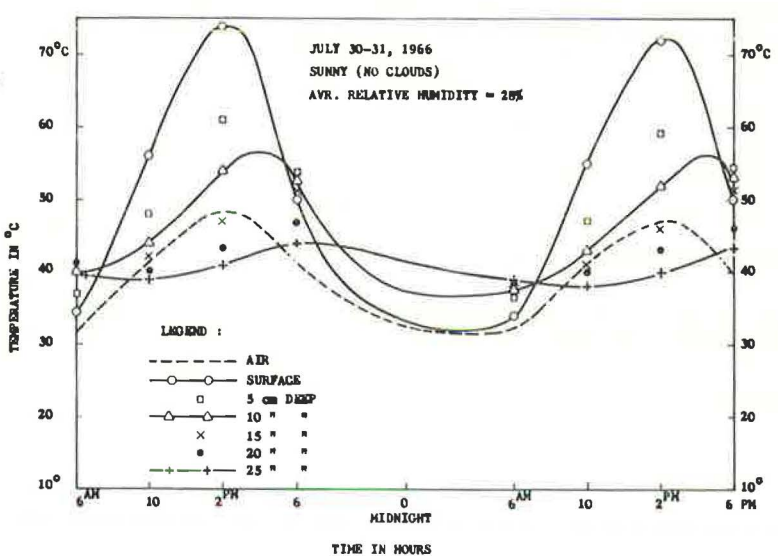

Figure 4. Typical pavement temperature cycle on an October day.

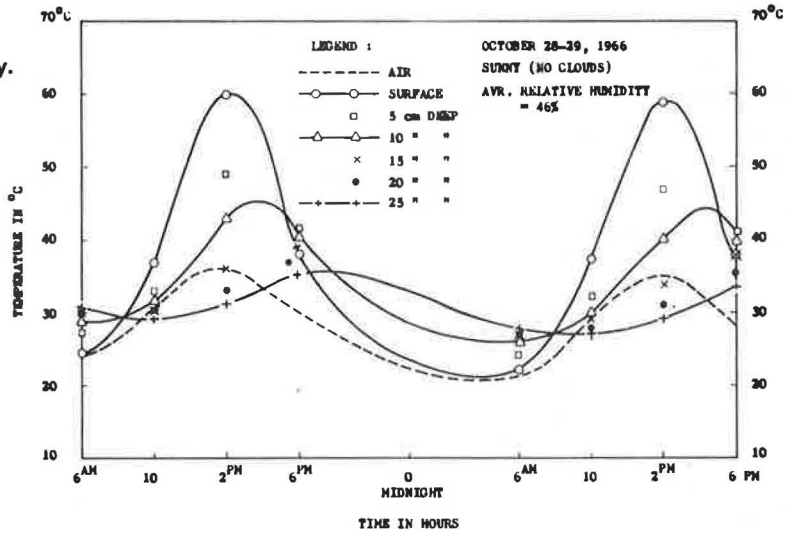

Figure 5. Typical pavement temperature cycle on a sunny winter day.

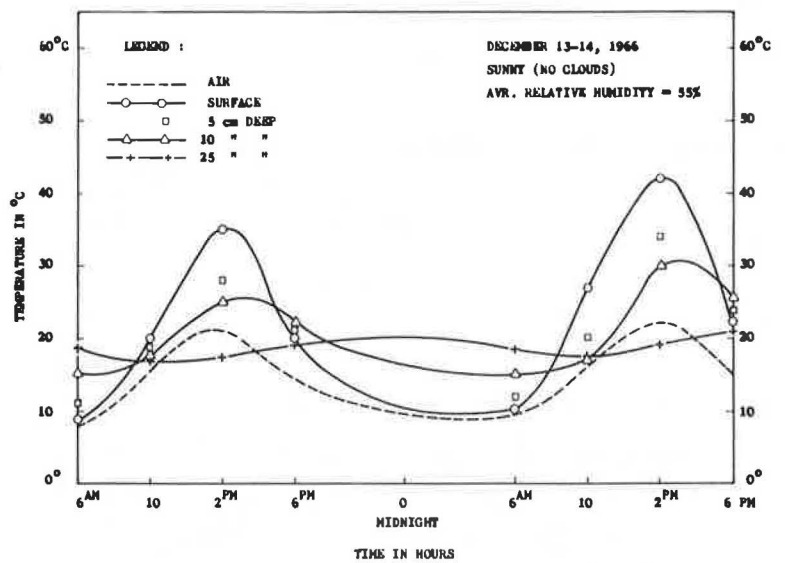

Figure 6. Typical pavement temperature cycle on a cloudy winter day.

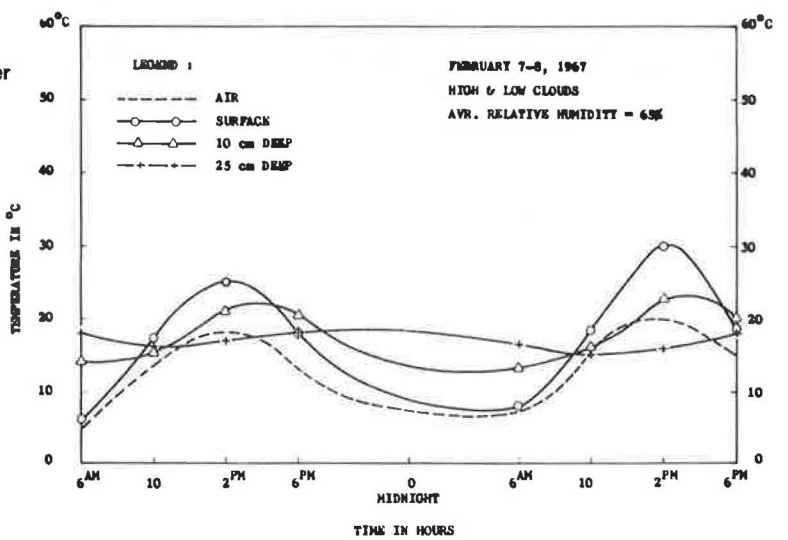

Figure 7. Typical pavement temperature cycle on an April day.

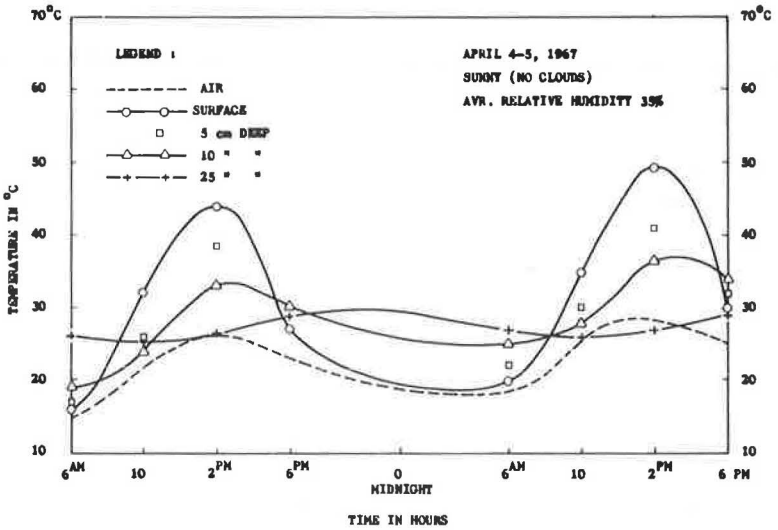

Figure 8. Temperature and solar radiation cycles on a sunny summer day in July.

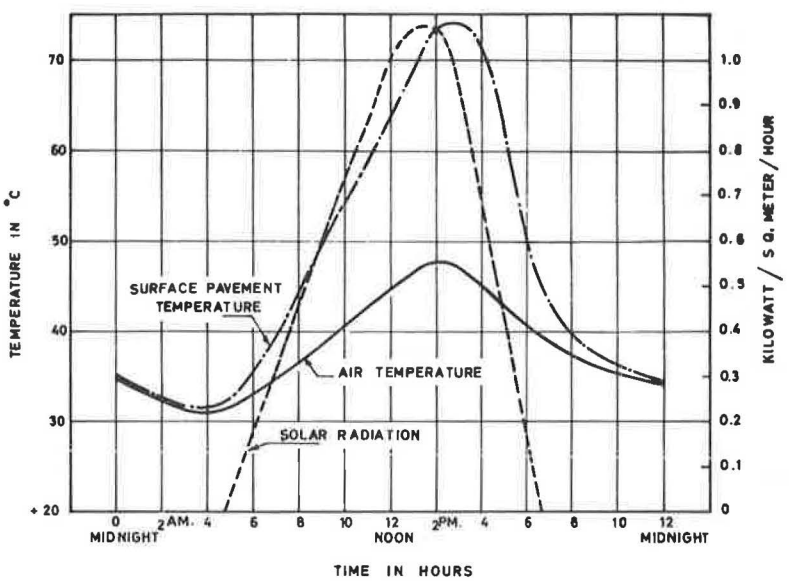

Figure 9. Temperature and solar radiation cycles on a sunny winter day in January.

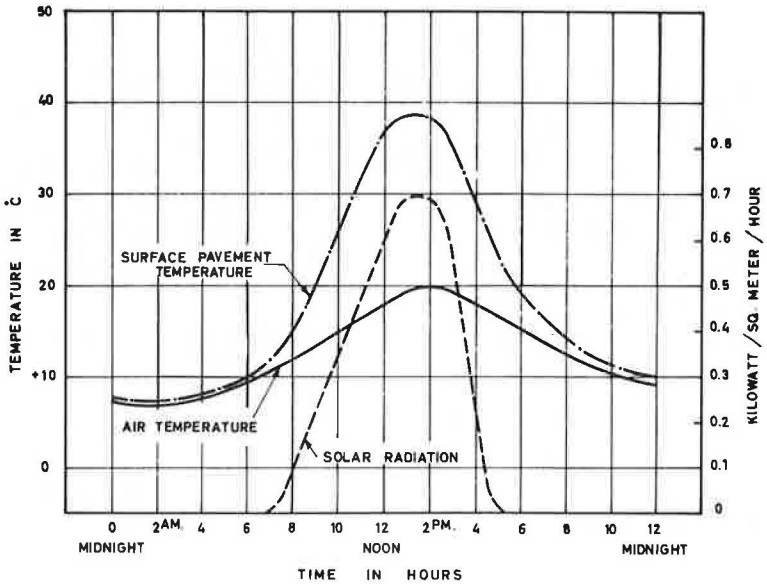

Figure 10. Monthly change in surface pavement temperatures.

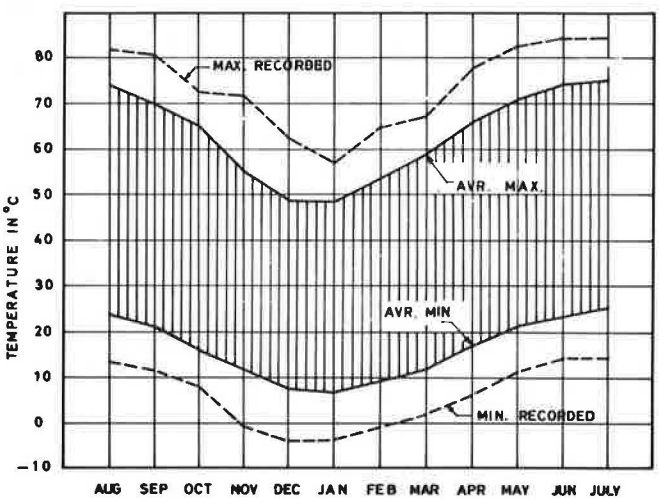

Lower Level Temperatures

Pavement temperatures at levels 5, 10, 15, 20, and 25 cm from the surface are shown in Figures 3 through 7. Similar to the surface temperature, the temperatures measured at deeper levels show their correspondence to the amount of solar radiation absorbed. As the depth increases, the extreme temperatures are delayed slightly from the layer above, depending on the time required for the heat conduction to the respective depth. On a summer day in July, the 5-cm pavement level cools during the early morning hours (6:00 a.m.) to 37 C and warms up to 60 C at 2:00 p.m. These temperatures are higher than the air temperature recorded on that date, which indicates the effect of solar radiation. At deeper layers, the daily variation in temperature is less extreme. At the 25-cm level, the temperature during July varies only between 39 and 44 C. Figure 11 shows the temperature gradient measured at 6:00 a.m. and 2:00 p.m. on sunny summer and winter days. At levels of 5, 10, 15, 20, and 25 cm from the surface, the maximum temperatures experienced during the recorded months were 74, 63, 57, 51, 47, and 45 C respectively. The minimum temperatures experienced at the surface (5, 10, and 25 cm) were 7, 11, 14, and 15 C.

RECORDED PAVEMENT TEMPERATURES IN KUWAIT AND IN OTHER CLIMATES

From the temperature readings taken during the test period, many inferences might be made; however, the temperature differences according to environment may be better shown through comparison.

Maximum Pavement Temperatures

Comparison of temperature gradients measured under maximum temperature conditions at Kuwait with other hot and cold climate areas gives some indication of the relative summer environments. Figure 12 shows that the maximum surface temperatures measured in Kuwait are 3 C higher than those measured in hot-climate areas like Tucson (3) and 12 C higher than those measured in colder climate areas like Maryland (1) and Potsdam, New York (2). However, the author feels that, in Kuwait, higher surface pavement temperature than that measured during the test period could occur. This is indicated by the maximum recorded temperatures over the 10-year period by means of the black-bulb thermometer (Fig. 10). Another reason is that surface temperatures have been measured with simple thermometers, which give approximate results and do not compare well with thermocouples fixed flush with the pavement surface.

Figure 12 shows also that, at the 10-cm level from the pavement surface, the minimum temperature measured in Kuwait is very close to that measured in southern Arizona (3) and is about 8 C and 11 C higher than that measured in Maryland (1) and Potsdam (2) respectively. At a deeper level than 10 cm the asphalt pavement is considerably less affected by the solar radiation conditions prevailing in the area that is the top pavement layer.

Temperature Prediction Methods

Southgate and Deen (7) have developed a set of figures for predicting pavement temperatures at depths up to 30 cm (assuming that the temperature at this depth is a function of the surface temperature, amount of heat absorption, and the air temperature of of the previous 5 days). This method has been recently used in Kuwait (10) to predict mean pavement temperature for the performance of Benkelman beam deflections.

The temperatures measured have been compared with those predicted by using Southgate's nomographs at 1:00 p.m. On a sunny summer day (July 31, 1966) surface pavement temperature was 74 C, and 5-day mean air temperatures were 40, 38, 37, 35, and 36 C. The following measurements were made:

Figure 11. Temperature gradient in asphalt pavement.

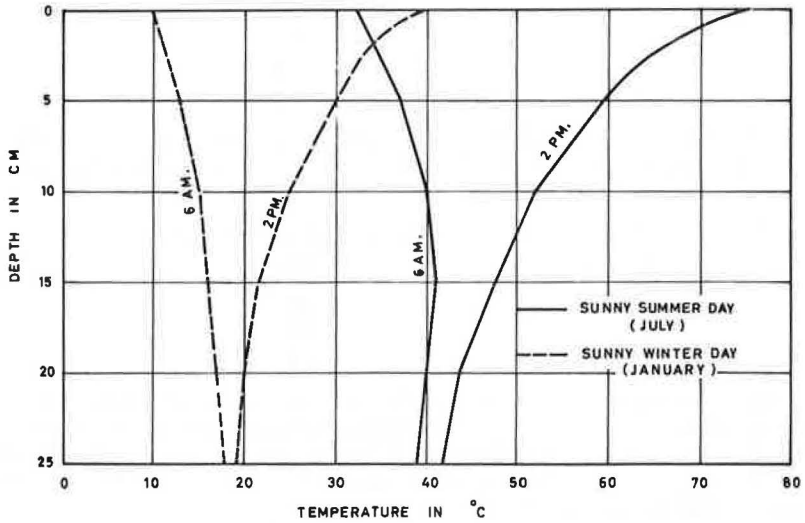

Figure 12. Comparison of asphalt concrete temperature gradient measured at different climates under maximum temperature conditions.

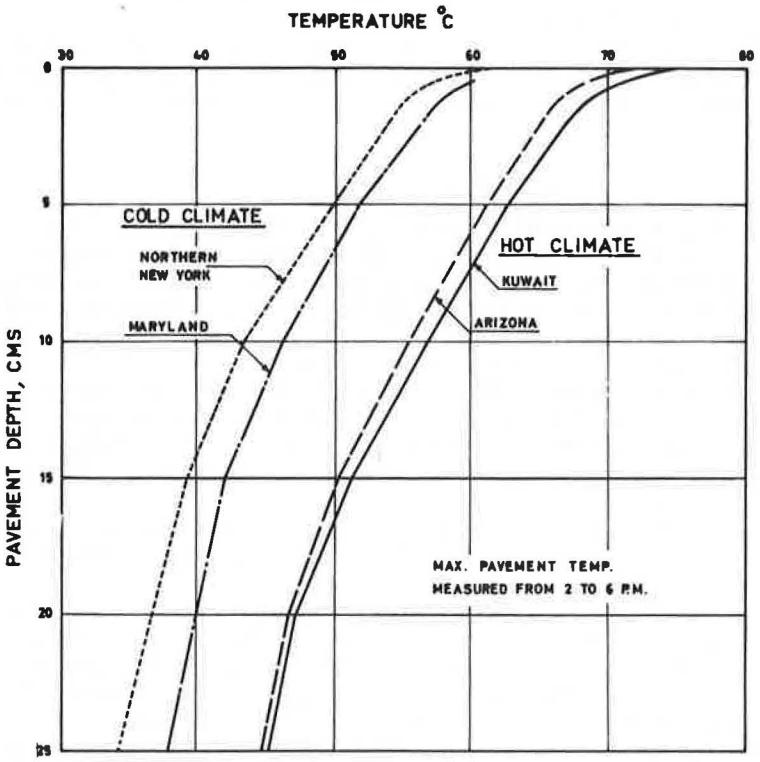

Depth (cm)	Recorded Temperature (deg C)	Predicted Temperature (deg C)
5	59	61
10	53	56
20	44	50

On a sunny winter day (December 13, 1966) surface pavement temperature was 36 C, and 5-day mean air temperatures were 15, 17, 20, 17, and 17 C. The following measurements were made:

Depth (cm)	Recorded Temperature (deg C)	Predicted Temperature (deg C)
5	30	29.5
10	25	26
20	20	24

This comparison does not show a close correlation between recorded and predicted temperatures, especially at deeper levels. The measured temperature gradient in Kuwait is steeper than that predicted by Southgate. This can be attributed to the relatively high amount of absorbed solar radiation in the top surface layer and the respective low heat conduction to the deeper levels.

The empirical curves developed by Rumney and Jimenez (3) for predicting upper layer peaks from air temperatures and solar radiation data have been compared with recorded values in Kuwait. Except for the air temperatures and solar radiation values that occur during the daytime in July and are higher than the range of these curves, the predicted maximum pavement temperatures from these figures correlate to the recorded values with an accuracy of ±4 F.

In all cases, it may be impossible to get a close correlation between measured and predicted values because of the number of variables involved in temperature predicting methods. A standard error of ±5 F as mentioned by Rumney and Jimenez (3) would be more realistic.

Frequency Distribution of Pavement Temperature

Because the temperature data collection at different pavement depths was limited to 1, 48-hour run each month (repeated during 5 months of the year), the temperature durations could be only approximated. Pavement temperatures at a depth of 10 cm have been predicted for various hours of the day by applying the method developed by Southgate and Deen (7).

From the surface temperature data, it can be seen that, during half of the year (May to October), the temperature is above 20 C 100 percent of the time and above 60 C about 8 percent of the time. During June, July, and August, the temperature reaches 70 C and remains above that about 5 percent of the time. Surface temperatures of 75 C and above were also recorded during the 3 summer months but did not remain for any appreciable length of time.

For asphalt concrete at a depth of 10 cm, the temperature was above 20 C 100 percent of the time during April to November. During June, July, and August the temperature reaches 55 C about 5 percent of the time.

In many parts of the United States, pavement temperatures do not reach the levels recorded in Kuwait. Figure 13 shows that, in Kuwait, the percentage of duration of pavement temperatures at a depth of 10 cm exceeding 43.3 C is higher than equivalent recorded values in the United States. The comparison indicates that, in general, the temperature of asphalt pavement at a 10-cm level ranges between 10 and 32.2 C about half of the year in both the cold and the hot climatic areas considered here. However, during the other half of the year, the temperature ranges between 32.2 and 54.4 C in hot climate areas like Kuwait and Arizona (3) and between -12 and +10 C in cold areas like northern New York (2).

A comparison of the percentage of time durations of asphalt concrete temperatures at 10 cm in depth laid in England (8) and Melbourne (9) with that recorded in Kuwait is

shown in Figure 14. The comparable results for 1 year show that asphalt pavement temperature at this level laid in Kuwait is about 15 and 8 C warmer than similar pavement material laid in England and Melbourne respectively.

HIGH-TEMPERATURE EFFECTS ON ASPHALT PAVEMENTS

On the basis of the relatively high pavement temperatures reported in this paper, the author suggests further investigation of high-temperature effects on asphalt pavements.

Design of Asphalt Mixtures

Current practice in designing asphalt mixtures does not explicitly recognize the high-temperature service requirements that prevail in Kuwait and other hot climatic areas. Current methods of designing asphalt mixtures specify minimum stability, deformation limits, and a range of air voids at 60 C, which is the assumed maximum service temperature.

Based on the pavement temperature data reported in this paper, the asphalt concrete surface layer of 5 cm thickness laid in Kuwait experiences temperatures between 60 and 75 C about 5 percent of the entire year. In many cases, it is difficult to follow the physical and chemical specification restrictions on the binder and aggregate components necessary to provide adequate stability of the mix at temperature service conditions exceeding 60 C. This might be due to the nonavailability of low-temperature susceptibility asphalt cements and/or the expensive well-crushed, angular, and graded aggregate material.

The design and performance of asphalt mixtures at temperatures higher than 60 C may need different test procedures from those normally used because of the nonlinear mechanical or viscoelastic properties of asphalt mixtures within this range of temperatures (18, 19, 20). It is suggested that the use be continued of the standard 60 C stability test for evaluating the physical and mechanical properties of asphalt mixes. However, it would be desirable in the future to study means for reducing the rate of absorption of solar radiation by asphalt pavement surfaces. This could be possibly achieved by increasing the surface texture of surface air gaps of the asphalt surface mix and also by changing the dark black color to a gray or any lighter color. This might result in lowering the surface temperature by about 5 to 8 C.

For asphalt base courses, it has been indicated by Khalifa and Herrin (11) and by McLeod (14) that increasing the maximum particle size up to 50 mm results in producing a mixture of higher stability at high-temperature conditions. The stiffness modulus determined by McLeod of asphalt base mixtures with a maximum size of 50 mm at the maximum temperature condition prevailing in Washington, D. C., was about double its value for a base mixture with a maximum size of 19 mm at the same temperature. Consequently, a substantial economy could be obtained by constructing asphalt pavement base courses in hot climatic areas, made with aggregates of larger maximum size because of the lower structural thickness requirement.

Structural Design

High-temperature design differs from that of low-temperature design because the stiffness modulus of the asphalt-bound material is very strongly temperature dependent. The results of the analysis done by Monismith and others (12, 13) on the effect of low stiffness value of the asphalt-bound material at high temperatures indicates that the granular base course exhibits a very low modulus of resilience. This is because of the tendency for tensile horizontal (radial) stresses to develop in the granular base course beneath the asphalt concrete layer.

It is suggested that, for the thickness design of asphalt pavements based on layered system theory, the stiffness values determined at the maximum and minimum layer temperatures in service be used instead of an assumed average stiffness of modulus for the asphalt-bound layer. The design principles concerning the horizontal (radial) tensile strain on the underside of the asphalt-bound layer and the vertical compressive strain in the surface of the subgrade are highly dependent on the pavement

Figure 13. Comparison of pavement temperature durations at depth of 10 cm.

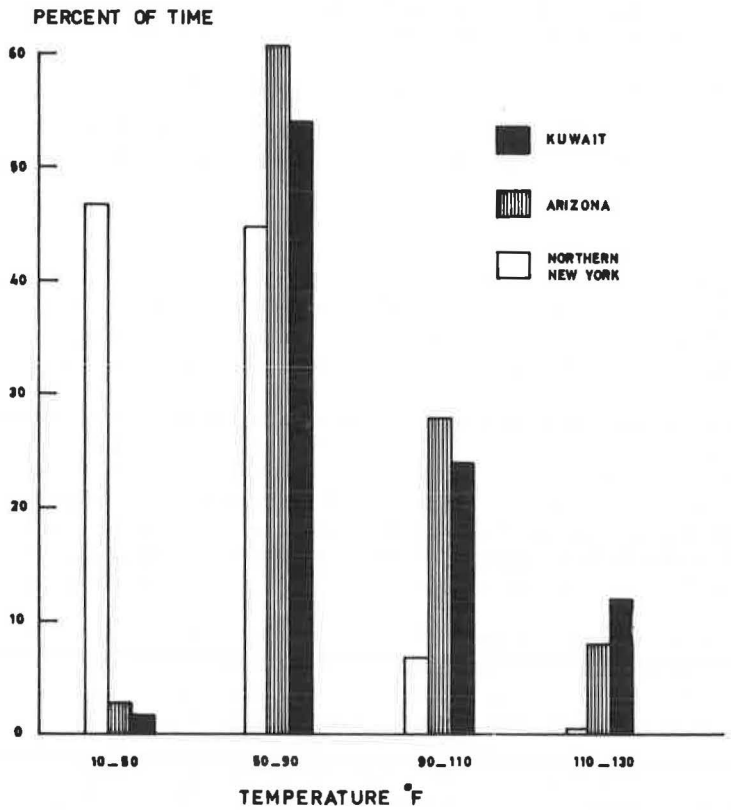

Figure 14. Frequency distribution of temperature over 1-year period.

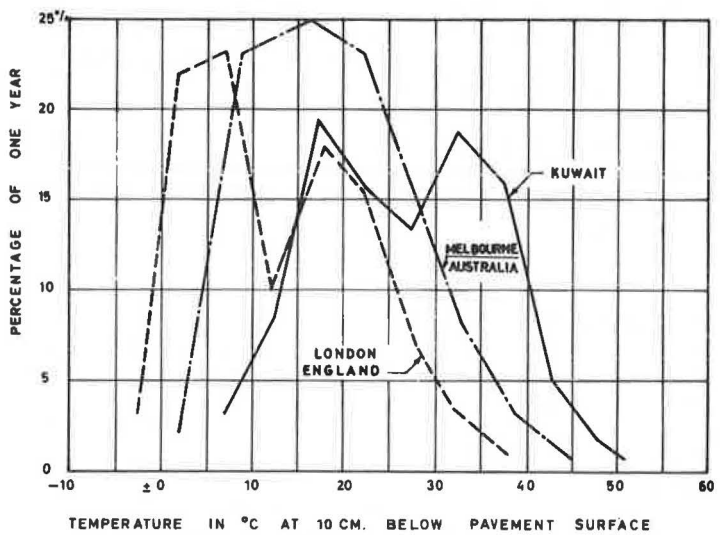

Figure 15. Details of three-layer pavement system.

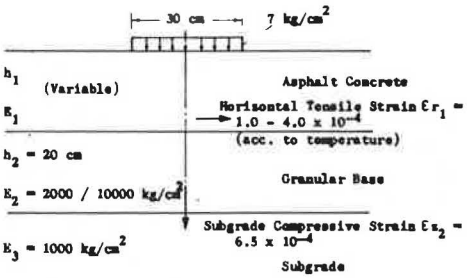

Figure 16. Required asphalt concrete thickness in hot and cold climates.

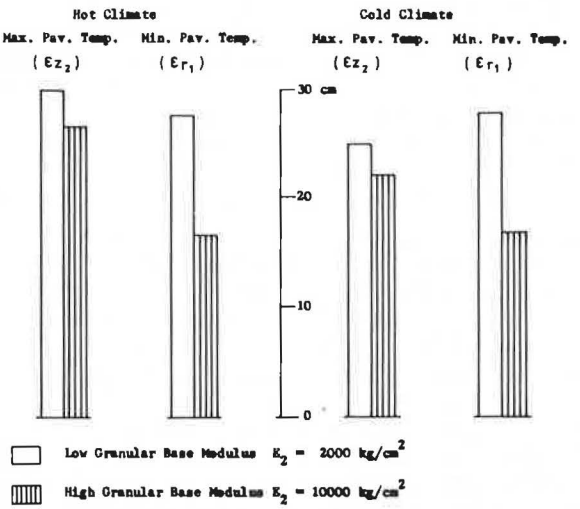

Table 1. Stiffness modulus of asphalt concrete as a function of layer temperature in hot climate (Kuwait).

Asphalt Pavement Depth (cm)	Maximum Service Temperature			Minimum Service Temperature		
	Temperature (deg C)	Stiffness Modulus[a] (kg/cm²)		Temperature (deg C)	Stiffness Modulus[a] (kg/cm²)	
		Asphalt Cement[b]	Asphalt Concrete[c]		Asphalt Cement[b]	Asphalt Concrete[c]
5	67	0.15	450	9	750	140,000
10	60	0.4	850	12	500	84,000
20	52	1.2	2,000	14	400	70,000
30	45	3.5	4,000	15	350	70,000

[a]Loading time: 0.04 sec (4 cps).
[b]Asphalt cement (recovered): penetration, 25 C, 100 grams, 5 sec = 50; viscosity at 60 C = 9,000 poises; penetration index = 0.0; and base temperature = 55 C.
[c]Asphalt concrete: 5 percent asphalt content by weight, 4 percent air voids, and concentration volume = 0.885.

Table 2. Stiffness modulus of asphalt concrete as a function of layer temperature in cold climate (northern New York).

Asphalt Pavement Depth (cm)	Maximum Service Temperature			Minimum Service Temperature		
	Temperature (deg C)	Stiffness Modulus[a] (kg/cm²)		Temperature (deg C)	Stiffness Modulus[a] (kg/cm²)	
		Asphalt Cement[b]	Asphalt Concrete[c]		Asphalt Cement[b]	Asphalt Concrete[c]
5	53	0.4	1,000	-14	5,000	245,000
10	47	0.6	1,500	-13	4,000	220,000
20	40	3.0	3,500	-11	3,500	196,000
30	34	7.5	7,000	-8	3,000	175,000

[a]Loading time: 0.04 sec (4 cps).
[b]Asphalt cement (recovered): penetration, 25 C, 100 grams, 5 sec = 90 (assumed); viscosity at 60 C = 2,000 poises; penetration index = 0.0; and base temperature = 49 C.
[c]Asphalt concrete: 5 percent asphalt content by weight, 4 percent air voids, and concentration volume = 0.885.

temperature conditions. This dependence is related to variations in stiffness of asphalt concrete layer due to temperature changes.

An analysis of the response of an asphalt pavement system using the elastic theory at both high and low temperatures is shown in Figures 15 and 16 and Tables 1 and 2. The stiffness modulus of asphalt concrete has been determined by means of a procedure described by McLeod (14) as a function of maximum and minimum in-service layer temperatures reported in Kuwait and in northern New York. Burmister's (15) three-layer elastic theory was employed to determine the thickness of asphalt concrete for a certain wheel load and subgrade supporting conditions. An average of the moduli-of-stiffness values for the number of pavement layers was employed to provide the overall average modulus-of-stiffness value substituted in the elastic layer theory at both maximum and minimum temperature service conditions in each case.

Permissible values for compressive strain in the subgrade were obtained from experience with pavements designed according to CBR curves and correlations with the AASHO Road Test results (16). Laboratory fatigue data presented by Heukelom and Klomp (17) were used to establish strain-load repetition relations for the asphalt layer, and the influence of temperature was considered.

The following conclusions were reached from the theoretical analysis.

1. The design of asphalt concrete layer thickness at the temperatures prevailing in Kuwait is controlled by the design criterion of the vertical compressive strain in the surface of the subgrade. In the case of colder climates (northern New York) the asphalt concrete thickness is controlled by the design criterion of the horizontal tensile strain on the underside of the asphalt concrete layer.
2. The required thickness of asphalt concrete layer at high-temperature conditions (Kuwait) is more than that required in colder climates for the same wheel load, subgrade, and granular base supporting conditions.
3. At high-temperature conditions, the thickness of asphalt concrete layer has a more significant effect on the magnitude of vertical compressive strain in the surface of the subgrade than the thickness of granular base course or its modulus of resilience.

CONCLUSIONS

In Kuwait, investigation of pavement temperature conditions has only recently been started. Additional studies and further measurements of these temperatures and their variation with depth are necessary.

The temperature data reported indicate the following.

1. Pavement temperatures are directly related to major climate factors of air temperature and solar radiation and will vary greatly with depth.
2. Asphalt surface courses in Kuwait experience substantial extremes in temperature. Within 9 hours on a summer day, the surface pavement temperature fluctuates between 32 and 74 C. During the year, asphalt surface temperatures fluctuate between an average minimum of 5 C and an average maximum of 74 C.
3. In Kuwait asphalt base courses (at depths of more than 10 cm from the surface) are subject to smaller temperature fluctuations—between an average minimum of 15 C and an average maximum of 50 C.
4. A comparison of measured pavement temperatures in Kuwait with those in other climates shows the importance of studying the effect of the relatively high pavement temperatures on structural design, performance analysis, and laboratory testing.

ACKNOWLEDGMENTS

This study was made possible by the support of the Roads and Drainage Department, Ministry of Public Works, Kuwait, in cooperation with the Federal Highway Administration, Kuwait Division. The author wishes to express grateful acknowledgments to the organizations and individuals who willingly contributed to this work. Credit must also be given to authors who have done previous work on this subject.

REFERENCES

1. Kallas, B. F. Asphalt Pavement Temperatures. Highway Research Record 150, 1966, pp. 1-11.
2. Straub, A. L., Schenck, H. N., Jr., and Przybycien, F. E. Bituminous Pavement Temperature Related to Climate. Highway Research Record 256, 1968, pp. 53-77.
3. Rumney, T. N., and Jimenez, R. A. Pavement Temperatures in the Southwest. Highway Research Record 361, 1971, pp. 1-13.
4. Climatological Data for Kuwait. Government of Kuwait, Meterological Service.
5. Allison, T. R. Factors Affecting the Design and Construction of Buildings and Roads in Kuwait. Government Research Station, Ministry of Public Works, Kuwait, 1966.
6. Galloway, J. W. Temperature Durations at Various Depths in Bituminous Roads. Gt. Brit. Road Research Laboratory, RRL Rept. LR 138, 1968.
7. Southgate, H. F., and Deen, R. C. Temperature Distribution Within Asphalt Pavements and Its Relationship to Pavement Deflection. Highway Research Record 291, 1969, pp. 116-131.
8. Trott, J. J. An Apparatus for Recording the Duration of Various Temperatures in Records. Roads and Road Construction, Vol. 41, 1963, p. 491.
9. Scala, A. J., and Dickinson, E. J. The Use of Asphalt Pavement Structures in the Australian Environment. Proc. 2nd Internat. Conf. on Structural Design of Asphalt Pavement, Univ. of Michigan, 1967.
10. Asphalt Overlays and Pavement Rehabilitation. The Asphalt Institute, Manual Series 17, 1969.
11. Khalifa, M. O., and Herrin M. The Behavior of Asphaltic Concrete Constructed With Large-Sized Aggregate. Proc. AAPT, Vol. 39, 1970.
12. Monismith, C. L., Seed, H. B., Mitry, F. G., and Chan, C. K. Prediction of Pavement Deflections From Laboratory Tests. Proc. 2nd Internat. Conf. on Structural Design of Asphalt Pavements, Univ. of Michigan, 1967.
13. Duncan, J. M., Monismith, C. L., and Wilson, E. L. Finite Element Analyses of Pavements. Highway Research Record 228, 1968, pp. 18-33.
14. McLeod, N. W. Discussion of paper Factors Influencing Dynamic Modulus of Asphalt Concrete (Shook, J. F., and Kallas, B. F.). Proc. AAPT, Vol. 38, 1969, pp. 166-178.
15. Jones, A. Tables of Stresses in Three-Layer Elastic Systems. HRB Bull. 342, 1962, pp. 176-214.
16. Dormon, G. M., and Metcalf, C. T. Design Curves for Flexible Pavements Based on Layered System Theory. Highway Research Record 71, 1965, pp. 69-84.
17. Heukelom, W., and Klomp, A. J. G. Dynamic Testing as a Means of Controlling Pavements During and After Construction. Proc. Internat. Conf. on Structural Design of Asphalt Pavements, Univ. of Michigan, 1962.
18. Barksdale, R. D. A Nonlinear Theory for Predicting the Performance of Flexible Highway Pavements. Highway Research Record 337, 1970, pp. 22-39.
19. Bissada, A. F. On the Deformation Mechanism and Visco-Elastic Behavior of Asphalt Mixture by Statical Loads. Tech. Univ., Darmstadt, West Germany, PhD thesis, 1962.
20. Monismith, C. L., and Secor, K. E. Visco-Elastic Behavior of Asphalt Concrete Pavements. Proc. Internat. Conf. on Structural Design of Asphalt Pavements, Univ. of Michigan, 1962.

ASPHALT CEMENT VISCOSITIES AT AMBIENT TEMPERATURES BY A RAPID METHOD

Herbert E. Schweyer, University of Florida

This paper describes a method for determining the apparent viscosity and shear susceptibility of asphalt cements at 25 C and other ambient temperatures. Although it is based on another study, the present work utilizes a modified barrel and sample holder to permit improved productivity in running tests. A modified plunger is used that eliminates certain interferences. Apparent viscosity is evaluated at a selected shear rate, and shear susceptibility is measured by the complex flow index that is the exponent in the power law equation for non-Newtonian fluids. It is believed that the proposed method is adaptable for a routine testing procedure by using carefully standardized capillaries and more sensitive load cells with sophisticated temperature control. When such a test is developed by cooperative effort, it is believed it would replace the penetrometer and other empirical flow tests to provide rheological information of practical value for explaining service behavior. In fact, such information should be useful in design for applications where the rheology of the asphalt component is a critical factor.

•THERE is a demand for a simple, rapid test to measure the consistency in absolute units of asphalt cements in the ambient temperature range of 10 to 60 C. Methods have been proposed in ASTM standards (1) for this purpose, but they are complicated and generally not suitable except for research studies. The method discussed in this paper will be proposed as an alternative method for consideration by a task force of ASTM Committee D04.40. The extrusion method proposed is based on an earlier study in a companion paper by Schweyer and Busot (2), which discussed in detail certain theoretical and empirical aspects of the method.

The test is applied to asphalts sufficiently fluid that they can be extruded through an appropriate capillary without exceeding the safe loads of the apparatus. Accordingly, the limits of viscosity for the test will depend not only on the viscosity of the asphalt but also on the specific geometry (diameter and length of the capillary) that is employed for the determination. The test procedure is for use at 25 C but would also apply for other temperatures where the viscosity of the asphalt or the combination of diameter and length of the capillaries employed were such that satisfactory results would be obtained. Under these conditions, the preparation step on the samples for 25 C would necessarily have to be altered for whatever temperature was being used.

The object of the evaluations is to determine the apparent viscosity of the asphalt in terms of the ratio of the shearing force divided by the corrected rate of shear at a standard condition for rate of shear. In addition, the shear susceptibility is evaluated as the constant in the power law equation.

STUDY PROCEDURE

The procedure is similar to a previous one (2) except that the component equipment design has been changed to provide greatly increased productivity and simplicity. In

Sponsored by Committee on Characteristics of Bituminous Materials.

the earlier methods, a very expensive and cumbersome barrel (into which the sample is poured) was used; it has been replaced by a simple sample tube. These inexpensive sample tubes, which carry a capillary and can be filled in multiples and then brought to temperature, are inserted into a simple barrel holder for each run. They are then removed quickly and replaced by a new sample tube and capillary containing the next sample that had previously been brought to temperature and that is ready to run.

Figure 1 shows the rheometer assembly, and Figure 2 shows the rheometer components.

STUDY RESULTS

The results of the modified sample tube method as compared with the long barrel method (2) are given in Table 1 for 25 C and in Table 2 for 15.5 C.

In general, the data for 25 C for a rheometer barrel and sample tube are in good agreement (Table 1). In Table 2, the data for 15.5 C show anomalies because the sample tube data are in good agreement, but the data for the barrel and tube do not agree. Based on recent experimental work, the explanation for the difference is in the flow of asphalt in a very thin layer in front of the O-ring between the tube wall and the plunger. The high drag in this region apparently is accentuated for the low temperature data. The plunger has been redesigned to minimize this interference.

Comparison of Methods

A comparison of certain data obtained by using the capillary rheometer, the cone and plate (1, 3), and the sliding plate procedures (1, 4) is given in Table 3. These procedures compute the viscosity at 0.05 reciprocal sec without the power law correction for rate of shear (2). These data were developed through a joint effort with R. N. Traxler of the Texas Transportation Institute and V. T. Puzinauskas of The Asphalt Institute in connection with studies of a task force of committee ASTM D4.44 on rheological tests. The agreement over a range of data is shown in Figure 3. The solid line indicates exact agreement. The Florida method data are corrected for geometry and the Rabinowitsch correction (2). The complex flow indexes given in Table 3 were computed by the author from graphs supplied by the other investigators. For the cone and plate method, the plot of log viscosity versus log shear rate was used. A straight line was drawn from the viscosity at 0.05-sec^{-1} shear rate through the points at higher shear rates to provide an estimate of complex flow. For the sliding plate method, the reciprocal slope of log shear rate versus log shear stress was evaluated. For this method, the data are close together, and it is possible to make errors in estimating the true slope.

Shear Susceptibility

The effect of shear susceptibility on the apparent viscosity is shown in Figure 4. The complex flow index indicates that asphalt D is definitely more shear susceptible than asphalt B. At $\dot{\gamma} = 0.1$ sec^{-1}, both asphalts have about the same consistency; at $\dot{\gamma} = 1.0$ sec^{-1}, the D sample has only 50 percent of the viscosity of sample B. These effects are accentuated for the harder asphalts that have a low value of the complex flow index. Samples M and F are similar at 0.05 sec^{-1}, but at 1.0 sec^{-1} the M sample has only about 20 percent of the viscous resistance as the F sample. This could be of significance in service applications under stress. The data in Figure 4 at other than 0.05 and 1.0 sec^{-1} are for values at a constant power input. As shown by the data and the plot, comparative data at a constant power input occur at different rates of shear depending on the consistency of the asphalt cement and the degree of complex flow that results from the nature of the basic rheological relation. Data for Figure 4 are given in Table 4.

Because shear susceptibility is an important property in distinguishing among asphalt cements, it should be considered in more than a cursory manner. Because it affects the deformation profile under stress, shear susceptibility must be considered in the theoretical analysis of viscosity data. Current ASTM procedures do not consider these implications, but they do arbitrarily state that comparisons should be made at some

Figure 1. Rheometer assembly.

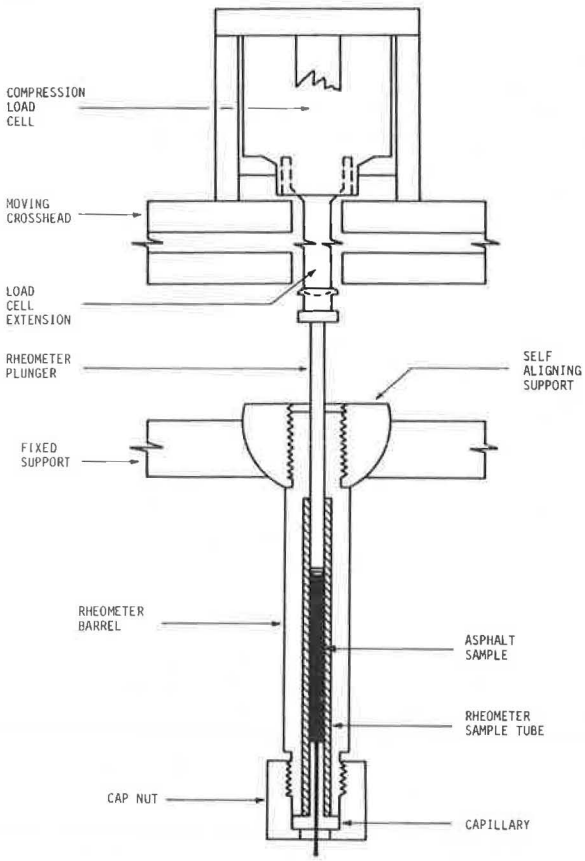

Figure 2. Rheometer components.

Table 1. Comparative data using Florida method for determination of apparent viscosity at 25 C and 180-deg entry for asphalt cements.

Asphalt	Penetration at 25 C	Equipment	Capillary (in.)	Sample Size (in.)	Tube Size (in.)	Apparent Viscosity (MP)	Complex Flow Index C
Smackover, S63-4	89	Barrel extrusion and conical plunger	1/16 by 1 1/4	4 1/2	-	1.64	0.82
						1.48[a]	0.84[a]
			3/16 by 3	3	-	1.91	0.86
		Tube extrusion and conical plunger	1/16 by 1 1/4	4 1/2	6	1.75	0.79
		Tube extrusion and blunt plunger	1/16 by 1 1/4	4 1/2	6	1.22	0.82
			1/8 by 1 1/4	4 1/2	6	1.78	0.80
Air-blown, S63-13	89	Barrel extrusion and conical plunger	1/16 by 1 1/4	4 1/2	-	0.60	0.64
						0.62[a]	0.64[a]
			3/16 by 3	3	-	0.66[a]	0.78[a]
		Tube extrusion and conical plunger	1/16 by 1 1/4	4 1/2	6	0.73	0.64
		Tube extrusion and blunt plunger	1/16 by 1 1/4	4 1/2	6	0.84	0.64
			1/8 by 1 1/4	4 1/2	6	0.98	0.65
Panuco, S63-19	90	Barrel extrusion and conical plunger	1/16 by 1 1/4	4 1/2	-	1.33	0.89
						0.98[a]	0.85[a]
			3/16 by 3	3	-	1.69[a]	0.82[a]
		Tube extrusion and conical plunger	1/16 by 1 1/4	4 1/2	6	1.28	0.84
		Tube extrusion and blunt plunger	1/16 by 1 1/4	4 1/2	6	0.93	0.80
			1/8 by 1 1/4	4 1/2	6	1.54	0.81
Los Angeles Basin, S63-20	89	Barrel extrusion and conical plunger	1/16 by 1 1/4	4 1/2	-	1.20	0.98
						1.34[a]	1.02[a]
			3/16 by 3	3	-	1.52[a]	1.05[a]
		Tube extrusion and conical plunger	1/16 by 1 1/4	4 1/2	6	1.31	0.96
		Tube extrusion and blunt plunger	1/16 by 1 1/4	4 1/2	6	1.31	1.11
			1/8 by 1 1/4	4 1/2	6	1.40	0.92
Kern River, S63-21	89	Barrel extrusion and conical plunger	1/16 by 1 1/4	4 1/2	-	-	-
			3/16 by 3	3	-	-	-
		Tube extrusion and conical plunger	1/16 by 1 1/4	4 1/2	6	-	-
		Tube extrusion and blunt plunger	1/16 by 1 1/4	4 1/2	6	1.17	1.17
			1/8 by 1 1/4	4 1/2	6	1.33	0.99

[a]Taken from Schweyer and Busot (2); 3-in. samples, 90-deg entry.

Figure 3. Comparative results below 4.0 MP for asphalt cements at 0.05 reciprocal sec.

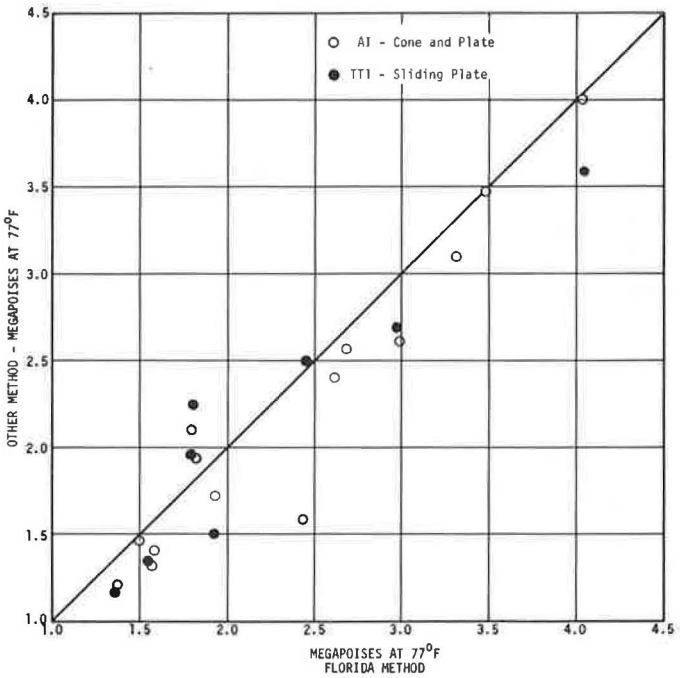

Figure 4. Shear susceptibility of various asphalts.

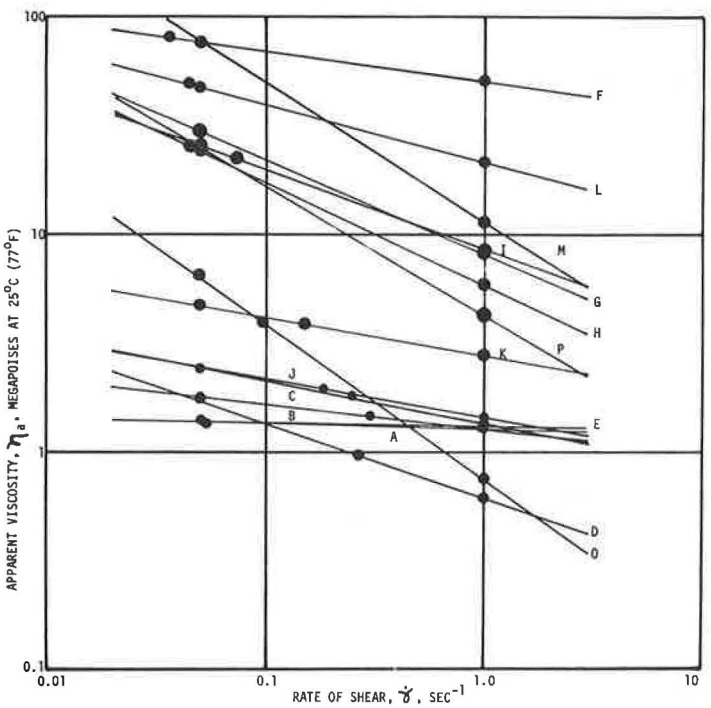

Table 2. Comparative data using Florida method for determination of apparent viscosity at 15.5 C and 180-deg entry for asphalt cements.

Asphalt	Penetration at 15.5 C	Equipment	Capillary (in.)	Sample Size (in.)	Tube Size (in.)	Apparent Viscosity (MP)	Complex Flow Index C
Smackover, S63-4	89	Barrel extrusion and conical plunger	1/16 by 1 1/4	3	-	22.3	0.78
			3/16 by 3	3	6	9.1	0.79
		Tube extrusion and conical plunger	1/8 by 1 1/4	4 1/2	6	10.5	0.84
			1/16 by 1 1/4	3	4	7.7	0.76
		Tube extrusion and blunt plunger	1/16 by 1 1/4	4 1/2	6	8.21	0.80
			3/16 by 3	4 1/2	6	8.12	0.81
			1/8 by 1 1/4	4 1/2	6	9.03	0.74
Air-blown, S63-13	89	Barrel extrusion and conical plunger	1/16 by 1 1/4	3	-	4.4[a]	0.72[a]
			3/16 by 3	3	6	4.7	0.74
		Tube extrusion and conical plunger	1/8 by 1 1/4	4 1/2	6	3.3	0.71
			1/16 by 1 1/4	3	4	3.8	0.68
		Tube extrusion and blunt plunger	1/16 by 1 1/4	4 1/2	6	4.18	0.63
			3/16 by 3	4 1/2	6	3.46	0.59
			1/8 by 1 1/4	4 1/2	6	3.73	0.56
Panuco, S63-19	90	Barrel extrusion and conical plunger	1/16 by 1 1/4	3	-	17.1[a]	0.90[a]
			3/16 by 3	3	6	8.7	0.89
		Tube extrusion and conical plunger	1/8 by 1 1/4	4 1/2	6	5.5	0.86
			1/16 by 1 1/4	3	4	8.5	0.87
		Tube extrusion and blunt plunger	1/16 by 1 1/4	4 1/2	6	4.22	0.83
			3/16 by 3	4 1/2	6	6.12	0.76
			1/8 by 1 1/4	4 1/2	6	7.62	0.70
Los Angeles Basin, S63-20	89	Barrel extrusion and conical plunger	1/16 by 1 1/4	3	-	49[a]	0.96[a]
			3/16 by 3	3	6	16.0	0.98
		Tube extrusion and conical plunger	1/8 by 1 1/4	4 1/2	6	8.1	1.03
			1/16 by 1 1/4	3	4	-[b]	-[b]
		Tube extrusion and blunt plunger	1/16 by 1 1/4	4 1/2	6	-[b]	-[b]
			3/16 by 3	4 1/2	6	6.90	1.09
			1/8 by 1 1/4	4 1/2	6	7.57	1.06
Kern River, S63-21	89	Barrel extrusion and conical plunger	1/16 by 1 1/4	3	-	-	-
			3/16 by 3	3	6	-	-
		Tube extrusion and conical plunger	1/8 by 1 1/4	4 1/2	6	-	-
			1/16 by 1 1/4	3	4	-	-
		Tube extrusion and blunt plunger	1/16 by 1 1/4	4 1/2	6	-	-
			3/16 by 3	4 1/2	6	8.34	1.03
			1/8 by 1 1/4	4 1/2	6	10.4	0.90

[a]Taken from Schweyer and Busot (2). [b]Did not reach an equilibrium value.

Table 3. Comparative data of methods used.

Sample	Penetration at 25 C	Florida Method (corrected for geometry)		Cone and Plate Method		Sliding Plate Method	
		Complex Flow Index C	Apparent Viscosity (MP)	Complex Flow Index C	Apparent Viscosity (MP)	Complex Flow Index C	Apparent Viscosity (MP)
8621	60	0.69	4.04	0.61	4.00	0.89	3.60
8693	55	0.98	2.62	0.89	2.40	-[a]	-[a]
8610	62	0.73	3.48	0.62	3.47	-[a]	-[a]
8581	59	0.85	2.99	0.87	2.60	0.91	2.70
8594	58	0.81	3.32	0.74	3.10	-[a]	-[a]
8617	90	0.81	1.56	0.74	1.32	1.07	1.44
8580	82	0.86	1.94	0.90	1.23	1.10	1.50
8590	87	0.70	1.59	0.75	1.40	-[a]	-[a]
8589	77	0.76[b]	1.50[b]	0.72	1.45	0.98	2.94[c]
8620	65	0.74	2.69	0.72	2.56	-[a]	-[a]
A (S63-20)	89	0.98	1.37	0.92	1.23	0.98	1.16
B (S63-19)	90	0.89	1.81	0.75	1.95	0.81	2.26
D (S63-13)	89	0.65	1.79	0.56	2.12	0.94	1.96
F (8757A)	20	0.86	75.8	-[a]	-[a]	1.13	57.6
G (8659A)	30	0.57	30.0	0.35	39.0	0.66	25.6
H (8665B)	13	0.57	24.1	0.37	32.0	0.83	20.0
I (S64-22)	21	0.65	25.5	0.49	19.5	0.58	23.4
J (S64-42)	65	0.82	2.45	0.84	1.60	0.99	2.50
K (S64-46)	43	0.83	4.76	0.75	4.70	0.94	7.15
L (S64-47)	19	0.74	46.6	0.56	36.0	0.61	33.6
M (S67-15)	16	0.38	74.6	0.22	52.5	-[a]	Too hard
O (S64-33)	25	0.28	6.4	-[a]	-[a]	-[a]	-[a]
P (R71-8)	23	0.41	25.2	0.27	33.3	0.20	33.0

[a]Not run.
[b]A different sample of this material gave values of C = 0.71 and a viscosity of 2.63 MP. There may have been a sample mixup.
[c]Average of four determinations.

fixed value, usually 0.05 sec^{-1}. The data given in Tables 1 and 2 are at a constant power input because previous data were available at this condition.

In the original Florida study (2), it was recommended that comparisons be made at the same power input of 100,000 ergs/(sec-cm^3). If a constant rate of shear value is to be used, it is suggested that a value of 1.0 sec^{-1} be the standard. This suggestion is based on a very simple consideration.

The fundamental relation for a power law fluid is expressed mathematically as

$$\eta = \eta_0 \left| \dot{\gamma}/\dot{\gamma}_0 \right|^{C-1} \tag{1}$$

η is the apparent viscosity, in poises, at the point where $\dot{\gamma}$ is rate of shear, and η_0 and $\dot{\gamma}_0$ are corresponding values at some standard state with C being the exponent in the power function. It will be noted that, if the standard value of $\dot{\gamma}_0$ is taken as 1.0 sec^{-1}, the standard viscosity η_0 is numerically equal to the value of the standard shearing stress τ_0 where both τ_0 and $\dot{\gamma}_0$ must be measured at the same point in the fluid. This is true because the viscosity at any $\dot{\gamma}$ is also defined for the apparent viscosity η_a:

$$\eta_a = \tau/\dot{\gamma} \tag{2}$$

and if $\dot{\gamma}$ is 1.0 sec^{-1}, the value of the viscosity η_a, in poises, is numerically the same as τ, the shearing stress (given in dynes/cm^2).

Another form of Eq. 1, which relates shear stress to rate of shear, is

$$\tau = \eta \dot{\gamma}_0^C \tag{3}$$

which plots as a straight line on log-log coordinates with a slope of C whenever the power law is applicable. In this form, η is a correlation coefficient (which also is the viscosity in poises when C is equal to unity).

For most asphalt cements in the range of 85 to 100 penetration, observations will give measurements in the range of rates of shear of 1.0 sec^{-1}. Some correlations, however, possibly should be made at a constant power input as was originally suggested.

It should be noted that the data given in Tables 1 and 2 for the apparent viscosity in the Florida method are corrected for complex flow (Rabinowitsch) and for geometry. However, the rates of shear are the average values as used in evaluating the slope of $C = (d \ln \tau)/(d \ln \dot{\gamma})$ for the rheological diagram.

Recent studies by Lodge (5) have indicated that asphalts may show a pressure susceptibility that will accentuate shear-susceptibility effects. A method for correction for pressure was proposed if it becomes desirable to make such corrections. This subject is being explored further.

The present studies, using various instruments, show acceptable agreement in general for all three methods with paving grade asphalts as indicated in Figure 4. As might be expected, special asphalts are less in agreement probably because of non-Newtonian flow phenomena. However, even with these materials, one order of magnitude agreement is shown for the apparent viscosity values. The poorest agreement is in the complex flow index, but there is no apparent trend in disagreement.

In a recent paper, Lefebvre and Robertson (6) presented comparable data, using several different instruments, which indicated that the cone method tends to give lower values for the complex flow index at 25 C than does the capillary method. These were limited data on very soft asphalts (300 penetration).

Temperature Susceptibility

Certain nonlinear temperature effects noted for low temperatures on the ASTM chart were discussed by Lefebvre and Robertson (6). They also showed for one asphalt that there was a significant break of the plots at the region from 40 to 60 C. This was the region where the apparatus they used was changed from the efflux type to the cone and plate and cone-cone types. The authors commented that the temperature susceptibility appeared to be greater in the lower temperature regions. This was not confirmed in

the present study because the data plotted at the power input point show lower slopes than those at the higher temperatures. This effect appears to be accentuated with increased complex flow behavior.

The new procedure was used to develop data in the lower ambient range from 5 to 60 C (Table 5). These data, at a constant power input, 10^5 ergs/(sec-cm^3), were plotted with other high-temperature data up to 195 C as shown on a redrawn ASTM D2493 chart (log-log viscosity versus log of absolute temperature in degrees Rankine). These plots (and many others) show a good straight line for the efflux viscosities above 60 C when all are reported in poises. Below this temperature, Florida capillary method data give essentially a continuation of the high-temperature line for materials exhibiting essentially Newtonian flow as shown in Figure 5 for R70-56. However, for other asphalts such as R70-51 (Fig. 6), the line shows a definite offset from the higher temperature data. When data at different shear rates are plotted as shown in Figure 7, the best straight line appears to be at the power point. Shear-susceptible materials tend to show better agreement for the data at a constant power input, but whether this is universally true is not known. These materials also show larger viscosities at 60 C when the Florida capillary method is used than when the efflux method (Cannon-Manning) is used.

No explanation is given for the discrepancy of the data at 60 C by different methods except that possible pressure-viscosity effects, which Lodge (5) found at lower temperatures, may also be present. This is being investigated in a special study. (For temperatures substantially above and below 25 C, which was the controlled room temperature with primary environmental chamber control, special precautions were taken for ensuring that sample was at the indicated test temperature.)

COMMENTS ON PROCEDURES

The recommended procedure for the analysis of asphalt rheology given in the tables allows for the Rabinowitsch correction (2) and corrects for the sample tube geometry relative to the capillary geometry (2). This is not appreciable for a 1/16- by 1½-in. capillary until the complex flow index is 0.5 or less (at which point the observed viscosity should be reduced by about 5 percent). For a 3/16- by 1½-in. capillary, this correction is about 10 percent for a complex flow index of 1.00 and about 30 percent when C has a value of 0.5.

For analysis at 25 C, a nominal capillary of 1/16- by 1½-in. for asphalt cements of 80 to 100 penetration is suggested with expected range of results as shown at the lower values in Figure 1. The variability for values of apparent viscosities averaged about 7 percent of the mean value based on five check runs. For the complex flow index, the variability was within about 5 percent of the average value (2).

It has been found that capillaries with length-to-diameter ratios in excess of 15 are desirable for satisfactory results (2). In selecting a standard size for different ranges of viscosities at variable temperatures, several factors need to be considered. First, a small diameter uses less sample, provides good heat dissipation, and requires a shorter length to meet the length-to-diameter ratio requirement. However, small-diameter capillaries are more difficult to fabricate. Second, larger bores require longer sample tubes to accommodate greater length of capillary and require lower pressures (force per unit cross-sectional area), which minimizes certain problems of anomalous flow at high pressures. In addition, large-diameter capillaries require a geometric correction for the data depending on the sample tube diameter.

As a guide for capillary selection, the following tabulation is helpful for 85-penetration asphalt cements having an apparent viscosity of about 1 megapoise (MP) at 25 C. Softer asphalts would use the smaller diameters and harder asphalts the larger (Table 6).

In general, it is believed that shearing stresses should be less than 5×10^6 dynes/cm^2 as a maximum until further research determines that this can be raised. With this limit, certain problems of critical stress phenomena can be minimized.

Other observations of interest that have been noted are that 90-deg entry gives about the same result as does 180-deg (flat) entry. Stainless steel, brass, and amalgamated brass gave about the same results in tubes. It was also noted that heating the sample tubes showed little or no effect.

Table 4. Comparative data of asphalt cements at different shear rates at 25 C.

Asphalt[a]	Penetration at 25 C	Rheological Analysis: Complex Flow Index C	V25[b], Apparent Viscosity (MP): 0.05 sec^{-1}	1.0 sec^{-1}	10^5 ergs/sec-cm^3
A	89	0.98	1.37	1.27	1.36
B	90	0.89	1.81	1.28	1.48
C	89	0.80	2.44	1.32	1.78
D	89	0.65	1.79	0.62	0.98
E	89	0.99	1.37	1.31	1.33
F	20	0.86	75.8	50.3	80.1
G	30	0.57	30.0	8.07	30.8
H	13	0.53	24.1	5.90	25.3
I	21	0.65	25.5	8.6	22.4
J	65	0.82	2.45	1.46	1.93
K	43	0.83	4.76	2.82	3.93
L	19	0.74	46.6	21.3	49.4
M	16	0.38	74.6	11.4	141.0
O	25	0.28	6.4	0.75	3.90
P	23	0.41	25.2	4.22	25.6

[a]Samples A to E are paving asphalts; others are miscellaneous items including recovered paving asphalts and air-blown and roofing asphalts.
[b]V25 is used to designate absolute viscosity at 25 C.

Table 5. Comparative Florida rheometer data on asphalt cements at ambient temperatures.

Asphalt	5 C Viscosity (MP)	10 C Viscosity (MP)	15.5 C Viscosity (MP)	25 C Viscosity (MP)	40 C Viscosity (kP)	50 C Viscosity (kP)	60 C Viscosity (kP)
R70-50, 89 pen							
Complex flow index C	0.84	0.86	0.80	0.80	0.96	0.92	0.95
Rate of shear							
$\dot{\gamma}_{\infty}$, sec^{-1}	250	73.5	18.5	2.44	79	24.5	6.15
$\dot{\gamma}_1$, sec^{-1}	165	48.4	10.4	1.32	74	18.1	4.95
$\dot{\gamma}_p$, ergs/(sec-cm^3)	292	77.8	17.5	1.78	74	18.1	4.52
R70-51, 89 pen							
Complex flow index C	0.65	0.63	0.57	0.65	0.78	0.86	0.90
Rate of shear							
$\dot{\gamma}_{\infty}$, sec^{-1}	50.4	13.4	5.88	1.79	111	21.4	5.75
$\dot{\gamma}_1$, sec^{-1}	17.3	4.4	1.61	0.625	60	14.3	4.04
$\dot{\gamma}_p$, ergs/(sec-cm^3)	55.1	11.4	3.84	0.985	57	12.5	3.38
R70-55, 90 pen							
Comples flow index C	0.71	0.85	0.72	0.81	0.86	0.88	0.91
Rate of shear							
$\dot{\gamma}_{\infty}$, sec^{-1}	94.8	34.8	6.29	1.81	128	44.9	11.5
$\dot{\gamma}_1$, sec^{-1}	39.5	22.9	4.27	1.28	89	30.8	8.65
$\dot{\gamma}_p$, ergs/(sec-cm^3)	113.3	35.2	6.26	1.54	89	29.3	7.70
R70-56, 89 pen							
Complex flow index C	1.12	0.98	1.02	0.92	1.01	1.10	0.99
Rate of shear							
$\dot{\gamma}_{\infty}$, sec^{-1}	535	87.0	7.47	1.37	34	6.14	1.52
$\dot{\gamma}_1$, sec^{-1}	459	80.0	8.04	1.27	35	7.65	1.48
$\dot{\gamma}_p$, ergs/(sec-cm^3)	803	88.2	7.62	1.40	35	8.45	1.45

Figure 5. Temperature susceptibility of R70-56.

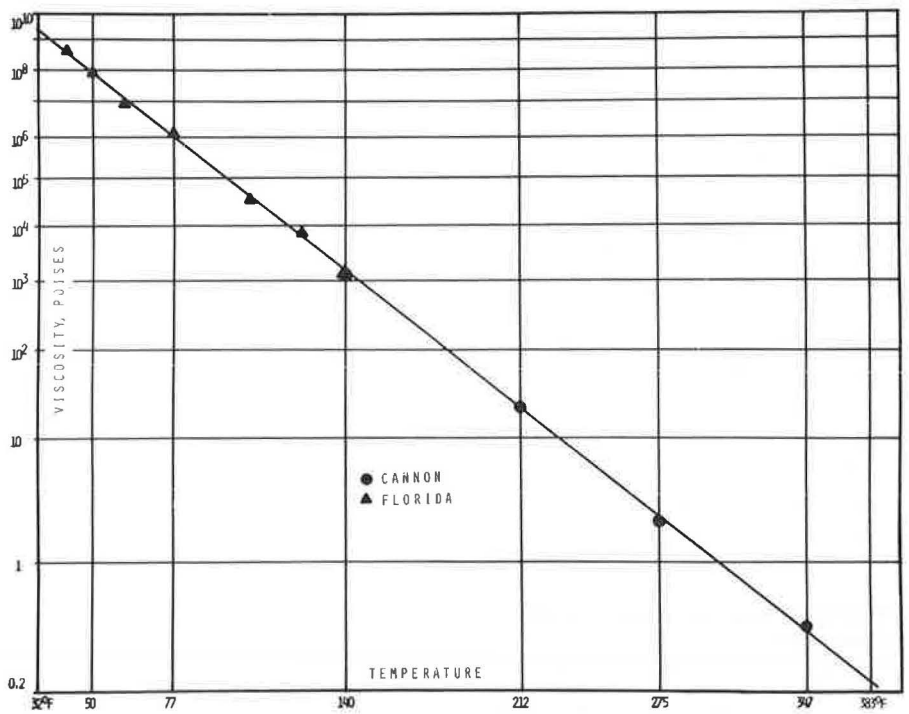

Figure 6. Temperature susceptibility of R70-51.

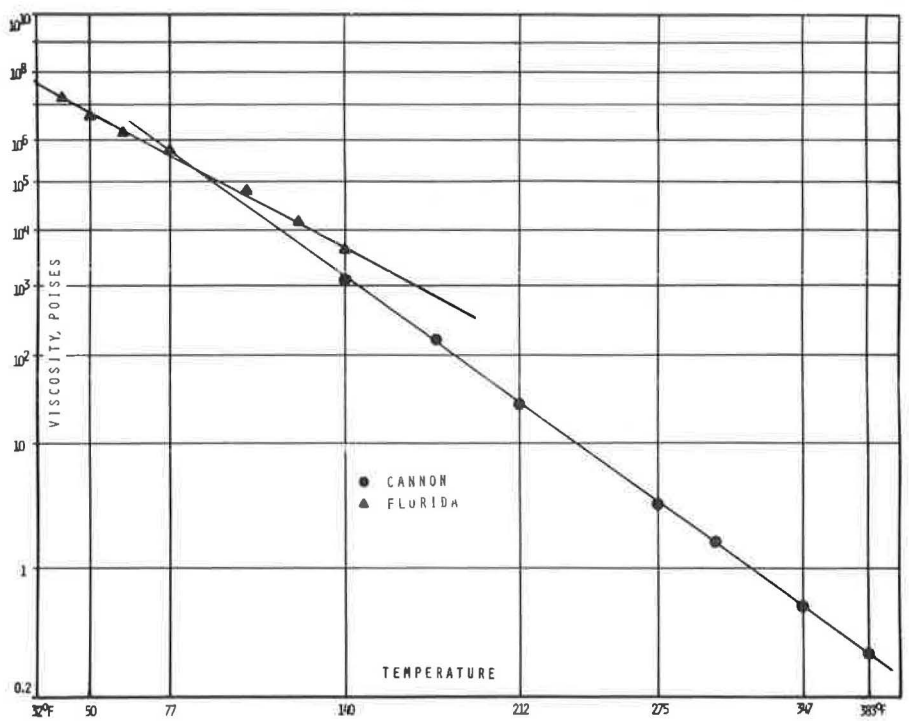

Figure 7. Low-temperature susceptibility of R70-51.

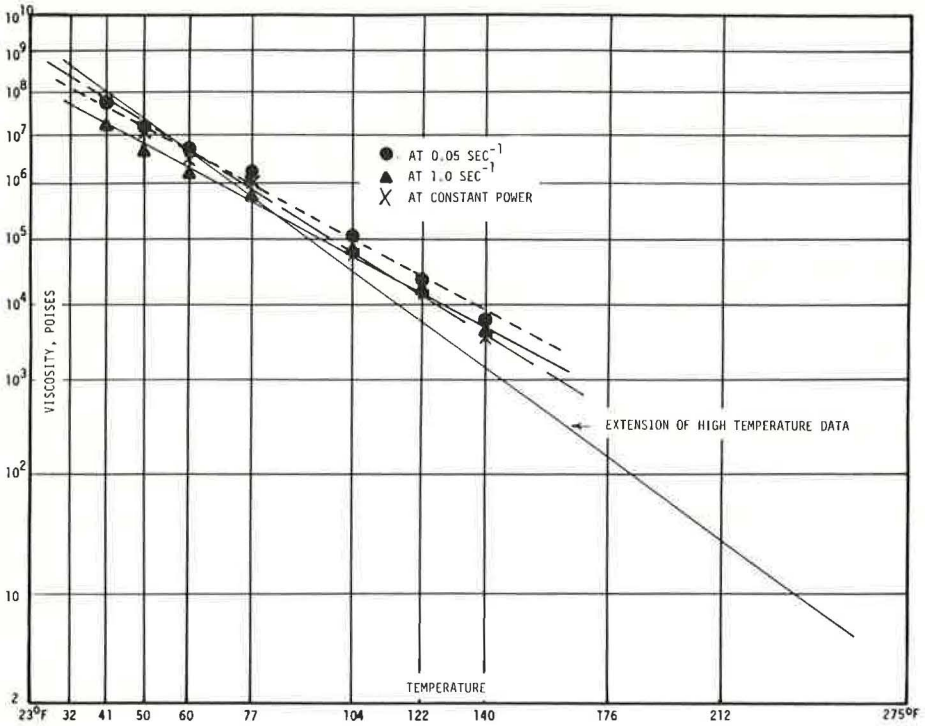

Table 6. Nominal capillary dimensions.

Temperature of Absolute Visocity (deg C)	Dimension (in.)		Temperature of Absolute Visocity (deg C)	Dimension (in.)	
	Diameter	Length		Diameter	Length
60	0.020	1.5	25	0.08	1.5
	0.030	1.5		0.120	1.5
50	0.030	1.5	15	0.120	1.5
	0.050	1.5		0.187	1.5
40	0.040	1.5	5	0.187	1.5
	0.060	1.5		0.25	1.5

In its present state of development, the Florida method can be used for general routine testing at low cost if a suitable inexpensive constant force drive or constant velocity drive apparatus is made available.

ACKNOWLEDGMENT

Certain initial work on this research was supported by the Florida Department of Transportation whose assistance is acknowledged. Also, the author is grateful for the advice of J. C. Busot in helping to develop the method used in this study.

REFERENCES

1. ASTM Standards. Part II, 1967.
2. Schweyer, H. E., and Busot, J. C. Experimental Studies on Viscosity of Asphalt Cements at 77 F. Highway Research Record 361, 1971, pp. 58-70.
3. Puzinauskas, V. T. Communication to Florida Department of Transportation and used by permission.
4. Traxler, R. N. Private communication and used by permission.
5. Lodge, R. W. Effect of Pressure in Asphalt Viscometry. University of Florida, M.Sc. thesis, Aug. 1971.
6. Lefebvre, J. A., and Robertson, W. D. Viscosity Characteristics of Two Canadian Asphalts. Proc. Canadian Tech. Asphalt Assn., Vol. 15, 1970.

ASPHALT ABSORPTION AS RELATED TO PORE CHARACTERISTICS OF AGGREGATES

Prithvi S. Kandhal, Pennsylvania Department of Transportation; and
Dah-yinn Lee, Iowa State University

Absorption of asphalt by aggregates is of paramount importance to account for the loss due to absorption because, in the design of densely graded bituminous concrete mixes, a relatively small variation in the asphalt content will result in mixtures that are too rich or too lean. Pore characteristics are the most important properties of the aggregates, especially in the absorption phenomenon. Most attempts have been made by the investigators to evaluate aggregate absorption without direct analysis of the pore characteristics. Review of literature on pore characteristics and methods of determination of asphalt absorption by aggregates are presented. Rock cores ½ in. in diameter from six Iowa limestones, having variable absorptive characteristics, have been used throughout this study. Mercury porosimetry has been employed to evaluate total effective porosity, pore-size distribution, pore-volume distribution, and extent of "ink-bottle" pores. Asphalt absorption has been determined by the immersion method and the bulk-impregnated specific gravity method. A relation between pore parameters and asphalt absorption has been established by regression analysis. Pore size in the range of 0.1 to 0.05 μm seems to determine the amount of water absorption, whereas pore size in the range of 0.7 to 0.05 μm determines the asphalt absorption.

•ABSORPTION of asphalt by aggregates is recognized as an important factor in the design of mixes for bituminous pavements. For the calculation of the quantity of asphalt required for a particular aggregate, the surface capacity of an aggregate has to be taken into account. The surface capacity is composed of three factors: surface area, which varies with gradation; variation due to the roughness of the aggregates; and variation due to true effective porosity or absorption in the aggregates themselves (1). The last factor determines the quantity of asphalt actually present on the surface of the aggregate and available as binder. Obviously, where the asphalt or any of its important constituents (in selective absorption) are absorbed, the absorbed portion can no longer act as part of the binder proper. This may lead to the failure of the pavement because (a) the resulting thin film around the aggregate is more susceptible to stress and weathering (especially water action) and (b) low-temperature cracking may occur because of the change in the physical and chemical properties of asphalt film.

Thus, the evaluation of exact absorption of asphalt by aggregates is of paramount importance to account for the loss due to absorption because, in the design of densely graded bituminous concrete mixes, a relatively small variation in the asphalt content will result in mixtures that are dangerously rich or dangerously lean (2).

Some aggregates are rejected for highway construction purposes if the absorption of asphalt is substantial. Increased consumption and the continued demand for higher quality aggregates, because of accelerated highway construction programs and expanded usage of concrete in the building industry, are rapidly exhausting many suitable aggregate sources, which results in a shortage of quality aggregates available at reasonable cost in many areas of the country. Therefore, tests and criteria on absorptive capacity

Sponsored by Committee on Characteristics of Aggregates and Fillers for Bituminous Construction.

of aggregates with respect to asphalt are needed to ensure high-quality paving mixtures and to ensure that so-called "marginal aggregates" are not rejected unjustifiably because of the lack of criteria.

The present work was undertaken to study the pore characteristics of six different aggregates and their absorptive capacity with respect to commonly used asphalts.

LITERATURE REVIEW

Aggregates may be considered as porous media (solid bodies containing pores) in the study of the process of absorption. Hence, the following review is divided into pore characteristics and asphalt absorption by aggregates as evaluated in the present study.

Pore Characteristics

The importance of pore size and pore-size distribution has been realized and studied extensively in the case of concrete aggregates. However, there have been no published data on the study of the pore-size characteristics of asphalt aggregates and their relationship to absorption other than that by Lee (3).

The pores in a porous system may or may not be interconnected. The interconnected part of the pore system is called the effective pore space of the porous medium.

The pores in rock are pictured as irregularly shaped cavities connected by capillaries that have varying shapes and diameters (4). The smallest entrance diameter to a pore is used as the measure of the size of that pore.

According to Scheidegger (5), the only unambiguous pore size should be the largest sphere that can be put into the space containing the point in question.

The pore characteristics that are generally determined are porosity, pore size, pore-size distribution, and a specific internal area called specific surface.

Porosity

Probably the most common method used in the casual investigation of aggregate porosity is to measure the absorption and assume that the volume of water absorbed equals the pore volume, i.e., to assume complete saturation. The result may be termed water-permeable or 24-hour soaked porosity. Dinkle (4) obtained vacuum-saturated porosity and reported good correlation among saturated porosity, 24-hour soaked porosity, and mercury intrusion porosity. The main point with respect to the absorption method as a measurement of porosity is that one rarely gets complete saturation (6).

Washburn and Bunting (7) employed a gas expansion method based on Boyle's law to determine porosity. Beeson (8) modified the apparatus, and most of the commercially available equipment is based on this principle.

Porosity can be determined visually on a polished or thin section of aggregate by measuring void area (pore space) microscopically by various camera-lucida or photomicrographic methods. Sweet (9) has used such optical methods on aggregates.

Dolch (10) determined the effective porosity of limestone aggregates with the McLeod gauge porosimeter as developed by Washburn and Bunting (11).

Pore Size and Specific Surface of the Solids

Brunauer, Emmett, and Teller (12) advanced BET theory for obtaining specific surfaces from sorption isotherms. Surface adsorption has also been used to obtain indirectly a curve for pore-size distribution.

Other methods (13, 14) for pore size and specific surface are small angle X-ray scattering, heat of immersion, rate of dissolution, ionic adsorption, and radioactive and electrical means; however, these have been little used.

The method (15) most frequently used is that of injection of mercury into the pore system. This method has been adopted in the present study. Washburn (16) was the first to suggest the use of pressed mercury in determining the pore-size distribution of porous solids (assuming the model is based on a system of circular capillaries).

The relation developed by him may be stated in the following form:

$$p(r) = -2\sigma \times \cos\theta \qquad (1)$$

where p is the pressure applied, r is the pore radius, σ is the surface tension of mercury, and θ is the contact angle of the mercury with respect to the solids.

Ritter and Drake (17) put Washburn's conception to practical use and developed the apparatus. The apparatus generally referred to as a mercury porosimeter has been described by Purcell (18). Subsequently, Drake (19) utilized a high-pressure mercury porosimeter and made measurements up to 60,000 psi to measure pore radii down to 20 Å. The method was applied successfully to concrete aggregates by Hiltrop and Lemish (20).

Determination of Percentage of Asphalt Absorption

Many investigators have attempted to evaluate aggregate absorption with kerosene and have applied suitable corrections for the amount of asphalt absorbed by aggregates in mixture design. Hveem (1) devised the Centrifuge Kerosene Equivalent (CKE) test in 1942. Lohn (21) and Donaldson et al. (22) proposed some modifications to the Hveem CKE test. Because kerosene has wetting properties similar to asphalt, it is believed to be a better representative absorption agent than is water (23). Oils have also been used by some investigators (1, 24) to evaluate the absorptive capacity of coarse aggregates.

In 1942, Goshorn and Williams (2) developed the immersion method in which the coarse aggregate is immersed in a tarred wire basket in asphalt at 275 F for 3 hours. Because the aggregate is in contact with an unlimited supply of asphalt at relatively low viscosity for extended periods of time, the absorption is much higher than would be expected in a bituminous mixture. However, the values can definitely be taken as the absorptive potentials of aggregates used for bituminous mixtures (25).

Rice (26) proposed a procedure to determine the maximum specific gravity of the mixture by using volumetric flasks. The absorption of asphalt by aggregate in a mixture can be calculated if the maximum specific gravity of the mixture (after Rice's method), the asphalt content, and the bulk specific gravity of the aggregate used in the mixture are known.

The U. S. Corps of Engineers (27, 28) developed and used the bulk-impregnated specific gravity method in the design and control of bituminous paving mixtures. It has also been used to determine the asphalt absorption by porous aggregates.

In this study, asphalt absorption of rock cores has been determined by using two methods: immersion method and bulk-impregnated specific gravity method.

INVESTIGATIONS

Materials

Six major limestone aggregates, having variable absorptive characteristics, have been studied.

In the present study, which also includes the pore characteristics of the aggregate, rock cores ($\frac{1}{2}$ in. in diameter) drilled from stone blocks received from the respective quarries were used. This was done to have consistent and comparable results in studying pore characteristics and asphalt absorption because of the following.

1. Rock cores taken from one stone block are more likely to be homogeneous and uniform, and correlation between absorption and pore characteristics can be more realistic.
2. Rock cores or cylinders allow uniform drying of surface for saturated surface dry condition in ASTM Test C 127-59 for determination of bulk specific gravity and thus give reproducible results to be used in the immersion and bulk-impregnated specific gravity methods for calculating asphalt absorption.

The source and designation of the aggregates (cores) studied are given in Table 1. Hereinafter, the cores shall be referred to in this study by name of quarry from which the stone blocks were received. Two asphalt cements have been included in this study. The properties of the two asphalts studied are given in Table 2.

Testing Procedure

Water-Permeable or 24-Hour Soaked Porosity—The water-permeable porosity was computed by multiplying the percentage of water absorption by the bulk specific gravity where both were determined on ½-in. diameter rock cores from the standard 24-hour soaked procedure as per ASTM Test C 127-59.

Effective Porosity or Mercury-Intrusion Porosity—Effective porosity was determined with mercury capillary apparatus or mercury porosimeter apparatus. The effective pore volume was the volume of mercury injected into the rock core at a pressure of 2,000 psia. The bulk volume was that occupied by the rock surrounded by mercury at a pressure of 5 psia. In other words, the effective porosity, as defined in this study, is the ratio of the interconnected permeable pores in the pore-entry radius range, from 21.32 to 0.05 μm, to the total bulk volume of particle including pores, expressed as a percentage.

Pore Size and Pore-Size Distribution—The pore size and the pore-size distribution were determined by using a mercury porosimeter apparatus manufactured and distributed by Ruska Instrument Corporation, Houston, Texas, under license of the Shell Development Company. The apparatus and procedure have been described in detail elsewhere (3, 20). The data of the cumulative volume of pores or volume of mercury absorbed at various applied pressures or corresponding pore radii can be treated in various ways. The data in this study are as follows.

Nonnormalized Pore-Size Distribution Curve—The distribution curve represents the frequency of occurrence of one particular pore size. The curve indicates at what size (for example, r) the greatest number of pores occurs. Ritter and Drake (17) derived the equation for a nonnormalized distribution curve:

$$D(r) = p/r \times [d(Vo - V)dp] \quad (2)$$

where

$D(r)$ = distribution function;
p = applied pressure, psia;
r = pore-entry radius, μm;
$Vo - V$ = volume of mercury injected from zero to pressure p, cc/gram; and
$d(Vo - V)/dp$ = slope of Vo - V versus pressure as determined from pressure-pore volume curve.

All the terms on the right side of Eq. 2 are known or determinable. Values of the derivation are readily obtained by graphical differentiation. Plotting D(r) against r gives the distribution curve.

Porosity Distribution Curves—Curves of cumulative porosity versus pore radius were plotted for all rock cores. The cumulative porosity is the cumulative pore volume divided by total bulk volume of a particle.

Percentage of Porosity in Various Pore-Radius Ranges—The porosity for pores between certain radii is the ratio of the pore volume in these sizes to the total bulk volume of an aggregate including pores, expressed as a percentage. These porosities were determined for the following pore radius ranges in microns: 21 to 11, 21 to 5, 21 to 2, 21 to 1, 11 to 1, 5 to 1, 1 to 0.5, 1 to 0.1, 1 to 0.05, 0.1 to 0.05, and 0.7 to 0.05.

Hysteresis in Mercury Porosimetry—When the pressure is systematically released in the mercury porosimeter, the depressurization curve does not follow the original pressurization curve, and some of the mercury is retained in the sample even on complete removal of pressure. The phenomenon was also observed by Ritter and Drake (17), who attributed the action to the so-called "ink-bottle" shape of the pores. Curves illustrating hysteresis have been obtained for all rock cores.

Determination of Asphalt Absorption by Immersion Method

The method used is essentially that developed by Goshorn and Williams (2) for coarse aggregates, with the exception that the rock cores were immersed in asphalt at 300 F

(instead of 275 F) for 1 hour only (instead of a total of 3 hours). Also, the samples were not cooled at room temperature and reheated at 275 F before the cores were removed from the asphalt. It is felt that, by using this modification, (a) the time required to complete the test can be greatly reduced, (b) the conditions more nearly approach the field operation of hot mix, and (c) the absorption should be more indicative of the maximum or potential absorptive capacity of an aggregate (25).

Determination of Asphalt Absorption by Bulk-Impregnated Specific Gravity of Aggregates

The procedure used in determining the bulk-impregnated specific gravity is essentially that described by Ricketts et al. (28).

RESULTS AND DISCUSSION

Pore Properties

Water-Permeable or 24-Hour Soaked Porosity—Results of water-permeable or 24-hour soaked porosity, bulk specific gravity, and water absorption as determined from ASTM Test C 127-59 for ½-in. rock cores are given in Table 3.

Effective Porosity or Mercury-Intrusion Porosity—Effective porosity covers the pore-entry radius from 21.32 to 0.05 μm. The results are given in Table 4.

Pore Size and Pore-Size Distribution—Plots were made from the data of the cumulative volume of pores or volume of mercury absorbed at various applied pressures or corresponding pore radii. From these, graphs were drawn after necessary computations.

Porosity Distribution Curves—Curves of cumulative porosity (percent) versus pore radius for rock cores are shown in Figure 1.

Nonnormalized Pore-Size Distribution Curves—The curves representing the frequency of occurrence of one particular pore size, as mentioned earlier, are shown in Figure 2.

Percentage of Porosity in Various Pore-Radius Ranges—The porosity for pores between certain radii was determined for the following pore-radius ranges in microns: 21 to 11, 21 to 5, 21 to 2, 21 to 1, 11 to 1, 5 to 1, 1 to 0.5, 1 to 0.1, 1 to 0.05, 0.1 to 0.05, and 0.7 to 0.05. The last range was included in the study based on six nonnormalized pore-size distribution curves that had a range of 0.05 to 0.7 μm for the most frequently occurring pore radius. The porosities are given in Table 4.

Statistical Analysis Results—Out of the various pore-size ranges, important ranges (which will be specified later) were selected. Linear correlation coefficients between these main pore properties were determined so as to study how they vary. The computed correlation coefficients are given in Table 5.

The pore-size ranges given in Table 5 were selected on the basis of their correlation with asphalt absorption. Those with poor or no correlation were not included. It appears that mercury-intrusion porosity is mainly dependent on the porosities in the following ranges of pore size: 0.7 to 0.05 μm, 1 to 0.05 μm, 1 to 0.1 μm, and 1 to 0.5 μm. The porosities in the following ranges have fair correlations with mercury-intrusion porosity and show a general trend: 5 to 1 μm, 11 to 1 μm, 21 to 2 μm, and 0.1 to 0.05 μm. Based on the determination of 24-hour soaked porosity and mercury-intrusion porosity, the following plots show good correlations.

24-Hour Soaked Porosity Versus Mercury-Intrusion Porosity—Correlation coefficient between methods is 0.7093. Menlo and Linwood cores behave similarly. Cook and Alden cores tend to absorb less water, whereas Keota and Pints cores absorb more water as compared to mercury intrusion.

Mercury-Intrusion Porosity Versus 0.7- to 0.05-μm Porosity Range—Because values of pore radius r corresponding to maximum value of D(r) in the nonnormalized pore-size distribution curves (Fig. 2) range from 0.05 to 0.7 μm, this range was correlated with mercury-intrusion porosity. The correlation coefficient is 0.9553 (Table 5). Porosity in the 1- to 0.05-μm range is the controlling factor for total mercury intrusion, whereas for water absorption the range is 0.1 to 0.05 μm. The correlation coefficient between this porosity and water absorption is 0.9782.

Table 1. Aggregates studied.

County	Quarry	Beds or Ledges	Geological Formation
Adair	Menlo	3 to 6 Argentine	Missourian series, Pennsylvanian system
Black Hawk	Pints	Rapid	Cedar Valley formation, Devonian system
Hardin	Alden	—	Gilmore City formation, Mississippian system
Scott	Linwood	Davenport	Devonian system
Story	Cook	—	St. Louis formation, Mississippian system
Washington	Keota	Beds 14 to 22	Osagian series, Mississippian system

Table 2. Properties of asphalts studied.

Property	Asphalt	
	A (85 to 100 penetration)	B (120 to 150 penetration)
Penetration, 77/100/5	92	127
Specific gravity	1.0077	1.0237
Flash point, F	600	605
Fire point, F	670	665
Softening point, F	120	118
Viscosity at 140 F, poises	1,144	727
Viscosity at 77 F, poises	3.95×10^6	1.58×10^6
Thin-film loss on heating 5 hours at 325 F, percent	0.10	0.08
Penetration of residue, 77/100/5	54	72
Percentage of original penetration (thin-film residue)	57.4	53.3
Soluble in CCl_4, percent	99.84	99.83
Ductility at 77 F, cm	130+	130+
Ductility at 77 F (thin-film residue), cm	130+	130+
Spot test	Negative	Negative

Table 3. Bulk specific gravity, water absorption, and porosity of rock cores.

Cores	Bulk Specific Gravity	Water Absorption (percent)	24-Hour Soaked Porosity (percent)
Menlo	2.637	0.90	2.37
Pints	2.271	7.22	16.40
Alden	2.510	1.72	4.32
Linwood	2.636	0.90	2.37
Cook	2.565	2.16	5.54
Keota	2.489	3.12	7.77

Table 4. Porosity in different pore-size ranges.

Pore-Size Range (μm)	Quarry (percent)					
	Menlo	Pints	Alden	Linwood	Cook	Keota
21 to 11	0.17	0.12	0.10	0.13	0.17	0.71
21 to 5	0.26	0.18	0.28	0.24	0.25	1.52
21 to 2	0.36	0.32	0.50	0.32	1.10	2.29
21 to 1	0.43	2.30	1.12	0.36	7.0	2.68
11 to 1	0.26	2.18	1.02	0.23	6.83	1.97
5 to 1	0.17	2.12	0.84	0.12	6.75	1.16
1 to 0.5	0.08	6.20	5.28	0.08	5.30	0.22
1 to 0.1	0.45	12.9	8.29	0.51	10.0	0.97
1 to 0.05	0.55	14.65	8.45	0.54	10.4	1.98
0.1 to 0.05	0.10	1.75	0.19	0.03	0.40	1.01
0.7 to 0.05	0.52	10.45	5.80	0.49	7.2	1.86
21 to 0.05[a]	0.98	16.88	9.60	0.90	17.44	4.66

[a]Mercury-intrusion porosity.

Figure 1. Cumulative porosity distribution.

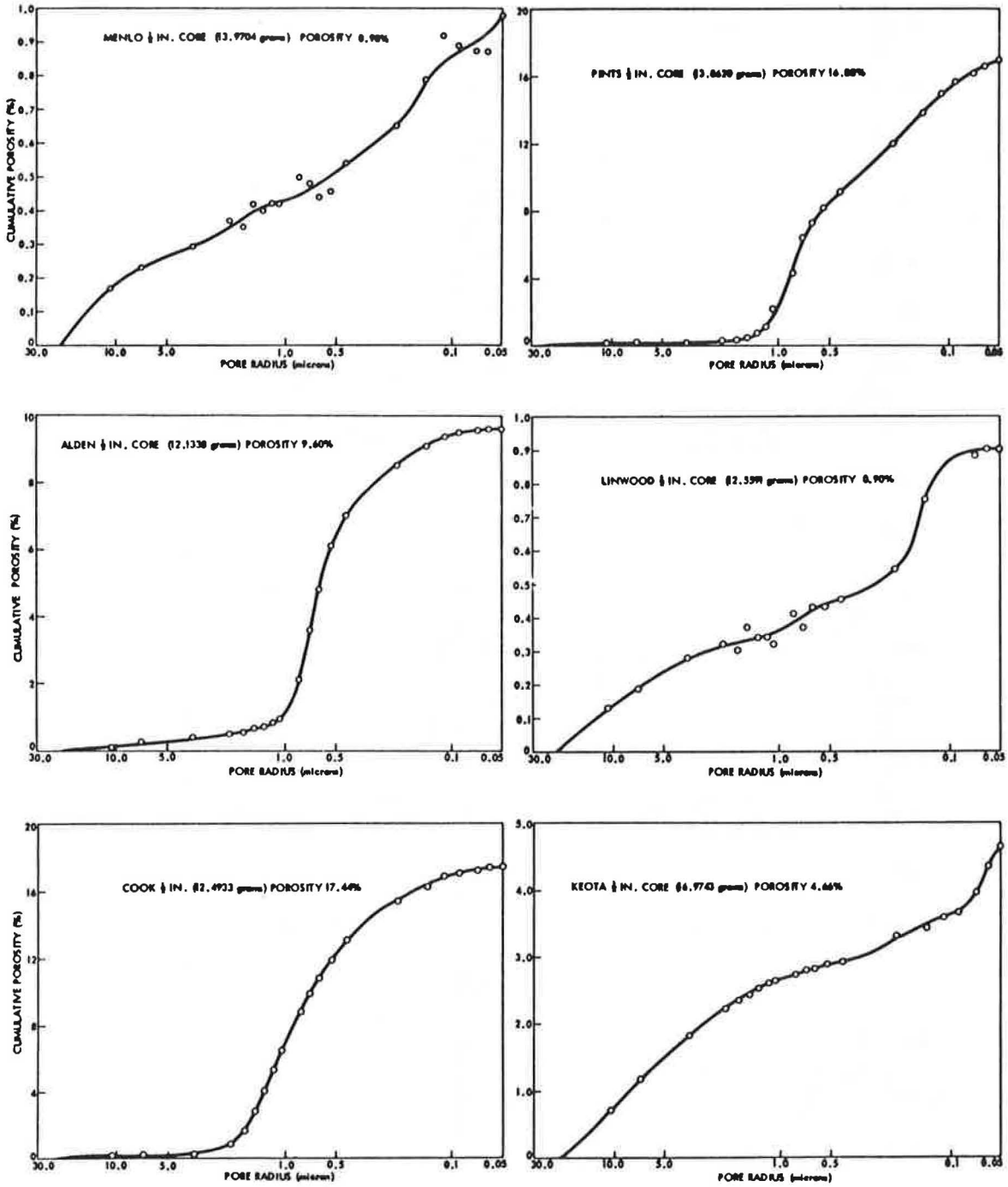

Figure 2. Nonnormalized pore-size distribution.

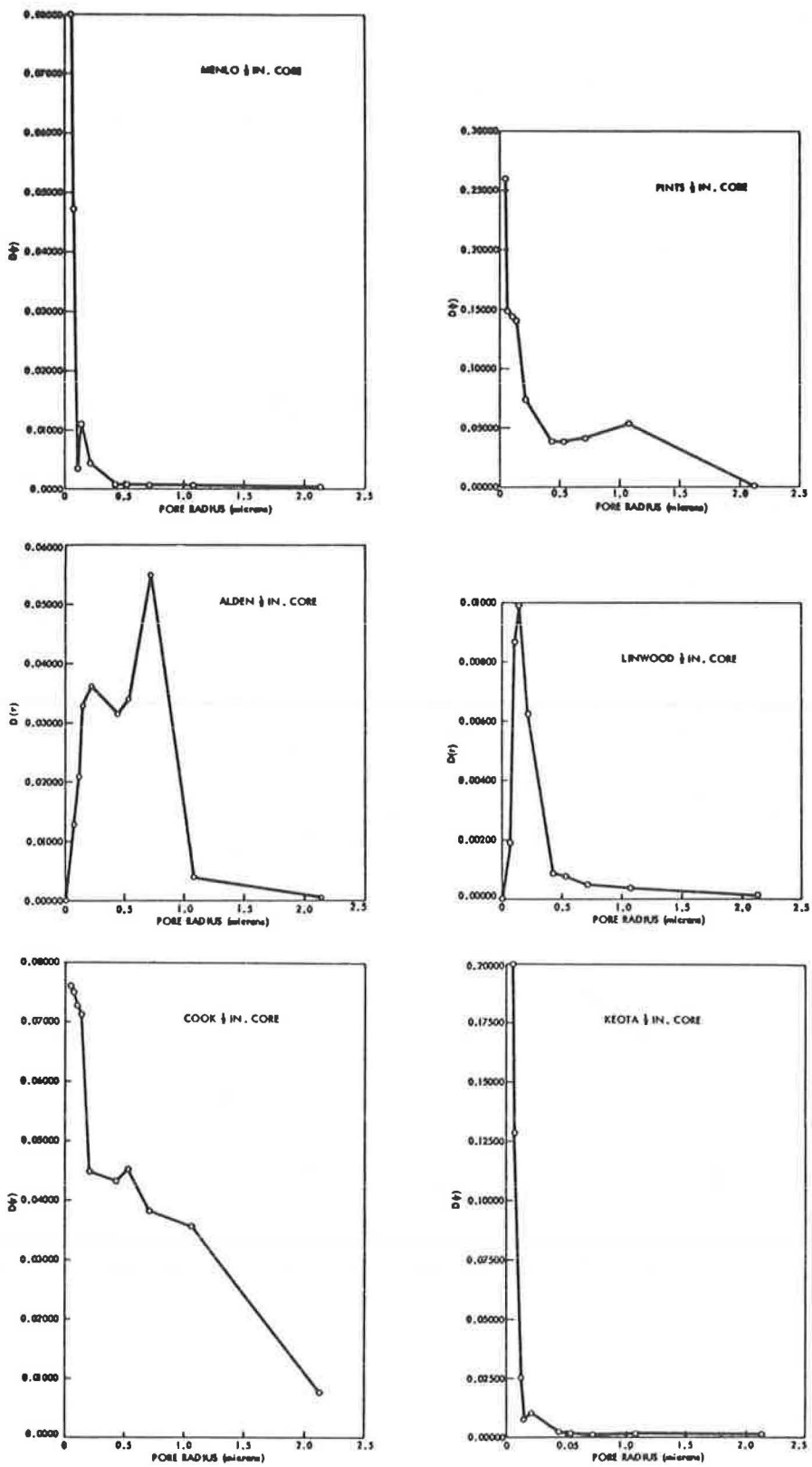

Hysteresis in Mercury Porosimetry—Curves illustrating the phenomenon of hysteresis are shown in Figure 3. If the pores are cylindrical with a uniform diameter or V-shaped, the points of penetration and retraction of mercury in pressure-penetration curve will fall on the same line, provided the advancing and receding contact angles are also equal. However, pores with a narrow throat, the so-called "ink-bottle" pores, would not be expected to empty when the pressure is released and thus are responsible for hysteresis. Estimation of the major dimensions of the interior cavities can be made from the phenomenon of hysteresis. Detailed interpretation of data on individual rock's pore properties, based on the pore-size distribution graphs and hysteresis, can be done and has been reported elsewhere (29).

Asphalt Absorption

As mentioned earlier, asphalt absorption was determined for the ½-in. diameter rock cores by using two methods: (a) bulk-impregnated specific gravity method and (b) immersion method. Two asphalts having penetrations of 85 to 100 (referred to as asphalt A) and 120 to 150 (referred to as aspahlt B) were used to compare their relative absorption by the rock cores. Duplicate determinations of asphalt absorption were done in each test. The results of absorption tests are given in Table 6.

Absorption by Bulk-Impregnated Specific Gravity Method—The percentage of absorption (using asphalt A) varied from a low of 0.30 for Menlo cores to a high of 2.01 for Pints cores. Results of absorption for asphalts of different penetrations (A and B) are shown in Figure 4. The correlation coefficient is 0.9861, which is excellent. There is no appreciable difference in percentage of asphalt absorption as far as the two asphalts are concerned, though the absorption of asphalt B is slightly higher than asphalt A, as expected. This could be because the viscosity difference between the two asphalts at testing temperature (280 F) was too small.

Asphalt Absorption by Immersion Method—The percentage of absorption (using asphalt A) varied from 0.44 for Linwood cores to 2.11 for Pints cores. Results of differential absorptions of asphalts A and B are shown in Figure 4. The correlation coefficient is 0.9505. Again, the slope and intercept of the regression line indicate a general trend of no appreciable difference between absorption of asphalts A and B.

Comparison of Two Methods—Table 6 shows that the absorption values from the immersion method are higher than those obtained by using the bulk-impregnated specific gravity method. Figure 5 shows a comparison of the two methods. The correlation is excellent for asphalts A and B. The correlation coefficients are 0.9883 and 0.9862 respectively. Slopes of the regression lines indicate, in general, a constant difference in the values obtained by two methods. It is indicated that the immersion method gives higher values, which can be taken as the absorptive potentials of the rock cores used in this study. The values obtained by using the specific gravity method can be considered as the "realistic" maximum value (25), which can occur during mixing, hauling, spreading, and cooling of the paving mixture and in service under traffic.

Pore Properties Versus Asphalt Absorption

Porosity in different pore-size ranges has been determined for rock cores as well as the absorption of asphalt by using two methods and two types of asphalt. All these results were put to statistical analysis to find the pore-size ranges or other porosity characteristics that may have some correlation with asphalt absorption. Correlation coefficients and regression coefficients (slope and Y-intercept of the regression line) were determined. It was thought that there could be a pore-size range (or ranges) that is optimum for asphalt absorption.

Correlations

Water Absorption and Asphalt Absorption—Efforts have been made in the past (24, 28) to correlate water absorption of aggregates to asphalt absorption because the former is relatively a very simple standard test. In this study, the linear correlation coefficients range from 0.8398 to 0.9341, which is excellent. However, experience has

Figure 3. Hysteresis in mercury porosimetry.

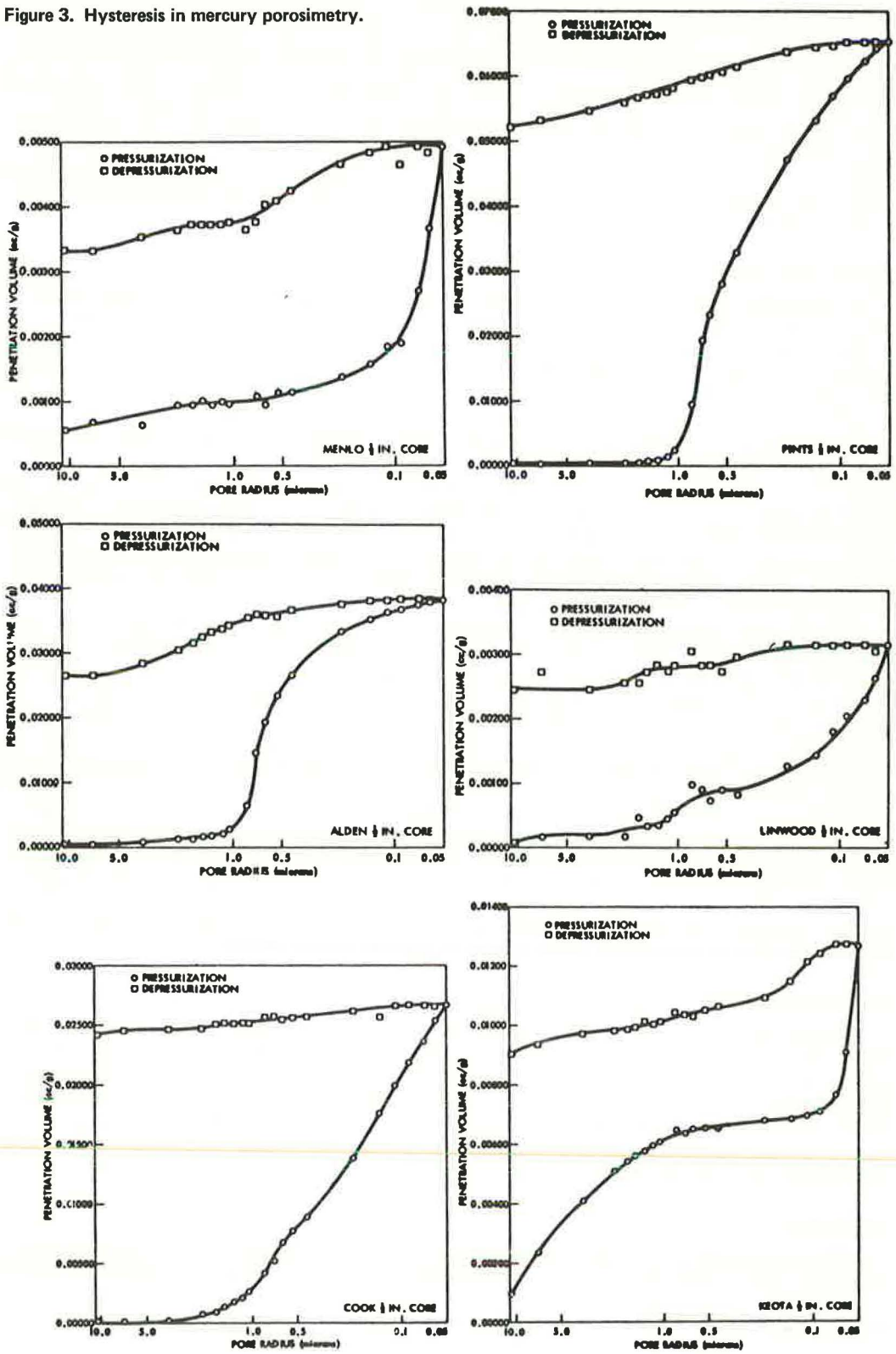

Table 5. Linear correlation coefficients among main pore properties.

	Porosity						
Porosity	24-Hour Soaked	Mercury-Intrusion	0.7- to 0.05-μm	0.1- to 0.05-μm	1- to 0.05-μm	1- to 0.1-μm	1- to 0.5-μm
24-hour soaked	1.0						
Mercury-intrusion	0.7093	1.0					
0.7- to 0.05-μm	0.7716	0.9553	1.0				
0.1- to 0.05-μm	0.9782	0.5510	0.6510	1.0			
1- to 0.05-μm	0.7405	0.9548	0.9987	0.6128	1.0		
1- to 0.1-μm	0.6733	0.7084	0.9894	0.5341	0.9953	1.0	
1- to 0.5-μm	0.5664	0.9275	0.9566	0.4188	0.9687	0.9854	1.0

Figure 4. Asphalt absorption: asphalt A versus asphalt B.

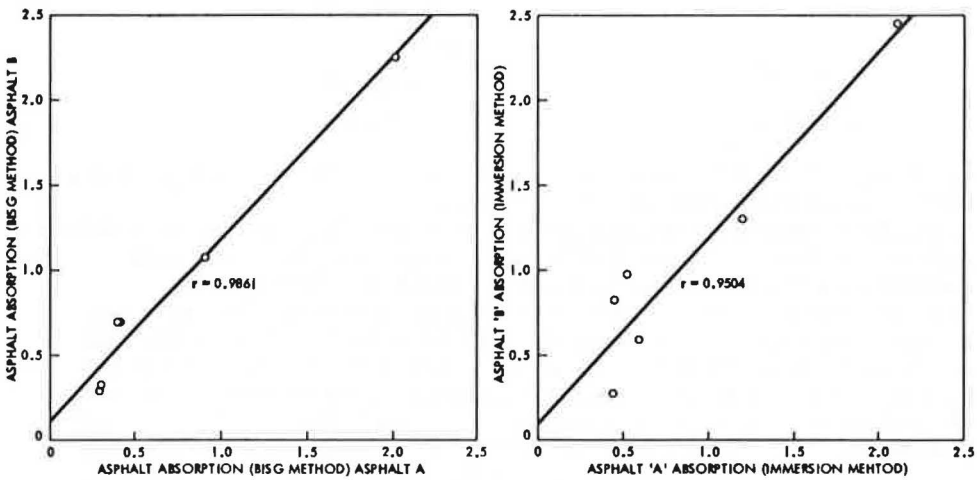

Table 6. Asphalt absorbed by rock cores (percentage by weight of rock cores).

	Bulk-Impregnated Specific Gravity Method		Immersion Method	
Rock Core	Asphalt A	Asphalt B	Asphalt A	Asphalt B
Menlo	0.30	0.30	0.59	0.59
Pints	2.01	2.27	2.11	2.47
Alden	0.91	1.08	1.20	1.31
Linwood	0.30	0.33	0.44	0.28
Cook	0.40	0.70	0.45	0.83
Keota	0.41	0.69	0.52	0.98

Figure 5. Asphalt absorption: bulk-impregnated specific gravity method versus immersion method.

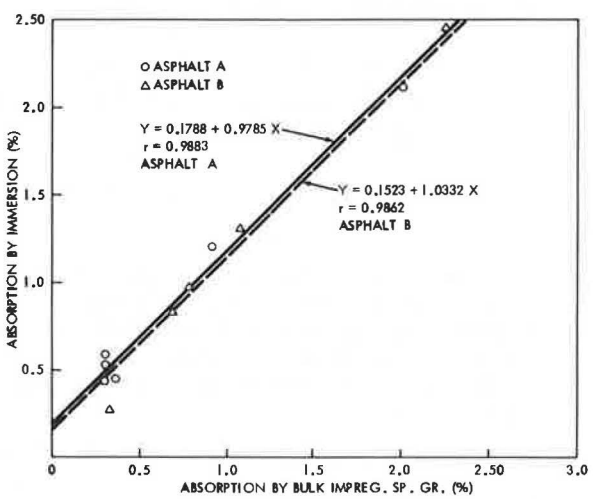

shown that the water absorption is not a reliable test for predicting asphalt absorption because of noted exceptions. Bitumen-water absorption ratios have reportedly ranged from 1 to 100 percent. Aggregates have been reported to show higher bitumen absorption than water absorption in rare cases (28).

Porosity and Asphalt Absorption—Correlation coefficient for porosity in various pore-size ranges and asphalt absorption was determined. It has been noted that the correlation is poor in the following pore-size ranges (in microns): 21 to 11, 21 to 5, 21 to 2, 21 to 1, 11 to 1, and 5 to 1. For the remainder of the pore-size ranges, the correlation coefficients in decreasing order are as follows.

Mercury-Intrusion Porosity Range (μm)	Range of Correlation Coefficients
0.7 to 0.05	0.8760 to 0.7708
1 to 0.05	0.8594 to 0.7595
0.1 to 0.05	0.8566 to 0.7226
1 to 0.1	0.8170 to 0.7247
1 to 0.5	0.7563 to 0.6806
21 to 0.05	0.7136 to 0.5517

The porosity in the 0.7- to 0.05-μm range (as determined by the mercury porosimeter) has excellent correlations with asphalt absorption.

Effective porosity or mercury-intrusion porosity (21- to 0.05-μm range) has correlation coefficients ranging from 0.7136 to 0.5517 with asphalt absorption. However, effective porosity does indicate the general trend of asphalt absorption.

It seems that different pore-size ranges control the absorption of different liquids depending on their viscosities, surface tensions, and contact angles with solids. The correlation coefficients given in Table 5 reveal that 0.1- to 0.05-μm porosity has the best correlation (r = 0.9782) with 24-hour soaked porosity and hence may be regarded as the main controlling pore-size range for water absorption as far as limestone rock cores in this study are concerned; porosity in the 0.7- to 0.05-μm range has the best correlation with asphalt absorption (r = 0.8760 to 0.7708). As expected, water having good wettability has a lower range of 0.1 to 0.05 μm, whereas asphalt has a controlling range of 0.7 to 0.05 μm.

The equations for regression lines for the linear correlations with a 0.7- to 0.05-μm range are as follows. (X = percentage of porosity in the 0.7- to 0.05-μm range, and Y = percentage of asphalt absorption.)

Pore-Size Range (μm)	Absorption Method	Asphalt	Equation for Regression Line
0.7 to 0.05	Specific gravity	A	$Y = 0.1294 + 0.135\ X$
		B	$Y = 0.1977 + 0.1563\ X$
	Immersion	A	$Y = 0.3640 + 0.1255\ X$
		B	$Y = 0.3362 + 0.1593\ X$

In all cases, correlations are better in the case of asphalt B, which has more penetration than asphalt A. Also, absorption values obtained from the specific gravity method have better correlation with the porosity in the preceding pore-size ranges than those obtained from immersion test.

The following conclusions can be drawn from the pore-size and absorption correlations.

1. Pore-size distribution has a direct effect on asphalt absorption. Figure 6 shows the cumulative pore-size distribution of Menlo and Pints cores on the same scale. Considerable difference in asphalt absorption between these two types of rock cores is reflected by the significant variation between the two curves. This is also evident in

Figure 6. Cumulative porosity distribution (Menlo and Pints cores).

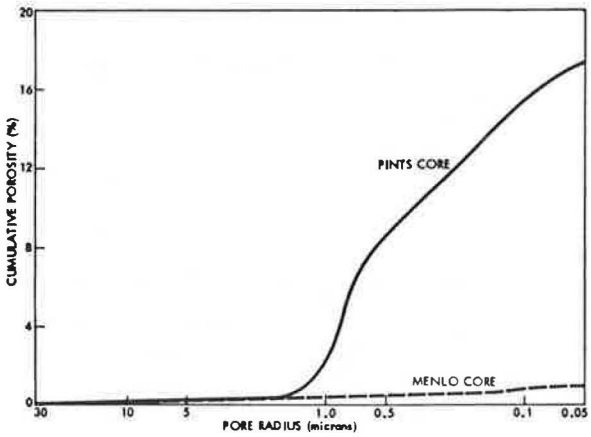

Figure 7. Hysteresis in mercury porosimetry (Menlo and Pints cores).

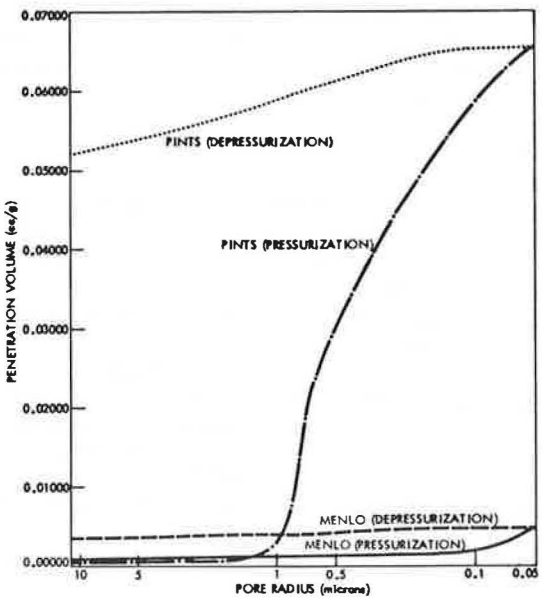

Figure 8. Porosity in 0.7- to 0.05-μm range versus asphalt absorption.

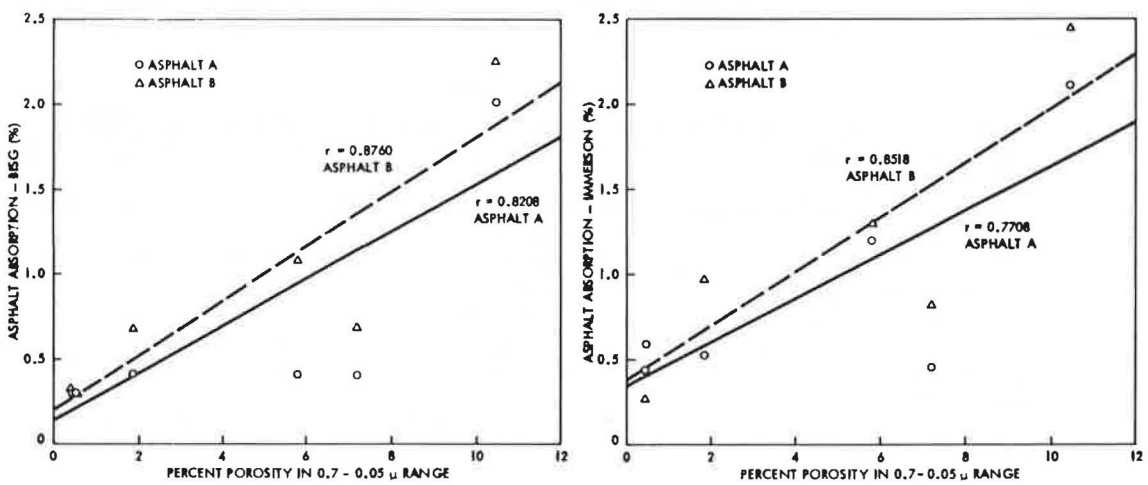

Figure 7, which combines curves of hysteresis in mercury porosimetry of Menlo and Pints cores.

2. Porosity in the 0.7- to 0.05-μm range has a direct effect on asphalt absorption. The relation is linear. Figure 8 shows these relations for both methods.

3. Effective porosity indicates a general trend of absorption of asphalt.

SUMMARY AND CONCLUSIONS

Pore characteristics are the most important properties of aggregates, especially with regard to the absorption phenomenon. Most attempts have been made by the investigators to evaluate aggregate absorption without direct analysis of the pore characteristics. This paper is based on study of absorption of asphalt by aggregates as related to their pore characteristics.

The following conclusions are drawn from the present study.

1. Effective porosity has fair linear correlation with asphalt absorption and thus indicates only the general trend of absorption of asphalt. Cores having more effective porosity are likely to absorb more asphalt and vice versa.

2. Absorption obtained by using the immersion method gives high values that can be regarded as the absorptive potentials of the rock cores, whereas absorption values obtained by using the specific gravity method can be considered as "realistic" maximum values that can occur in certain circumstances that require higher mixing temperatures.

3. Rock cores tend to absorb more asphalt of higher penetration than of lower penetration.

4. Though excellent linear correlations have been found between the percentage of water absorption and asphalt absorption, the former cannot be recommended for predicting asphalt absorption because of the exception found by various investigators.

5. The presence of "ink-bottle" pores is indicated in all cores. The probable dimensions of the pore throats and internal cavities vary from one core to another and seem to affect asphalt absorption.

6. Pore-size distribution of an aggregate has a direct effect on the degree of asphalt absorption. Very good correlation was found between the percentage of porosity in the 0.7- to 0.05-μm pore-size range and the asphalt absorption. This range seems to control the asphalt absorption by limestone aggregates included in this study, whereas pore size in the range of 0.1 to 0.05 μm seems to determine the amount of water absorption. Thus, different pore-size ranges control the absorption of different liquids depending on their viscosities, surface tensions, and contact angles with solids. This emphasizes the importance of pore characteristics in study of absorption by aggregates.

ACKNOWLEDGMENTS

The research included in this paper is the partial result of Project HR-142 sponsored by the Iowa State Highway Commission for the study of absorptive aggregates in asphalt paving mixtures. Sincere thanks are due to John Lemish for making available the mercury porosimeter used in this study and to June Viozzi for editing and typing this paper.

REFERENCES

1. Hveem, F. N. Use of Centrifuge Kerosene Equivalent as Applied to Determine the Required Oil Content for Dense Graded Bituminous Mixtures. Proc. AAPT, Vol. 13, 1942, pp. 9-40.
2. Goshorn, J. H., and Williams, F. M. Absorption of Bituminous Materials by Aggregates. Proc. AAPT, Vol. 13, 1942, pp. 41-51.
3. Lee, D. The Relationship Between Physical and Chemical Properties of Aggregates and Their Asphalt Absorption. Proc. AAPT, Vol. 38, 1969, pp. 242-275.
4. Dinkle, R. E. Freezing Resistance in Mortar Related Pore Properties of Rock Particles. Univ. of Maryland, College Park, MS thesis, 1966 (unpublished).
5. Scheidegger, A. E. The Physics of Flow Through Porous Media. Macmillan Co., New York, 1957.
6. Dolch, W. L. Porosity in Tests and Properties of Concrete. ASTM, STP 169-A, 1966, pp. 443-461.

7. Washburn, E. W., and Bunting, E. N. Porosity VI. The Determination of Porosity by the Method of Gas Expansion. Jour. Amer. Ceramic Soc., Vol. 5, 1922, pp. 112-116.
8. Beeson, C. M. The Kobe Porosimeter. Amer. Institute of Mining, Metallurgical, and Petroleum Engineers, Vol. 189, 1950, pp. 313-315.
9. Sweet, H. S. Research on Concrete Durability as Affected by Coarse Aggregates. Proc. ASTM, Vol. 48, 1948, pp. 988-1019.
10. Dolch, W. L. Studies of Limestone Aggregates by Fluid Flow Methods. Proc. ASTM, Vol. 59, 1959, pp. 1204-1215.
11. Washburn, E. W., and Bunting, E. N. Porosity VII. The Determination of the Porosity of Highly Vitrified Bodies. Jour. Amer. Ceramic Soc., Vol. 5, 1922, pp. 527-529.
12. Brunauer, S., Emmett, P. H., and Teller, E. Absorption of Gases in Multimolecular Layers. Jour. Amer. Chemical Soc., Vol. 60, 1922, pp. 309-311.
13. Carman, P. C. Flow of Gases Through Porous Media. Academic Press, New York, 1956.
14. Dallman, R. S. Analysis of Pore Size Distribution by Diffusive Counterflow. Iowa State Univ., Ames, MS thesis, 1966 (unpublished).
15. Ritter, H. L., and Erich, L. C. Pore Size Distribution in Porous Materials. Anal. Chem., Vol. 20, No. 7, July 1948, pp. 665-670.
16. Washburn, E. W. Note on a Method of Determining the Distribution of Pore Size in a Porous Material. Proc. Nat. Acad. Sci., Vol. 7, 1921, pp. 115-116.
17. Ritter, H. L., and Drake, L. C. Pore-Size Distribution in Porous Materials. Ind. and Eng. Chem., Anal. Ed., Vol. 17, 1945, pp. 782-786.
18. Purcell, W. R. Capillary Pressures—Their Measurement Using Mercury and Calculation of Permeability Therefrom. Trans. AIME, Vol. 186, 1949, pp. 39-48.
19. Drake, L. C. Pore Size Distribution in Porous Materials. Ind. and Eng. Chem., Vol. 41, April 1949, pp. 780-785.
20. Hiltrop, C. L., and Lemish, J. Relationship of Pore Size Distribution and Other Rock Properties to Serviceability of Some Carbonate Aggregates. HRB Bull. 239, 1960, pp. 1-23.
21. Lohn, R. N. A Method to Determine Aggregate Absorption and Control of Bituminous-Aggregate Properties. Proc. AAPT, Vol. 15, 1943, pp. 188-196.
22. Donaldson, J. A., Loomis, R. J., and Krchma, L. C. The Measurement of Aggregate Absorption. Proc. AAPT, Vol. 16, 1947, pp. 353-372.
23. Nevitt, H. G., and Krchma, L. C. Absorption of Liquid Bituminous Cements by Aggregates. Proc. AAPT, Vol. 13, 1942, pp. 52-68.
24. Lettier, J. A., Fink, D. F., Wilson, N. B., and Fraley, F. F. Mechanism of Absorption of Bituminous Materials by Aggregate. Proc. AAPT, Vol. 18, 1949, pp. 278-300.
25. Lee, D. Study of Absorptive Aggregates in Asphalt Paving Mixtures. Iowa State Univ., Eng. Research Institute, Res. Rept. HH-127, Feb. 1968.
26. Rice, J. M. Maximum Specific Gravity of Bituminous Mixtures by Vacuum Saturation Procedure. ASTM, STP 191, 1956, pp. 43-61.
27. Investigation of the Penetration of Asphalt Into Porous Aggregates as Related to and Affecting the Specific Gravity of the Aggregate. Waterways Exp. Station, U.S. Corps of Engineers, Misc. Paper No. 4-88, 1954.
28. Ricketts, W. C., Sprague, J. C., Tabb, D. D., and McRae, J. L. An Evaluation of the Specific Gravity of Aggregates for Use in Bituminous Mixtures. Proc. ASTM, Vol. 54, 1954, pp. 1246-1257.
29. Kandhal, P. S. Asphalt Absorption as Related to Pore Characteristics of Aggregates. Iowa State Univ., Ames, MS thesis, 1969 (unpublished).

GRADING ASPHALT CEMENTS BY PENETRATION OR VISCOSITY AT 77 F

Norman W. McLeod, McAsphalt Engineering Services, Toronto, Ontario

ABRIDGMENT

•THE author would like to make it clear at the beginning that he is not opposed to grading asphalt cements by viscosity. For reasons about to be presented, he is firmly opposed to viscosity grading at 140 F. He could fully support grading by viscosity at 77 F; however, until a rapid test for viscosity at 77 F has been developed and generally accepted, it seems doubtful that any organization would be willing to substitute viscosity at 77 F for penetration at 77 F for routine asphalt consistency control.

Any attempt to modify current specifications for asphalt cements should emphasize two major objectives:

1. It should facilitate high-temperature construction operations, and 275 F is a representative temperature for the high-temperature construction tasks of mixing, spreading, and breakdown rolling; and
2. It should improve long-term pavement performance, particularly under the low winter temperatures that occur in at least half of the United States and in all of Canada, and 77 F is a reasonably average pavement service temperature in much of North America.

This abridgment, which for brevity must omit many of the details in the paper itself, will show that neither of these two objectives is achieved by the AASHO specification based on grading asphalt by viscosity at 140 F. On the other hand, grading asphalt cements by penetration or viscosity at 77 F, plus a viscosity requirement at 275 F (Fig. 1), forms the basis for a simple but highly effective improved specification for asphalt cements, one that satisfied both of these objectives. First, however, because it is essential to the discussion that follows, some general information on asphalt cements will be presented.

BASIC CHARACTERISTICS OF ASPHALT CEMENTS

Temperature Susceptibility

Figure 2 shows that two asphalt cements with the same viscosity or penetration at 77 F can have widely different viscosities at all other temperatures. This occurs because of differences in their temperature susceptibilities, which is measured by penetration index (PI). All asphalt cements currently used in Canada lie within a PI of 0.0 and -1.5. In the United States, a PI range of +0.5 to -2.0 would include practically all paving asphalts.

Penetration Index

Figure 3 shows the relation between grading asphalt cements by penetration at 77 F and grading them by viscosity at 140 F. Line A in Figure 3 represents a PI of 0.0, whereas line B represents a PI of -1.5. If an asphalt cement of, for example, 200 penetration from a given crude oil has at 140 F a viscosity that places it on the upper boundary of line A, asphalt cements of other penetrations at 77 F made from the same

Sponsored by Committee on Characteristics of Bituminous Materials.

Figure 1. Grading asphalt cements by penetration at 77 F.

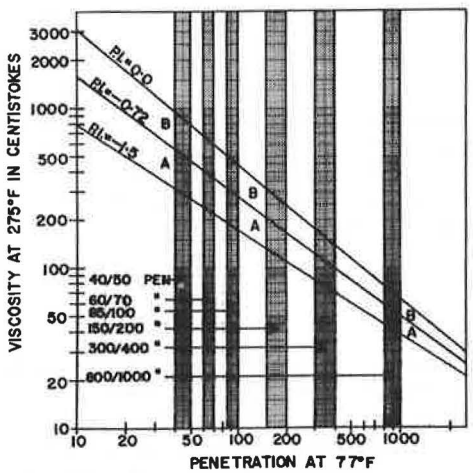

Figure 2. General relations among viscosity, temperature, and penetration indexes for asphalt cements.

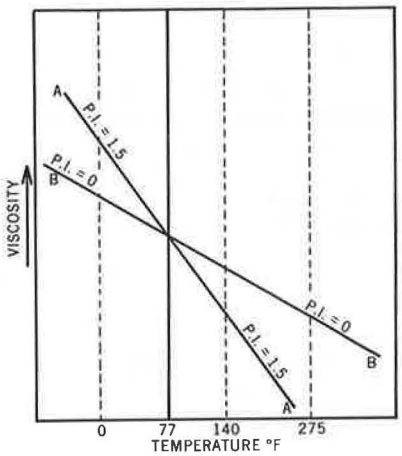

Figure 3. Correlation between viscosity at 140 F and penetration at 77 F.

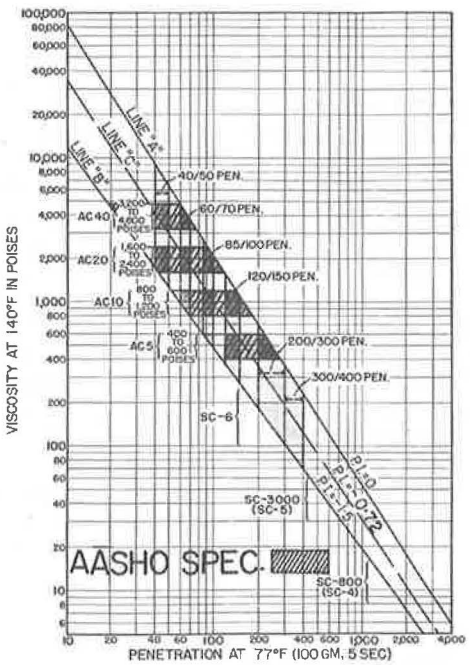

crude oil will have at 140 F viscosities that also tend to lie on the upper boundary of line A. Similarly, all asphalt cements from another crude oil will have penetrations at 77 F and corresponding viscosities at 140 F, which will tend to place them along a line that is approximately parallel to the upper boundaries of lines A and C.

Influence of Temperature

Figure 4 shows that grading asphalt cements by penetration or viscosity at 77 F avoids the very wide range of viscosity at -10 F associated with grading by viscosity at 140 F, which is responsible for a corresponding wide range of low-temperature transverse cracking. It also avoids the very broad range in viscosity at 275 F, which would result from grading asphalt cements by penetration or viscosity at 32 F (which in turn would greatly increase high-temperature construction problems).

VISCOSITY GRADING AT 140 F

Low-Temperature Transverse Pavement Cracking

Figure 5 shows a typical example of low-temperature transverse pavement cracking, which occurs because asphalt pavements tend to contract in cold weather. This is currently a serious pavement performance problem in Canada, and it appears to be a severe problem in at least the colder half of the United States. Figure 6 shows that there are four basic types of transverse pavement cracks. In our experience the most significant crack is type 1, which extends across the entire width of a traffic lane.

Figure 3 shows that the AC10 grade, for example, includes all asphalt cements between 50 to 60 and 150 to 200 penetration. Figures 7, 8, and 9 show the very serious differences in transverse cracking in pavements made with 85- to 100- and 150- to 200-penetration asphalt on a 9-mile test road in southern Ontario. Figure 7 shows the very serious transverse cracking that occurred in the several miles of pavement made with 85- to 100-penetration asphalt. Figure 8 shows no transverse cracks of any kind in the several miles paved with 150- to 200-penetration asphalt. In Figure 9, the pavements made with 85- to 100- and 150- to 200-penetration asphalt were laid in adjacent lanes over a length of 1,700 ft. The transverse cracks in the 85- to 100-penetration pavement in the right lane cross the centerline about 6 in. and disappear in the 150- to 200-penetration pavement in the left lane in which no transverse cracks occurred.

Therefore, the wide range of penetration at 77 F associated with each viscosity grade AC5, AC10, AC20, and AC40 is a most damaging criticism of grading asphalt cements by viscosity at 140 F in any area where pavements are subjected to low winter temperatures. This situation is worsened by the fact that changing to a lower viscosity grade, for example from AC10 to AC5, would not necessarily reduce the number of transverse cracks. For example, an engineer in northern Minnesota, Wisconsin, or North Dakota could experience serious transverse cracking with an AC10 grade of 150 to 200 penetration and decide to change to the supposedly softer AC5 grade. However, he might obtain an AC5 of 120 to 150 penetration and would have much more severe transverse pavement cracking than before.

A major conclusion drawn from pavement cracking investigations conducted in Canada is that low-temperature transverse pavement cracking occurs when the asphalt cement (the pavement) has been chilled to a critical high viscosity value. Figure 10 shows that, for asphalt cements of the same PI from a given crude oil, transverse pavement cracking can be avoided at lower pavement temperatures by using softer asphalt cements at 77 F.

Figure 11 shows that, for two asphalt cements of the same consistency at 77 F but with different PI values, a pavement containing the asphalt cement with the higher PI can be chilled to the lower temperature without transverse cracking occurring. The figure also shows that, if an asphalt cement of a given penetration or viscosity at 77 F with a high PI just avoids transverse cracking when a pavement containing it is cooled to, for example, -20 F, under the same conditions a much softer (higher penetration or lower viscosity at 77 F) asphalt cement must be slected if its PI is low.

Figure 4. Influence of temperatures selected for grading asphalt cements on viscosity ranges at -10 F and at 275 F.

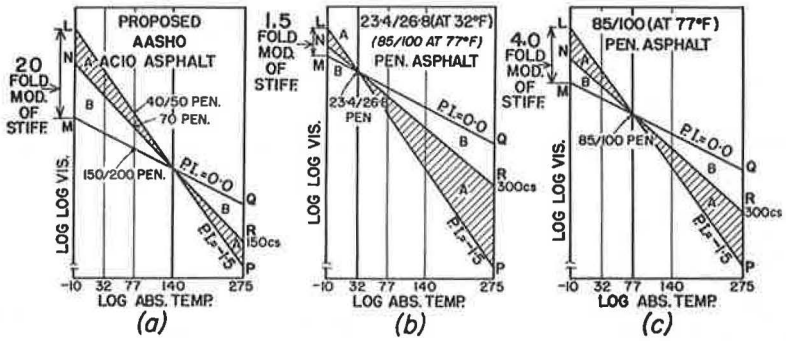

Figure 5. Typical low-temperature transverse pavement cracking (4-year old pavement made with 150- to 200-penetration asphalt).

Figure 6. Types of transverse pavement cracks.

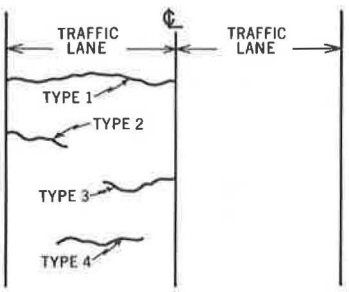

Figure 7. Transverse cracking (4-year old pavement made with 85- to 100-penetration asphalt).

Figure 8. Four-year old pavement made with 150- to 200-penetration asphalt.

Figure 9. Transverse cracking (85- to 100-penetration asphalt, right lane).

Figure 10. Relation among pavement temperature, softness of asphalt, and PI.

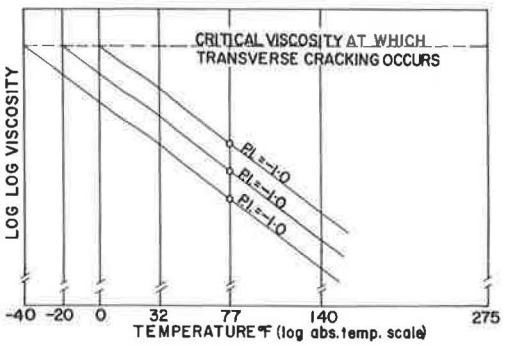

Figure 11. Relation between a low PI asphalt cement and a high PI asphalt cement at 77 F.

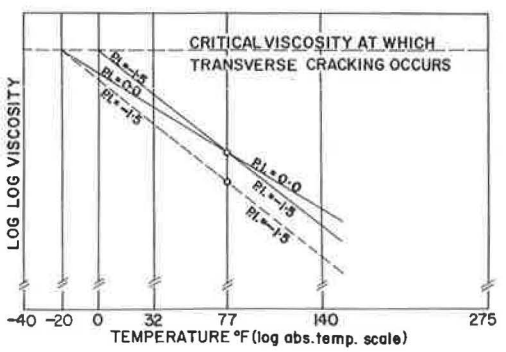

Figure 12. Guide for selecting grades of asphalt cement to avoid low-temperature transverse pavement cracking.

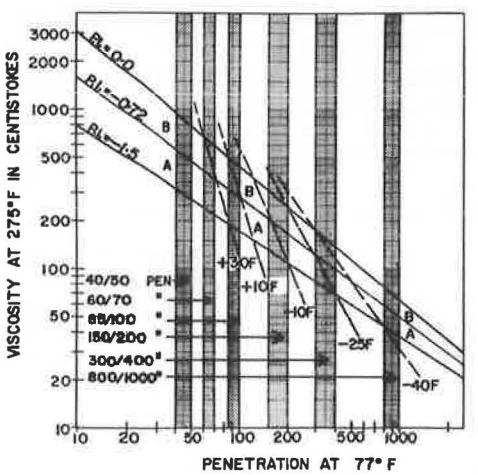

Figure 13. Relations between penetration indexes of original 85- to 100-penetration asphalt cements and number of type 1 transverse pavement cracks per lane mile after 8 years of service.

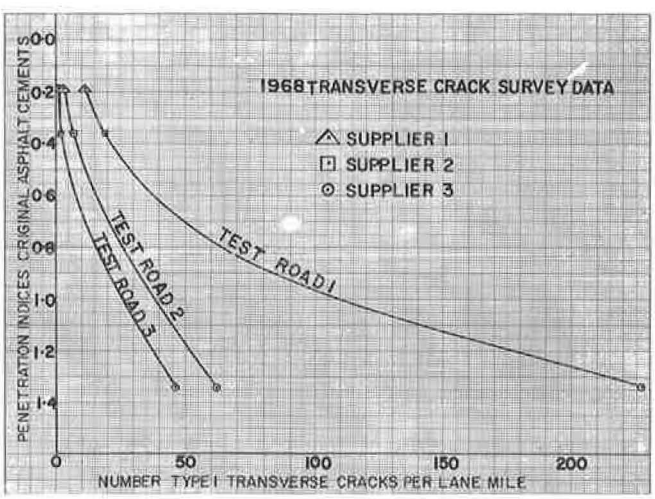

Avoidance of Low-Temperature Transverse Pavement Cracking

Based on information obtained in Canada, the author has developed Figure 12 as a guide to the selection of asphalt cements that will avoid low-temperature transverse pavement cracking throughout their service lives, provided they have been properly designed and constructed. An original asphalt cement should be selected that lies to the right of the diagonal line (Fig. 12) that represents the lowest temperature that is expected during the pavement's service life at a pavement depth of 2 in. If an engineer selects an asphalt cement that lies to the left of the oblique line (Fig. 12) that represents the critical minimum temperature, he is gambling with the probability that low-temperature transverse pavement cracking will occur sometime during the service life of the pavement.

Figure 12 shows that it is no longer acceptable to select the grade of asphalt cement for a paving job merely on the basis of its penetration at 77 F, as has been common engineering practice for at least the past 50 years. Figure 13, based on transverse crack surveys on three Ontario test roads, shows very clearly that this practice should not be continued. Figure 13, which indicates the results of a low-temperature transverse crack survey on asphalt pavements on three Ontario test roads after 8 years of service in a climate with moderate winter temperatures, shows that low-temperature transverse pavement cracking can be largely avoided when an 85- to 100-penetration asphalt with a PI of 0.0 is used. Severe transverse cracking may occur if an 85- to 100-penetration asphalt with a PI of -1.5 is employed. Consequently, if low-temperature transverse pavement cracking is to be avoided, engineers in colder climates should select the grade of asphalt cement on the basis of both its penetration at 77 F and its PI, as shown by the oblique temperature-labeled lines in Figure 12.

Grading Asphalt Cements by Viscosity at 140 F

Figure 14 shows the result obtained when the AC5, AC10, AC20, and AC40 viscosity grades shown in Figure 3 are plotted on Figure 12. Figure 14 shows very clearly that grading asphalt cements by viscosity at 140 F results in a fundamental fallacy insofar as low-temperature pavement performance is concerned.

Figure 12 shows that, if transverse pavement cracking is to be avoided, as the PI's of the asphalt cements become lower, the penetration at 77 F to be selected must become higher. On the other hand, when asphalt cements are graded by viscosity at 140 F, for any given viscosity grade, something else occurs. Figure 14 shows that, with respect to low-temperature transverse pavement cracking, as the PI's of the AC10 asphalts become lower, the penetration at 77 F to be selected must also become lower. This is contrary, as indicated by the oblique temperature-labeled lines in Figure 12, to what all practical field experience and theoretical considerations concerning the low-temperature transverse pavement cracking problem have taught us to date.

Consequently, any organization that adopts grading by viscosity at 140 F is including in its specification for asphalt cements the basic fallacy that is so clearly shown in Figure 14. Furthermore, Figure 14 shows that the only way in which grading asphalts by viscosity at 140 F can eliminate low-temperature transverse pavement cracking is by restricting asphalt cement production to crude oils that provide asphalt cements with high PI's. For example, if the critical minimum pavement temperature is -10 F, Figure 14 shows that only the portion of the AC5 grade with a PI above about -0.7 and the portion of the AC10 grade with a PI higher than about -0.3 lie to the left of the oblique line representing the critical minimum temperature. Consequently, grading by viscosity at 140 F carries a very heavy penalty in the form of the limited number of crude oils from which asphalt cements capable of avoiding low-temperature transverse pavement cracking can be made. Figure 15 shows that the viscosity graded specifications of Saskatchewan and Alberta are such that they are not subject to the low-temperature transverse pavement cracking that results from the use of asphalt cements of the same viscosity range at 140 F but with low penetrations at 77 F. Asphalt specifications like those of Alberta and Saskatchewan (Fig. 15) place very severe restrictions on the number of crude oils from which asphalt cements can be made.

Figure 14. Grading asphalt cements by viscosity at 140 F.

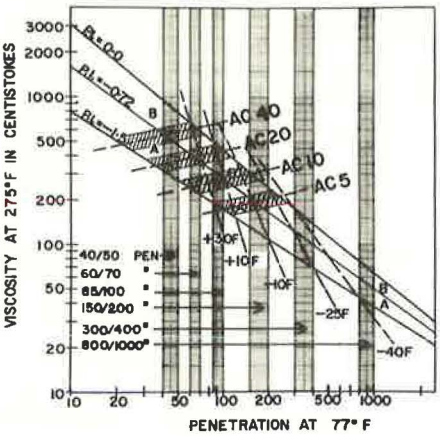

Figure 15. Correlation between viscosity at 140 F and penetration at 77 F.

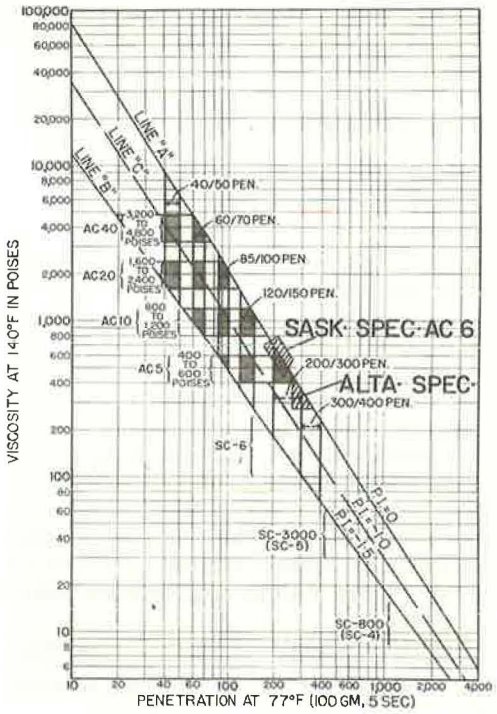

Figure 16. Comparison of actual viscosities at 275 F and AASHO requirements.

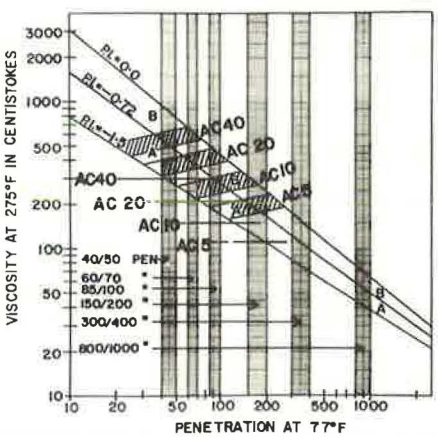

On the other hand, Figures 12 and 14 show that, when asphalt cements are graded by penetration (or viscosity) at 77 F plus a viscosity requirement at 275 F, it is a very simple matter to select an asphalt cement with the combination of PI and penetration at 77 F, which will lie to the left of the oblique line representing the critical minimum pavement service temperature. Furthermore, this selection can be made without any restriction on the crude oils from which asphalt cements are produced.

AASHO SPECIFICATION BASED ON GRADING BY VISCOSITY AT 140 F

One of the principal reasons for promoting grading of asphalt cements by viscosity at 140 F is the construction problems caused by the wide range of high-temperature viscosity associated with each penetration grade (Figs. 1 and 3). Because 275 F is a representative temperature for the high-temperature construction operations of mixing, spreading, and breakdown rolling, it might have been expected that the AASHO specification based on viscosity grading at 140 F would include very rigid requirements for viscosity at 275 F.

Figure 16 shows quite clearly that the minimum viscosity requirements at 275 F stipulated in the AASHO specification for grading by viscosity at 140 F are much too deficient to necessarily facilitate high-temperature construction operations. Figure 16 shows that the minimum viscosity requirements at 275 F, represented by the horizontal lines, are far below the viscosities at 275 F, which are normally associated with the viscosity grades, AC5, AC10, AC20, and AC40. Furthermore, the minimum viscosity requirements are horizontal lines, whereas the viscosity grades themselves have a positive slope that places the low PI end of each viscosity grade much closer to its respective minimum viscosity limit at 275 F than the high PI end. In contrast, Figure 16 shows that the normal shape of the viscosity curve at 275 F for asphalt cements of any given PI is a straight line of negative slope.

It is apparent from Figure 16 that grading asphalt cements by penetration or viscosity at 77 F plus a viscosity requirement at 275 F would greatly improve construction operations at high temperature by dividing the viscosity range at 275 F (currently permitted for each penetration grade) into approximately two halves, categories A and B. Furthermore, for each penetration grade, a viscosity requirement at 275 F, which is normal for each grade, could be specified.

COMMENTS

By one method of analysis, asphalt cements consist of asphaltenes, asphalt resins, and oily constituents. The harder grades of asphalt are made by removing some of oily constituents present in the softer grades, usually by vacuum distillation. The oily constituent part of asphalts is highly desirable as cat-cracker feed stock at refineries, where it is converted into gasoline and other light distillates. Currently, the oily constituents are more valuable as cat-cracker feed stock than when sold in the form of asphalt. Apart from the increased hardness that results, there is no reduction or deterioration in asphalt quality by the removal of oily constituents.

In view of this, the AASHO viscosity graded specifications for AC5, AC10, etc., with their wide range of penetration at 77 F, are an invitation to petroleum refiners to produce the hardest grade permitted by the specification. The damaging effect this can have on low-temperature pavement performance has been emphasized earlier.

When we grade asphalt cements by viscosity at 140 F, we are implying for the AC10 grade, for example, that pavement performance will be the same whether it contains asphalt cement of 50 to 60 or 150 to 200 penetration. Can the petroleum refiner be blamed for assuming we know what we are doing?

On the other hand, when asphalt cements are graded by penetration or viscosity at 77 F, a petroleum refiner is restricted with regard to the amount of oily constituents that he can remove because he must provide the penetration grade that has been specified (Fig. 1).

If grading by viscosity at 140 F were adopted, there would be a complete break with all the pavement experience we have slowly and painfully accumulated over the

past 50 years because all current hot-mix pavement experience with design, construction, and service performance is related to the penetration test at 77 F on asphalt cements.

Grading asphalt cements by viscosity at 140 F will promote a proliferation of specifications for asphalt cements in an attempt to avoid the variable pavement performance (Figs. 7, 8, and 9) that will inevitably result from the very wide range of penetration at 77 F, which is associated with each viscosity grade (Fig. 3). It is significant that, of the seven specifications based on viscosity grading at 140 F, which have been adopted by AASHO and various highway departments in the United States and Canada, no two of these specifications are alike.

Regional specifications for asphalt cements should not be considered whenever national specifications are possible. Regional specifications for asphalt cements, like regional languages, increase the difficulty of communication when engineers from different parts of the country try to compare their experience, and in extreme cases they make any significant comparison impossible.

It is suggested that grading by penetration or viscosity at 77 F, preferably with a viscosity requirement at 275 F (Fig. 1), could serve very adequately as a national or international specification for asphalt cements.

SPONSORSHIP OF THIS RECORD

GROUP 2—DESIGN AND CONSTRUCTION OF TRANSPORTATION FACILITIES
John L. Beaton, California Division of Highways, chairman

BITUMINOUS SECTION
Jack H. Dillard, Virginia Department of Highways, chairman

Committee on Characteristics of Bituminous Materials
Frank M. Williams, Ohio Department of Highways, chairman
Stephen H. Alexander, P. J. Arena, Jr., L. W. Corbett, James R. Couper, William H. Gotolski, Felix C. Gzemski, A. J. Hoiberg, George M. Jones, Larry L. Kole, Dah-yinn Lee, John J. Lyons, Kamran Majidzadeh, Fred Moavenzadeh, Charles A. Pagen, J. Claine Petersen, Charles F. Potts, Vytautas P. Puzinauskas, J. C. Reed, F. S. Rostler, R. J. Schmidt, Herbert E. Schweyer, R. N. Traxler, J. York Welborn, Leonard E. Wood

Committee on Mechanical Properties of Bituminous Paving Mixtures
Rudolf A. Jimenez, University of Arizona, chairman
Grant J. Allen, P. J. Arena, Jr., H. W. Busching, A. B. Cornthwaite, Jon A. Epps, William J. Harper, Yang Hsien Haung, Ignat V. Kalcheff, Bernard F. Kallas, J. Hode Keyser, W. H. Larson, Dah-yinn Lee, Kamran Majidzadeh, Fred Moavenzadeh, Carl L. Monismith, Charles A. Pagen, Charles F. Potts, Donald H. Remick, Lowell H. Shifley, Jr., Jack E. Stephens, Ronald L. Terrel, B. A. Vallerga, Leonard E. Wood George H. Zuehlke

Committee on Characteristics of Aggregates and Fillers for Bituminous Construction
James M. Rice, Federal Highway Administration, chairman
J. T. Corkill, Charles R. Foster, Bob M. Gallaway, Richard D. Gaynor, William H. Gotolski, Donald W. Lewis, Robert P. Lottman, Charles R. Marek, G. W. Maupin, Jr., W. E. Meyer, Frank P. Nichols, Jr., Robert E. Olsen, Vytautas P. Puzinauskas, Garland W. Steele, Egons Tons

Committee on Bituminous Aggregate Bases
Donald R. Schwartz, Illinois Department of Transportation, chairman
Richard G. Ahlvin, Charles W. Beagle, Gail C. Blomquist, J. T. Corkill, Jon A. Epps, O. S. Fletcher, Charles R. Foster, Erling Hendrikson, Moreland Herrin, Jean A. Lefebvre, T. E. McElherne, Lionel T. Murray, Charles V. Owen, Charles F. Parker, David W. Rand, Robert M. Ripple, Paul J. Serafin, Thomas L. Speer, Stewart R. Spelman, Ronald L. Terrel, David G. Tunnicliff, Lansing Tuttle, Warren B. Warden

R. Ian Kingham, Highway Research Board staff

The sponsoring committee is identified by a footnote on the first page of each report.